Ultrastructural Studies of Corneal Scar Tissue

Thesis

UNRESTRICTED

Ultrastructural studies of corneal scar tissue

Ian Malcolm Rawe, BSc

Thesis submitted for the degree of
Doctor of Philosophy
in the discipline of
Biophysics.

The Biophysics Group,
Oxford Research Unit,
The Open University

September 1993

Date of submission : 13th September 1993
Date of award : 18th January 1995

ProQuest LLC.
789 East Eisenhower Parkway
P.O. Box 1346
Ann Arbor, MI 48106 – 1346

Acknowledgements

I would like firstly to acknowledge Dr Keith Meek for giving me the opportunity to carry out this project, for being a great supervisor and, at the same time, a good friend. I wish to acknowledge Professor Gerald Elliott for his expert running of the Research Unit and his good advice over the years. I am also very grateful to Bev and Lorna for all their technical support in producing manuscripts. I would like to thank Andrew and Nigel for their assistance in transforming me into an EM user and for keeping me company down the pub on many occasions along with Jason, Justyn and Sheila. My thanks also to Ted and David for help and advice during critical periods of car maintenance and thanks to the Fox and White Hart for just being there when they were needed!

Finally, I would like to acknowledge all the members of the Research Unit for making it such a great place to be. My special thanks to Dan, Mounia and Nageena for all their help in the final adjustments to this thesis.

Abstract

This thesis is concerned with the study of the ultrastructure of corneal scar tissue. The corneal scar tissue studied was produced in rabbits from three different corneal wounds. These were a manual anterior keratectomy, an excimer laser ablation and a full-thickness 2mm button wound. In each case, a number of animals was used which were sacrificed at different time intervals. For the manual keratectomy and laser ablation, electron microscopy, incorporating cuprolinic blue staining, was the main technique used to study the scar tissue arising from these wounds. The full-thickness wounds were examined using synchrotron X-ray diffraction at Daresbury, UK. From low angle and high angle X-ray diffraction patterns, average values were calculated for centre-to-centre collagen fibril separation, the spread of fibril separation, the fibril diameter and the intermolecular spacing within the collagen fibrils.

The electron microscope studies showed that the same pattern of healing was observed in both types of wounds. An inflated population of keratocytes was observed under the epithelium at one week of healing. Around these keratocytes were vacuoles in the tissue, which were associated with large numbers of abnormally sized proteoglycan filaments. Up to 2 weeks of healing the population of abnormal filaments increased, as did the vacuoles in the tissue, after which they decreased. However, after nine months of healing the scar tissue is still clearly structurally distinguishable from original stromal tissue.

A measure of the collagen fibril density (number per unit area), demonstrated a significant difference between the scar tissue and control. However, it also showed that the number density of fibrils increased with time in the scar tissue. A measure of the range of the collagen fibril diameters in scar tissue up to nine months, indicated that there is a small increase in the range of fibril diameters but the average diameter remained unchanged. Radial distribution functions, from normal corneal stroma and from nine month scar tissue, showed that the short range ordering of the collagen fibrils in the scar tissue was reduced.

The results from the X-ray diffraction showed that, the average spacing between collagen fibrils remains slightly above normal. There is a small increase in the average fibril diameter and the intermolecular spacing is slightly lower than normal. The greatest change was in the range of interfibrillar spacing. The ratio of height to width of the distribution gives a quantitative estimate of this spread. After 3 weeks, this ratio was 0.3, increasing to 1.9 after 21 months; this is still significantly lower than the normal controls (6.2).

X-ray diffraction of the Morquio syndrome cornea showed that the interfibrillar spacing was reduced 10% compared to normal and that the intermolecular spacing was normal. In the TEM, two populations of fibril diameters were observed, one at 24-30nm (the normal range for human corneal collagen fibrils), and the other at 32-44nm. Cuprolinic blue staining revealed abnormally large proteoglycan filaments scattered throughout the stroma many of which were associated with lacunae in the collagen matrix.

Abbreviations

ECM	Extracellular matrix
GAG	Glycosaminoglycan
MS	Morquio's syndrome
PRK	Photorefractive keratectomy
RDF	Radial distribution function
SEM	Scanning electron microscopy
SLK	Superficial lamellar keratectomy
TEM	Transmission electron microscopy

Contents

List of Figures

List of Tables

Chapter 1

1.0 Introduction

The cornea, with the precorneal tear film forms the primary refractive surface of the eye. In humans, myopia, or near sightedness, is usually associated with increased length of vitreous chamber (Garnet, 1981; Hosaka, 1988). The myopic eye focuses rays of light before they reach the retina; from the focal point, the rays begin to diverge, resulting in a blurred image. Photorefractive keratectomy, the central removal of a specific profile of Bowman's layer and anterior stroma using an argon fluoride excimer laser, has been introduced to change the anterior curvature of the eye. Originally, investigators hoped that the remarkable precision and smoothness of the ablated surface (Marshall et al., 1986) would be translated to an accurate change in refraction. Animal and clinical studies have shown, however, that photorefractive keratectomy evokes a wound healing response in the stroma resulting in the deposition of scar tissue (Gartry et al., 1991). The clinical effects of wound healing are seen by the appearance of a fine reticulated corneal haze and regression of the refractive effect.

This thesis is concerned with the study of regenerating corneal stromal tissue known as scar tissue. Of particular interest was the morphology of the proteoglycans and collagen in the regenerating tissue. The regenerated tissue is opaque and differs morphologically from the original stromal tissue. Studying regenerated tissue should therefore give insight into the process of scar formation and give an idea of the relative importance of

different structural parameters for the transparency of the cornea. The tissue studied was taken from rabbit corneas that had undergone manual anterior keratectomy and photorefractive keratectomy with a view to observing the difference in the healing response between the two techniques. The major technique used to study the morphology of these tissues was electron microscopy. Electron micrographs were evaluated quantitatively using a specifically commissioned computer software programme to measure the different structural parameters of the tissue under investigation. Full thickness stromal wounds of rabbits were also analysed using synchrotron X-ray diffraction. X-ray diffraction was used to calculate, at physiological hydration, the average interfibrillar spacing, intermolecular spacing and fibril diameter of the collagen in scar tissue at different time periods.

During the course of my studies I was presented with the opportunity of acquiring a very rare corneal specimen. The cornea obtained was from a patient with mucopolysaccharridosis type IV (Morquio's syndrome). This specimen was analysed with the same methods employed for the corneal scar tissue: electron microscopy and X-ray diffraction.

1.1 Anatomy of the Cornea

The cornea is made up of five distinct anatomic layers lying parallel to its surface.

(i) The epithelium, which is the outer layer of cells, supports the tear film and provides a smooth refractive surface. The epithelium is an almost perfect semipermeable membrane (Mishima & Hedbys, 1967)and a barrier to water-soluble agents from the tear film and to bacterial and fungal infections. It also reduces evaporation and minimises absorption of fluid from the tears, therefore helping to maintain proper corneal hydration.

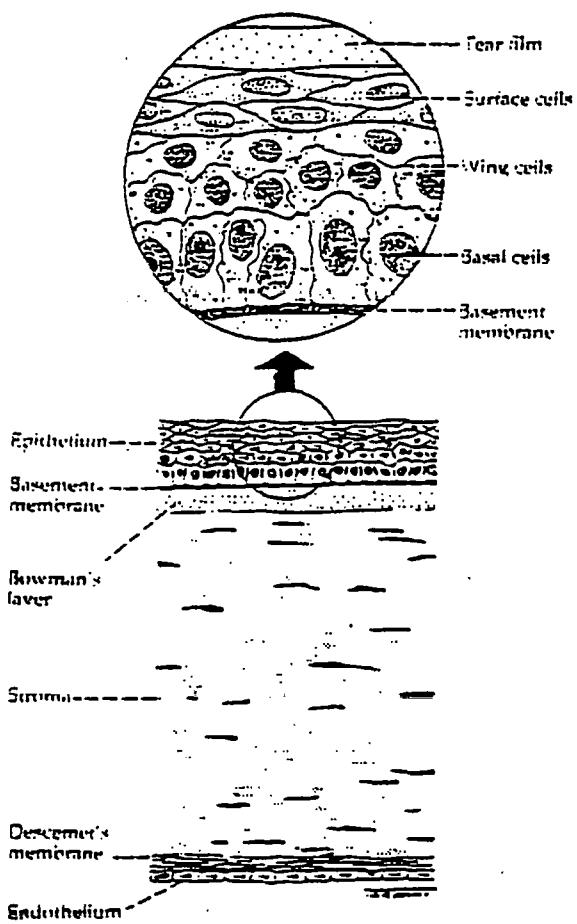

Figure 1.1 Anatomy of the cornea. Reproduced from Kanski, 1984

(ii) The basement membrane is composed of the epithelial basal lamina and Bowman's layer (in primates). Two collagens types, IV and VII, are present in the membrane. The basal layer of the epithelium is attached to the basal lamina by a series of hemidesmosomes and anchoring filaments.

(iii) The stroma constitutes about 84% of the corneal thickness (Buckley, 1987). It is formed mainly of collagen fibrils which provide tissue transparency and mechanical resistance to intraocular pressure. The collagen fibrils have a uniform narrow diameter and are formed into parallel bundles called lamellae. The cells of the stroma are keratocytes and these are scattered throughout the stroma primarily between the lamellae. They are involved in proteoglycan synthesis and secondary collagen fibrillogenesis (Birk & Trelstad, 1984).

(iv) Descemet's membrane is composed of a meshwork of collagen types IV and VIII along with glycoproteins laminin and fibronectin.

(v) The endothelium is a single layer of cells on the posterior stromal surface, 4 to 6um thick. It plays a major role in maintaining the state of hydration of the stroma by acting as a metabolic pump which opposes the osmotic properties of the hydrophilic stromal proteoglycans (Mishima & Kudo, 1967). To prevent fluid flow the cells possess elaborate interdigitation such that the length of the paracellular pathway is 10 times the thickness of the cell layer. Additional resistance to fluid flow is provided by specific junctional complexes.

1.2. Corneal Collagen

Collagens are a family of long-chain molecules entirely or partially composed of a triple helix formed of characteristic polypeptide chains. Differences in the component polypeptide chains have permitted several distinct collagen types to be distinguished. The basic structure of collagen is modified to meet specialised needs of particular tissues. The collagens in the normal rabbit cornea are predominantly type I and type VI with lesser amounts of type IV, V, VII and type VIII. In corneal scar tissue there is a decreased ratio of type VI to type I collagen (Cho et al., 1991) and scar tissue contains increased amounts of type III collagen (SundarRaj et al 1990).

1.2.1 Type I Collagen

Type I collagen is the predominant fibril forming collagen of the corneal stroma. Three polypeptide chains, each of a molecular weight of 100KDa, combine in a triple helical arrangement to form the 300nm long collagen molecule. A structural feature of this collagen and other fibril forming collagens is the repeating amino acid sequence Gly-X-Y in the constituent polypeptide chains, where X and Y are commonly the imino acids proline or hydroxyproline. Glycine at every third residue allows the three chains to twist around each other closely. Each polypeptide is stabilized by the steric repulsion of the pyrrolidine rings of the proline residues. The triple helix is cross-linked by hydrogen bonds between the three polypeptides which involve lysine and hydroxylysine (Nimni & Harkness, 1988). The triple helical molecule is bounded by small non-helical N- and C- domains

called telopeptides. The intermolecular cross-links occur mainly via the telopeptides due to their content of hydroxylysine residues (Bailey, 1975). The molecule is also stabilised by ionic interactions between charged residues on adjacent polypeptides (Parry, 1988).

Analysis of the constituents of type I collagen has shown that it is composed of two different polypeptides. They have been designated α 1(I) and α2(I). The type I molecule has been shown to consist of one α 2(I) and two α1(I) chains.

1.2.2 Type III Collagen

This collagen has a similar structure to type I and is a component of the small reticular fibrils in the dermis and other tissues. Recent studies have shown that type III collagen interacts with fibronectin and also copolymerises with type I collagen. In the cornea, the data on the existence of type III collagen in the collagen fibrils are conflicting. Some reports indicate the presence of type III collagen in the adult human, bovine and rabbit cornea, others indicate its presence only in foetal cornea. However it does occur in regenerating stromal tissues (SundarRaj et al., 1991) .

1.2.3 Type IV Collagen

Type IV collagen is a constituent of basement membranes, in the cornea it is located in Descemet's membrane and the basal lamina. It is a protein of 380KDa and contains, in a 2:1 ratio, two different disulphide-linked

polypeptide chains (Trueb et al., 1981). These chains are arranged in a single triple helical domain which is frequently interrupted by non helical sequences.

1.2.4 Type V Collagen

Type V collagen is similar to type I in that it contains a triple-helix of about the same length as the type I molecule, with non-collagenous propeptides attached at each end. The axial distribution of charged amino acid residues in type V collagen molecules has been shown to be very similar to that of type I molecules. Hybrid fibrils of type I and type V have a electron microscopical D- periodic banding pattern identical to that of pure type I fibrils (Adachi & Hayashi, 1987).

1.2.5 Type VI Collagen

Type VI collagen is a dumbbell shaped molecule with two large globular domains linked by a short, collagenous triple helix (Furthmayr et al., 1983; Engel et al., 1985). Monomers assemble into dimers, which in turn make tetramers by lateral association (Engvall et al., 1986). Tetramers are assembled end to end to produce thin filaments. The precise function of type VI collagen is unknown; recent studies suggest that it plays a role in anchoring basal lamina-containing organs within connective tissues and in restricting movement of collagen fibrils relative to each other (Keen et al., 1988). Type VI collagen is present in the stroma as filaments located between collagen fibrils (Zimmermann et al., 1986). Corneal transparency depends on the spacing of the collagen fibrils and it is likely that type VI

collagen and its interaction with proteoglycans may be responsible for this correct spacing (Cho et al., 1990).

1.2.6 Type VII Collagen

Type VII collagen forms the anchoring fibrils of the epithelium. These fibrils interact with other collagens in the basement membrane, especially type IV collagen, to form an extended anchoring network. Type VII collagen consists of three polypeptides of 350Kda which form a triple helix in the centre with globular extensions on each end.

1.2.7 Type VIII Collagen

Type VIII collagen is secreted by the endothelial cells; it forms the hexagonal lattice of Descemet's membrane (Labermeiery & Kenney, 1983; Kapoor et al., 1985). The type VIII collagen molecule contains three triple helical domains separated by non-collagenous linking regions.

1.3 Formation of Collagen Fibrils

Collagen molecules are synthesized in the rough endoplasmic reticulum (rER) and compartmentalized into intermediate tubules which transport the procollagen molecule to the Golgi apparatus. The intermediate tubules form into spherical distensions on the cis side of the Golgi were the procollagen molecules form into a triple helix. On the trans side of the Golgi cylindrical distensions occur were carbohydrate addition takes

place. The procollagen is passed into secretory granules and then cleavage of the propeptides occurs (figure 1.2)

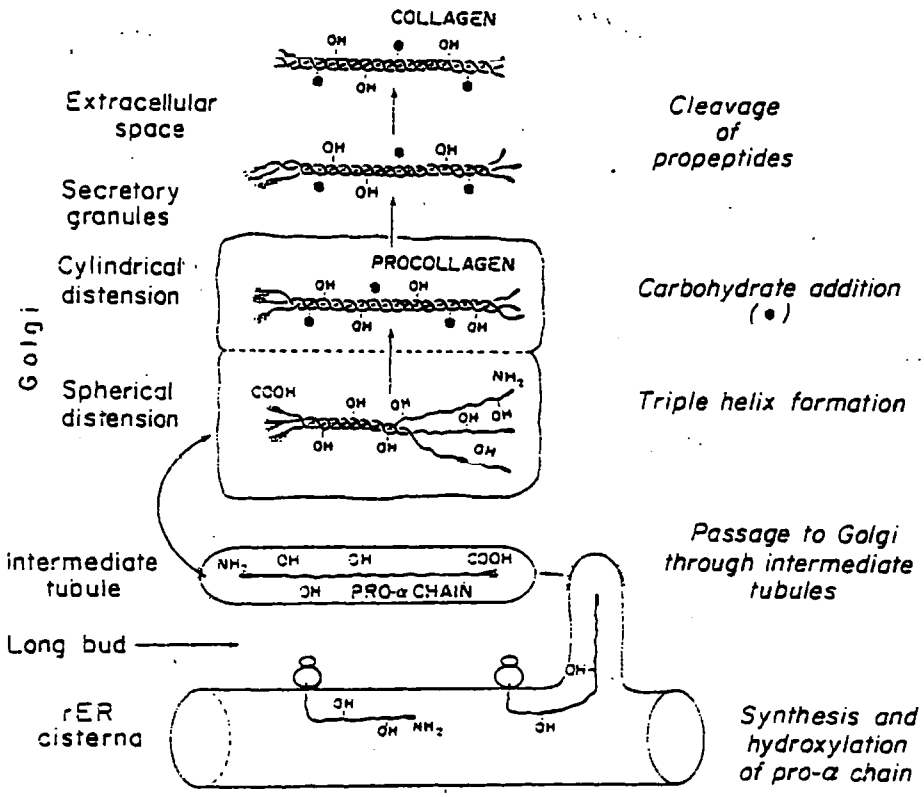

Figure 1.2 Formation of collagen fibrils (reproduced from Lepland, 1992)

1.4 Control of Collagen Fibril Diameters

The collagen fibrils of the corneal stroma have a narrow uniform diameter. Little is known of the factors that control fibril diameters. However a number of mechanisms may be involved. Type I and type V collagen co-polymerise in vitro, producing narrower fibrils with increasing concentrations of type V collagen (Birk, et al., 1990). Type III collagen

can also form hybrid fibrils with type I collagen so this also may be a controlling mechanism (Lapierre et al., 1977). Proteoglycans interact with collagen fibrils at specific locations (Scott & Haigh, 1985, 1988) and may influence fibril diameters (Scott, 1984) as might the content of hydroxylysine linked glycosides (Harding et al, 1980). Cellular control of the mixing of different macromolecules and post-depositional processing are probably also important in the control of fibril formation.

1.5 Proteoglycans

Proteoglycans (PG) are acidic macromolecules that are formed of at least one sulphated glycosaminoglycan (GAG) bound to a protein core. The GAGs characteristic of the cornea are keratan sulphate (KS) and chondroitin/dermatan sulphate (CS\DS) a hybrid of chondroitin-4-sulphate and dermatan sulphate. A GAG is a highly sulphated repeating disaccharide polymer of N - acetylglucosamine with either galactose (keratan sulphate) or glucuronic acid/iduronic acid (dermatan sulphate). Because of their highly charged sulphate and carboxylate groups, GAGs are extremely hydrophilic. Each proteoglycan forms a water-filled compartment, therefore most of the water present in the intercellular substance of connective tissue is in the form of solvation water of GAG molecules. Thus GAGs play a vital role in the regulation of tissue hydration, collagen fibril diameter (Katz et al., 1986) and spacing (Borcherding et al., 1975), and hence tissue transparency.

The proteoglycans in the cornea are fibromodulin, lumican, decorin and bilgycan (Hardingham and Fosang, 1992). They are low molecular weight

proteoglycans, with a core protein size of approximately 40 KDa. The GAGs attached to these proteoglycans are KS (fibromodulin, lumican), and or CS/DS (decorin and biglycan). Decorin and fibromodulin both bind type I and II collagen and therefore probably have a important role in matrix organisation. In vivo, decorin binds at the d & e bands of corneal collagen, and fibromodulin binds at the a & c bands (Scott & Haigh, 1985). During the development of the cornea there is normally a change in the component GAGs from dermatan sulphate (DSPG) in the foetus to keratan sulphate (KSPG) which is the predominant PG in the adult of most species.

1.6 Corneal Transparency

Collagen and associated proteoglycans, glycoproteins and other proteins combine in the corneal stroma to provide mechanical strength and transparency. Transparency is generally believed to depend upon a restriction in the cross-sectional diameter of the collagen fibrils and on the uniform spacing between the fibrils which produces destructive interference of scattered incident light (Maurice, 1957: Hedbys, 1961: Benedek, 1971). This ground substance consists mainly of proteoglycans, type VI collagen filaments (Zimmermann et al., 1986) and a number of other proteins and glycoproteins. Proteoglycans play an important role controlling corneal hydration and are thought to be involved in the maintenance of fibril separation (Borcherding et al 1975., Scott, 1985). An alteration in either the structure or the relative amounts of the collagen or of the proteoglycans can result in a degradation of the optical properties of the cornea.

1.7 Corneal Wound Healing

1.7.1 Epithelial wound healing

The corneal epithelium is a stratified non-keratinizing layer that provides stability for the tear film, a barrier to fluid influx to the cornea, and a pump mechanism that contributes to the maintainance of transparency by transporting fluid out of the stroma (Klyce, 1972). The basal epithelial cells are attached to the basement membrane by hemidesmosomes. From the hemidesmosomes, anchoring filaments of type VII collagen pass through the basal and reticular laminae of the basement membrane and spread out among the collagen fibrils to become attached to anchoring plaques up to 2μm within the corneal stroma (Gipson et al. 1987).

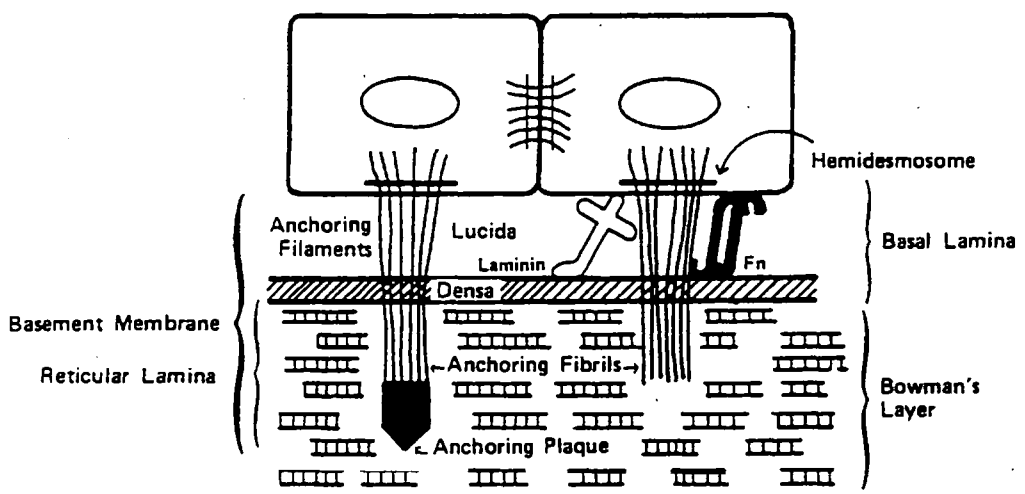

Figure 1.3 Attachment of human cornael epithelium to the stroma, reproduced from Beuerman, Crosson and Kaufman, 1989

Figure 1.3 Attachment of human corneal epithelium to the stroma, reproduced from Beuerman, Crosson and Kaufman, 1989

The initial progress of epithelial migration is similar following the loss of stromal tissue or epithelial debridement (Suda et al., 1982). Following a simple epithelial debridement there is a transverse rupture of the basal epithelial cells, and it is thought that portions of the hemidesmosomal complex may be preserved and re-utilised, which enables rapid and stable re-epithelialisation of the wound to occur. In contrast, following superficial keratectomy, a new attachment complex must be synthesized and assembled before firm epithelial reattachment is established, a process that may take up to three months in the primate (Khodadoust et al., 1968; Gipson et al., 1989). However, the formation of a basement membrane has been shown to be abnormal in monkey corneas 18 months after excimer laser keratectomy, with areas missing or fragmented and thickened (Hanna et al., 1990). Also, some regions of the epithelium overlying the basement membrane were devoid of type VII collagen anchoring fibrils (SundarRaj et al., 1990). The new hemidesmosomes and anchoring filaments appear synchronously, beginning at the periphery of the wound (Gipson et al., 1988), but the formation of anchoring structures may be delayed in the diseased cornea (Azar et al., 1989), and a failure to establish firm anchoring points may contribute to the pathogenesis of recurrent corneal erosion.

After an epithelial injury there is a latent phase, which in the rabbit and monkey is between 5-6 hours as the injured cells at the edge of the wound are desquamated and intercellular actin microfilaments polymerise prior to cellular migration (Crosson, 1986). The latent phase is followed by a

healing phase, during which wound closure occurs at a constant rate. The healing phase begins with cellular slide after hemidesmosomal attachments in a zone 50 to 70 um from the wound edge and cells adjacent to the wound begin to move as a monolayer to cover the defect. This initial movement is independent of cellular division (Kuwabara et al., 1976; Gipson & Anderson, 1977), but there is a secondary renewal from the epithelial basal layer and the germinal zone at the limbal and from the conjunctival epithelium (Thoft & Friend, 1983).

As epithelial cells migrate they temporally maintain an attachment to the corneal surface via macromolecules that are probably derived from the tears. The most important of these are thought to be the dimeric glycoproteins fibronectin and laminin. Both fibronectin and laminin can bind to type IV collagen of the basement membrane, while the other end of the fibronectin molecule attaches to the integrin-fibronectin receptor on the cell surface, and hence to intracellular actin. This provides a temporary matrix for epithelial adhesion during healing until the permanent attachment components are regenerated and the macromolecular binding complex is resorbed (Fujikawa et al., 1981; Fujikawa et al., 1984).

Temporary macromolecular bonds must be broken to permit further cell movement during cellular migration. Urokinase plasminogen activator (uPA) released by epithelial cells at the leading edge of the migrating sheet cleaves plasminogen to liberate plasmin, which severs through the fibronectin in a limited fashion to release the leading edge of the epithelium (Berman., 1989). When epithelial resurfacing is complete,

remaining subepithelial fibrin/fibronectin is thought to be resorbed by plasmin generated by tissue plasminogen activator (tPA).

1.7.2 Stromal Wound Healing

The production of a stromal injury is associated with inflammation, repair, and the removal of damaged tissue. Fibrin and fibronectin deposited on the surface of the wound from the tears, may act as a scaffold for neutrophils, macrophages and lymphocytes recruited to the wound, but as the cornea is avascular, granulation tissue is not formed. The keratocytes die back from a zone of about 200um around the wound surface (Matsuda & Smelser, 1973), possibly due to a change in the physiological environment of the anterior stroma. This acellular region becomes surrounded by a zone of between 200 and 500 um in which the keratocytes undergo proliferation before migrating to the wound surface. The activation of the keratocytes occurs after 48 to 72 hours and reaches a peak after 3 to 6 days, and histological examination at this stage demonstrates a prominent zone of keratocytes that have a dilated rough endoplasmic reticulum suggestive of active protein synthesis. However, an intact epithelial surface is required before stromal healing can begin (Dunnington & Wiemer, 1958). Keratocyte activity returns to normal after three months although hypercellularity of the wound may persist for years.

Digestion and resorbtion of damaged fibrils at the wound margin by keratocytes precedes the synthesis of scar tissue (Ten Cate & Deporter, 1975). This process is initiated by proteolytic enzymes from polymorphonuclear leukocytes from the corneal limbus and the tear film

and continued by macrophages, epithelial cells and keratocytes (Graf et al., 1972). Degradation of the extracellular matrix is mediated by a group of the structurally related metalloproteinases (collagenase, stromelysin, gellatinase) which will catalyse the degradation of native collagens of the cornea at neutral pH. Collagenase can not be detected in the unwounded cornea (Gordon et al., 1980) but gelatinase is expressed, suggesting a role in the maintenance of the extracellular matrix (Fini, 1990). Following injury the enzymes are secreted into the extracellular matrix either by resident epithelial and stromal cells or by invading inflammatory cells (Brown, 1970).

Corneal scar differs from normal adult stroma in that it is hazy, is less elastic and has a lower mechanical strength. The origin of the haze that is associated clinically with corneal scar formation is thought to derive from structural features of the scar tissue. The DSPG molecules that are deposited initially are associated with a reduction in the concentration of the KSPG in the wound (Hassell et al., 1983; Cintron et al., 1990a, 1990b). Increased levels of hyaluronic acid, which is present in only small quantities in human and rabbit cornea, are observed after laser keratectomy in the rabbit (Fitzsimmons, et. al. 1991). The main structural features of corneal scar tissue compared to normal stroma, are the reduction in the ordering of the collagen fibrils and the increased variation in fibril diameters. It has been reported that opaque corneal scars either contain collagen fibrils which show a considerable variation in their diameters (Kenyon, 1987), or that the collagen fibrils have a normal mean diameter but a greater spread of diameters (Manasche et al., 1988).

Transparency is thought to be acquired by the scar tissue when the interfibrillar spacing returns to normal (Cintron et al. 1977).

The turnover of collagen is normally very slow, but scar tissue undergoes remodelling to become less opaque with time. The ultrastructural dimensions of the collagen fibrils and biochemical features probably never return to normal (Cintron et al., 1978), therefore remodelling is never complete.

1.8 Drug Therapy

For excimer laser refractive surgery, ideally no stromal wound healing should take place. The prolonged administration of high concentrations of corticosteroids retards the healing of stromal wounds and reduces the deposition of scar tissue. The mechanism of the steroid effect is not certain, but it appears to be distinct from any anti-inflammatory effect. For example, the cellular effect of dexamethasone is to inhibit collagen production by reducing DNA synthesis by activated keratocytes, an anti-anabolic effect.

1.9 Electron Microscopy

Transmission electron microscopy was employed to study the structure of corneal scar tissue. Visualisation of the tissue was improved by the use of specific staining. For the collagen fibrils, heavy metals stains were used, uranyl acetate and phosphotungstic acid, and for the proteoglycans cuprolinic blue (3.1.2). Scanning electron microscopy was utilised to examine the lamellar structure of the scar tissue.

1.9.1 Positive staining of Collagen

Positive staining is used to enhance the contrast of embedded and sectioned biological tissues (Hayat, 1975). Heavy metal salts such as uranyl acetate and phosphotungstic acid are taken up by acidic and basic residues. When collagen is positively stained, a characteristic banding pattern is produced along the length of the fibrils. The bands are are normally labelled a to e (Hodge and Schmitt, 1960), and the banding repeats with a periodicity D, where D in the cornea is 65 nm (in tendon D=67 nm). The D periodicity in fibrils has its origins in the interactions that occur between the outwardly projecting side chains when two molecules come together in parallel association. The intermolecular attractions are greatest when the adjoining molecules are displaced axially by D (Hulmes et al., 1973). The D periodicity thus arises from an assembly of many molecules, with each D period being made up of two zones, one containing more molecules in a transverse cross section than the other-these are referred to as the overlap region and the gap region respectively.

1.9.2 Proteoglycan Staining

Cationic dyes, cupromeronic blue and cuprolinic blue (structural isomers) are stains that are used to enhance the electron density of proteoglycans. The cationic dyes are used in a critical electrolyte concentration (Scott, 1980; Scott et al., 1981). The concentration of electrolyte, usually magnesium chloride ($MgCl_2$), influences the extent to which the stain is taken up by the polyanionic glycosaminoglycans of the proteoglycans.

Cuprolinic blue causes the partial collapse of the glycosaminoglycans chains onto the protein core. The electron density of the cuprolinic dye complex is greatly enhanced by replacing the Cl^- with an anion of higher electron density, for example tungstate (Scott, 1980).

1.9.3 Proteoglycan and Collagen Interactions in the Cornea

Using cuprolinic blue, together with specialized and specific enzymes to digest GAGs, it has been shown that four separate proteoglycan binding sites occur within each D-period of type I collagen in rabbit cornea (Scott & Haigh, 1985: Scott, 1988).

X-ray diffraction mass distribution patterns of cupromeronic blue stained tissue sections suggest that approximately 12% of the stromal proteoglycans are with the specific binding sites in a well ordered arrangement, the rest being, to varying degrees, more randomly arranged (Meek et al., 1986).

1.10 X-ray Diffraction

In the cornea, the structure of the collagen fibrils and the regularity with which other components associate with the fibrils gives rise to a characteristic X-ray diffraction pattern. The study of corneal tissues using the technique of X-ray diffraction has a major advantages over electron microscopy. Tissue samples under study do not undergo any processing, therefore allowing analysis of the tissue much closer to its normal physiological condition.

X-ray diffraction patterns from collagen have several different components. There are sharp meridional reflections which result from the axial changes in the electron density caused by the D-periodicity along the collagen fibril. There are also the more diffuse reflections, termed equatorial reflections, which are caused by diffraction between the fibrils themselves (interfibrillar spacing) or between the laterally packed collagen molecules within the fibril (intermolecular spacing).

1.10.1 Equatorial X-ray Diffraction of Cornea

High-angle X-ray diffraction elucidates periodic structures on the nanometer scale and can therefore be used to calculate the intermolecular packing within collagen fibrils (Ramachandran, 1967).

The low-angle equatorial X-ray diffraction pattern from the corneal stroma gives a measure of the interfibrillar packing of the collagen fibrils (Goodfellow et al., 1978;Sayers et al., 1982; Worthington & Inouye,

1985). From this pattern accurate measurments can be made of the interfibrillar spacing, and the fibril diameter. The pattern has been analysed for a wide range of mammals, fish and birds (Gyi et al.,1988; Meek & Leonard, 1993).

1.10.2 Meridional X-ray Diffraction

The low-angle meridional pattern, which arises from the axial electron density profile of the collagen fibrils, is a series of orders of reflection with different intensities. The orders index on, and can therefore be used to obtain an accurate measurement of, the D-periodicity. The relative intensities of the different orders can be used to calculate the axial electron density of the collagen fibrils (Meek et al., 1981a,b).

1.11 Morquio's Syndrome

Mucopolysaccharide storage diseases are inborn errors of metabolism characterised by excessive storage of mucopolysaccharides and defective processes of degradation owing to deficiences of lysosomal acid hydrolases. In mucopolysaccharidoses, excess dermatan sulphate and keratan sulphate appear in the cornea, and heparan sulphate accumalates in the retina and central nervous system.

Morquio's syndrome is a mucoploysaccharidosis type IV which is inherited as an autosomal recessive trait and is associated with the accumulation of keratan sulphate in the tissues due to a deficiency of N-acetyl-galactosamine sulphatase. The areas that are primarily affected are

the cartilaginous and bony structures. Corneal clouding may occur, but is not strongly evident until after 10 years of age. Cloudiness may consist of a mild stromal haze, or it may be severe.

1.12 Aims of this Thesis

Using the techniques of electron microscopy and synchrotron X-ray diffraction the aims of this thesis were to:

1. Study the collagen and proteoglycans changes in stromal scar tissue following manual anterior keratectomy, in order to obtain an understanding of a wound healing process and to understand which factors affect transparency.

2. Study the collagen and proteoglycans in stromal scar tissue produced following laser ablation and compare these findings with the healing after manual wounding.

3. Examine full-thickness scar tissue with synchrotron X-ray diffraction to calculate the structural features of scar tissue at physiological hydration.

4. Examine the ultrastructure of a Morquio's syndrome cornea with electron microscopy and X-ray diffraction.

Chapter 2

2.0 Materials and Methods

2.1 Animal Specimens

2.1.1 Manual Keratectomy

The following procedures were carried out at the Institute of Ophthalmology, London, by Mr S. Tuft FRACS.

New Zealand white rabbits (16) were used in this study. All animals were approximately six months old (weight 2.5kg) at the time of surgery. Anaesthesia was induced by intramuscular injection of Hypnorm 0.5 ml/kg (Janssen Pharmaceuticals LTD.,Oxford UK) and topical proparacaine hydrochloride. Ocular akinesia was supplemented with intravenous diazepam 0.1 mg/kg. Only one eye of each animal was operated on, two animals were included for each observation period and the contralateral eyes served as controls. All the animals used in this study received adequate care and humane treatment in keeping with the ARVO Resolution on animal research.

For the superficial lamellar keratectomy wounds, the left eye was proptosed and a partial thickness incision was centred on the pupil with a 6.0 mm trephine. A superficial keratectomy was then completed with a razor fragment. At the end of the procedure 10 mg gentamycin was injected subconjunctivally and the eye taped shut until the animal had fully

regained consciousness (after approximately 2 hours). Animals were examined daily until re-epithelialization was complete, and at twice weekly intervals thereafter. Each animal received a drop of nonpreserved gentamycin 0.3% three times daily to the operated eye for four days, at which time all wounds had epithelialised. Steroids were not administered. All animals had a circular area of sub-epithelial haze in the central region of the cornea. This gradually reduced but was still present at 9 months post-wounding.

Animals were sacrificed (x2) at intervals of 1, 2, 4, 6, weeks and 2, 3, 6, 9 months with a 3 ml intravenous injection of sodium pentobarbitone (200 mg/kg) after prior sedation with an intramuscular injection of Hypnorm. Both eyes were enucleated and the corneas were dissected with scissors, removing the whole cornea which was then and processed immediately for electron microscopy (2.2).

2.1.2 Laser Ablated Corneas

The following procedures were carried out at the University of Minneapolis, Minneapolis, by Mr R. Zabel MD and Dr V. Chen.

The Dutch belted rabbits used in this study weighed between 1 - 2 kg. This weight corresponds to an age of approximately 3 months which was slightly less than that of the animals used in the manual keratectomy experiments. Thirty rabbits were used in the study, three of which received topical steroid post operatively. All the animals in the study received adequate care and humane treatment in keeping with the ARVO

Resolution on animal research. Laser ablations were performed under general anaesthetic (intramuscular ketamine hydrochloride, 100mg/ml, Aveco. Inc., Fort Dodge, IA and Xylazine, 20mg/ml, Mobay Corporation, Shawnee, KS) and topical (Acaine) anaesthetic.

Each rabbit was positioned to ensure proper alignment within the operative plane of the laser (Taunton Technologies, Monro). A circular impression was made in the corneal epithelium using an 8mm optical zone marker centred on the pupil and the contained epithelium was gently removed using a Tooke knife. A stromal wound with a "top hat" profile, 100 microns in depth and 6mm in diameter was ablated at a fluence measured at the operative plane of 125 mJ/cm^2. The laser was operated at 10Hz. Effluent was removed using a vacuum suction device. While anaesthetized, the eyes were taped shut to prevent corneal drying. Gentamycin 0.3% drops were instilled twice daily for one week. Selected eyes were treated with the topical steroid Fluoromethalone four times daily for five weeks.

Epithelialisation of the eyes was complete within one week. The rabbits were sacrificed at intervals of 1,2,4,8,16,35 and 45 weeks, and rabbits which had undergone steroid treatment at 15,35 and 45 weeks, under full general anaesthetic using intravenous T-61 euthanasia solution (Hoechst-Roussel, Somerville, NJ). Broad beam slit-lamp photography was performed prior to sacrifice. The whole scarred corneas and contralateral controls were excised and frozen in liquid nitrogen. Tissue was stored at $-70^{o}C$ until processed.

2.1.3 Full thickness corneal wounds

The following procedures were carried out at the Schepens Eye Institute, Boston, by Dr C. Cintron.

Twelve adult rabbits weighing approximately 2.5kg were anesthetised with an intravenous injection of sodium pentobarbital and topical application of proparacaine to each eye before the corneas were wounded. A 2mm diameter, full-thickness wound, was made in one eye of each rabbit and the other eye was used as a control. Rabbits were allowed to heal for 3 and 6 weeks and 7, 14 and 21 months and the scar tissue was clearly distinguishable from the adjacent normal cornea. The animals were then sacrificed with an overdose of sodium pentobarbital. To minimise dehydration the whole corneas were excised and immediately wrapped tightly in cling-film, then sealed in small plastic tubes and stored unfrozen, but on ice, whilst being transported directly to the synchrotron. The X-ray diffraction was carried out on the corneal scars within 20hrs of sacrifice and on completion the tissue was frozen and stored at -20°C.

2.1.4 Densitometry of Scar Tissue

The absorbance of the full thickness scar tissue was assessed using a scanning laser densitometer (LKB Ultrascan XL laser microdensitometer, Gaithersburg, MD) at a wavelength of 540nm. The whole corneas including the scars were individually thawed, laid flat on the densitometer with a small drop of water and scanned across the unscarred and scarred tissue. Increased absorbance relates to a decrease in transparency of the

scar tissue. On completion of the scan the scar tissue was cut out, cut into four pieces and placed in fixing solution (which contained no cuprolinic blue stain) and emmbedded (2.2).

2.2 Electron Microscopy

Transmission electron microscopy (TEM) was used to study the morphology and structure of corneal tissues. In most cases, a proteoglycan-specific dye, cuprolinic blue, was used to visualise the proteoglycans in the tissue (Scott, 1984). Scarred and unscarred controls of the same age were stained and processed together at all ages.

For processing, the central region of the cornea containing the scar, was isolated and cut vertically through the epithelium with a scalpel into approximately $1mm^2$ pieces, which were then immersed in 0.05% cuprolinic blue stain (BDH Ltd, Atherstone, Warwickshire, U.K.) containing 2.5% (w/v) glutaraldehyde and 0.1 M $MgCl_2$ in 25mM sodium acetate buffer. The pieces were rinsed three times each for 15 minutes in the buffer solution containing no cuprolinic blue and then counterstained using 3 x 15 minute changes of aqueous 0.5% sodium tungstate. This was followed by dehydration through an ethanol series and transfer to propylene oxide before embedding in Polarbed (Agar Aids Ltd). The corneal pieces were orientated in the embedding medium so that on sectioning, vertical sections through the cornea contained both the epithelium and endothelium. This allowed easy identification of the scar tissue below the epithelium as normal tissue in the section lay below the scar tissue and acted as an extra control. Sections approximately 90-

100nm (silver/gold colouring) thick were cut on a Reichert-Jung Ultracut E ultramicrotome, stained in 2% uranyl acetate or 2% uranyl acetate followed by 2% phosphotungstic acid, and were examined with a Philips 301 electron microscope. The microscope was calibrated with a 2160 lines/mm replica grating.

2.2.1 Analysis of Electron Micrographs

Electron micrographs were taken at 34k and 57k. In each series of micrographs, 3 calibration photographs were also taken of the 2160 lines/mm replica grating. When printed, scaling marks were added to each micrograph and the print was then taped against a vertical flat surface. A video camera (JVC TK-5310EG) linked to a PC (Opus Technology) and television screen was used to capture the image of the micrographs. The following properties of the image were computed-radial distribution functions and fibril diameter distributions. The radial distribution functions were calculated from 1000 fibrils, the centres having been indicated manually onto the television image using a mouse. Fibril diameter distributions were calculated from 250-500 fibrils by marking the approximate fibril centres manually.The program then used a 'Critical Chi-square', and a "grow fibrils" algorithm with a Kolmogorov-Smirnov test to find the centre of each fibril and to decide when to stop expanding the disc. The 'grown' fibrils could then be edited when necessary, and a printout of the fibril radii produced.

The sizes of the proteoglycan filaments seen after Cuprolinic blue staining were measured directly from prints of the electron micrographs, using a

metric ruler. Since the micrographs were calibrated and the print magnification was known, it was possible to convert measurements into nanometres. In prints from the scar tissue, the largest proteoglycans were measured to give an approximate maximum size. The number of measurements varied but in all cases sufficient measurements were made to give a reproducible estimate of filament dimensions for that particular tissue.

2.3 X-ray Diffraction

X-ray diffraction patterns were recorded at the SERC synchrotron source at Daresbury, UK. Corneas were either examined fresh (stored on ice and wrapped tightly in clingfilm to minimise drying during transportation) or frozen (also wrapped tightly in clingfilm to minimise drying during freezing and thawing). Although freezing is known to cause structural alterations to the collagen and GAGs within the stroma, these changes appear to be completely reversible on thawing (Quantock & Meek, 1990; Fullwood and Meek, 1994). During exposure the corneas were held in air-tight cells to which a small piece of watersoaked paper was added. This was to obviate water loss from the specimens during exposure. The X-ray beam was directed along the optical axis through the central part of the cornea. Low angle patterns were recorded using a long camera (2.4-4m), 90% of which was under vacuum to minimise air scattering. The beam for this camera was typically 0.5mm x 4mm, and the X-ray wavelength was 0.1540 nm. The first order exposure in the equatorial pattern required an exposure of 30-120 seconds and the higher orders required 30-40 minutes.

High angle patterns were collected on a short camera (11-12cm), on Station 7.2, with the specimen to film distance filled with helium to minimise air scatter. The beam had a circular cross-section of diameter 0.5mm and a wavelength of 0.1488nm. The exposure time was between 4-5 minutes.

The X-ray patterns were recorded on Caeverken Reflex 25 film (Caeverken, Strangnass, Sweden). The exposed X-ray films were scanned using an Ultrascan XL laser microdensitometer (LKB instruments Inc., Gaithersburg, MD). Backgrounds were fitted by eye. Both the densitometer traces and estimated backgrounds were digitized and subtracted using a Tetronix computer.

2.4 Analysis of X-ray Patterns

2.4.1 High Angle Patterns

The basic principle of X-ray diffraction is given in Bragg's equation:

$$n\lambda = 2d\sin\theta$$

were n is the order of reflection, λ is the wavelength of the radiation, the angle θ is half the scattering angle and d is the Bragg spacing (figure 2.1). Calibration can be accurately carried out by use of a specimen of known spacing. For high-angle X-ray diffraction, calcite crystals were used. Calcite has a diffracting structure with a periodic repeat of 3.04 Å. Thus,

for the first order (n=1), the wavelength λ, and d for the calibration specimen can be substituted into Bragg's equation and the scattering angle, 2θ, found. If r is the radius of the first order calcite ring on the X-ray film, and L is the specimen-to-film distance, then $\tan(2\theta)=r/L$ and from this relationship, L can be accurately determined. For any unknown reflection, r is measured from the pattern on the film and, by applying the above procedure in reverse, the Bragg's spacing of the unknown specimen can be determined (figure 2.2). The Bragg spacing is usually multiplied by a factor of 1.11 (Maroudas et al., 1991)) to convert it into an intermolecular spacing, on the assumption that the collagen molecules within the fibrils are packed in a quasi-hexagonal array.

Figure 2.1 Schematic diagram of X-ray diffraction from a perfect lattice showing the derivation of θ and d in Bragg's equation.

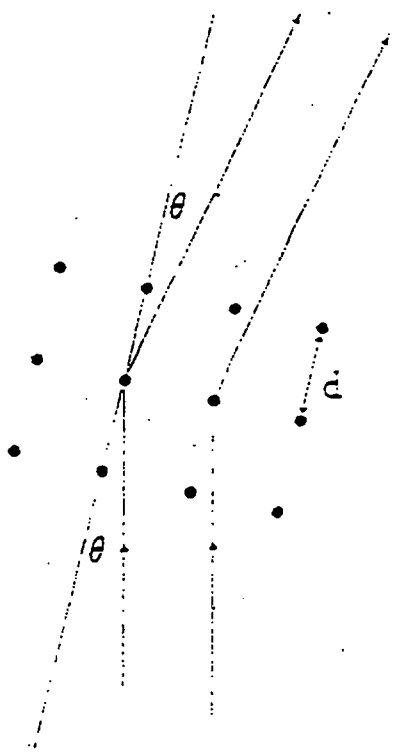

Figure 2.2 Schematic diagram of the X-ray camera arrangements.

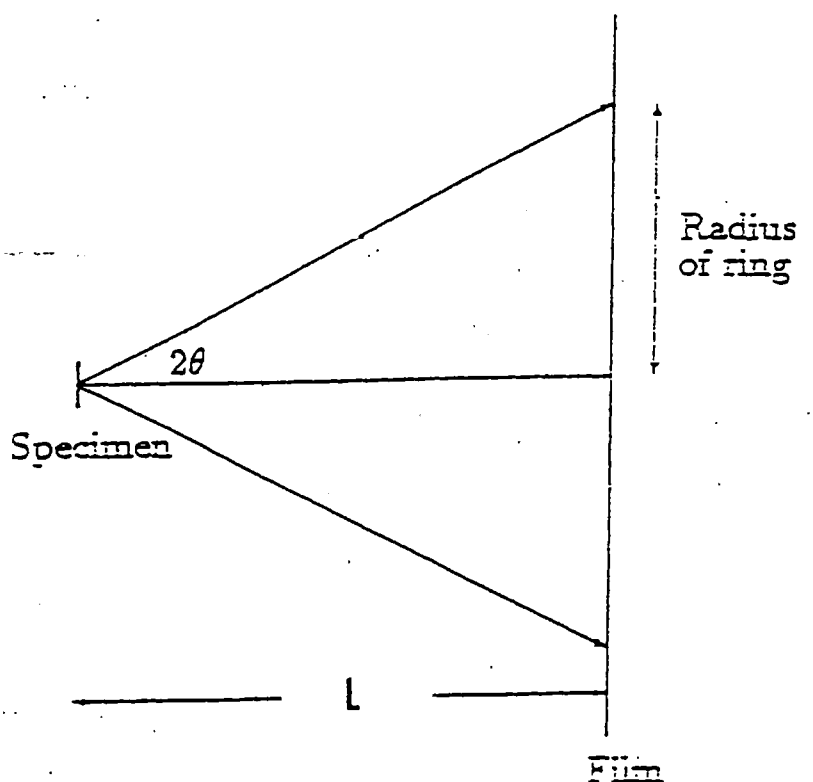

2.4.2 Low-Angle Patterns

In the corneal stroma the 1st order Bragg spacing, d, is related to the mean centre-to-centre interfibrillar spacing i, by i=1.12d (Worthington and Inouye, 1985). The low angle pattern was calibrated using the first order of the D-periodicity in rat tail tendon (67nm). If, on the X-ray film, r_t is the distance of this first order reflection from the centre of the pattern, and r is the corresponding distance of an unknown reflection, then the unknown Bragg spacing, d, is given by

$$d = \frac{67 \times r_t \text{ nm}}{r}$$

This method is valid for long camera lengths because for small angles, tan $\theta \approx \sin\theta$

The subsidiary maxima in the low angle pattern are thought to be due to the scattering from the individual cylindrical collagen fibrils (Worthington & Inouye, 1985). Therefore, the first of these would be expected to occur at:

$$R = \frac{5.14}{2\pi r_0}$$

where R is the reciprocal space coordinate of the reflection and r_0 is the fibril radius and the numerical factors derive from Bessel functions (Vainshtein 1966). The position of the maxima in the diffraction pattern therefore may be used to find R and hence calculate r_0 (Worthington and Inouye, 1985).

2.5 Morquio's Syndrome Cornea: Case Report

Patient born 28.3.59.

The patient was diagnosed Morquio's Syndrome by analysis of mucopolysaccarides in the urine, at the Sick Childrens Hospital in Toronto. The patient was first seen in the Department of Ophthalmology, Ottawa General Hospital in 1983. Refraction at that time was +5 +1.25 x 80 and +4.25 +2.50 x 90 for visual acuities of 20/70 and 20/40 right and left eye respectively. The cornea showed diffuse clouding - full thickness and limbus to limbus. The crystilline lenses were clear. The posterior pole revealed myelinated nerve fibres and diffuse washout of the retinal pigment epithelium. In August 1992 the visual acuities had dropped to 20/400 due to progressive clouding of the cornea.

The patient underwent penetrating keratoplasty in the left eye in October 1992. She was most recently seen in Febuary 1993. A refraction of +3.25 +1.0 x 45 gave an acuity of 20/80.

Immediately after surgery, sections were taken from the cornea and stained with cuprolinic blue and fixed and embedded as before. To provide confirmation of Morquio's Syndrome a piece of corneal tissue was saved for enzyme analysis, however this was not carried out and therefore Morquio's Syndrome was not confirmed.

Chapter 3

3.0 RESULTS

3.1 Electron Microscopy

The TEM was used to analyse the cuprolinic blue stained corneal tissue of the rabbits that had undergone manual and laser keratectomy. The focus of attention was the anterior area below the epithelium were stromal tissue regeneration should occur. This included the tissue of three rabbits that, after laser keratectomy, were treated with a steroid (fluoromethalone). It was also necessary to examine normal rabbit corneas as controls.

3.2 Electron Microscopy of Normal Rabbit Corneal Stroma

Analysis of normal rabbit cornea at low magnification in the TEM showed the layered arrangement of lamellae that make up the corneal stroma (figure 3.1). It also revealed the sparse population of keratocytes that are present throughout the stroma. At higher magnification the collagen that makes up the lamellae of the stroma can be seen (figure 3.2A). These collagen fibrils lie approximately parallel to one another. Figure 3.2B shows the collagen fibrils in cross-section with their regular interfibrillar spacing and uniform fibril diameters. Staining with cuprolinic blue reveals the distribution of proteoglycans in relation to the collagen fibrils. Proteoglycan filaments are situated at regular intervals along the individual collagen fibrils and run crosswise from one fibril to its neighbour

Figure 3.1 A TEM micrograph of normal rabbit corneal stroma showing the lamellar structure and the location of stromal keratocytes. Stained with cuprolinic blue and counterstained with uranyl acetate. Magnification 8K.

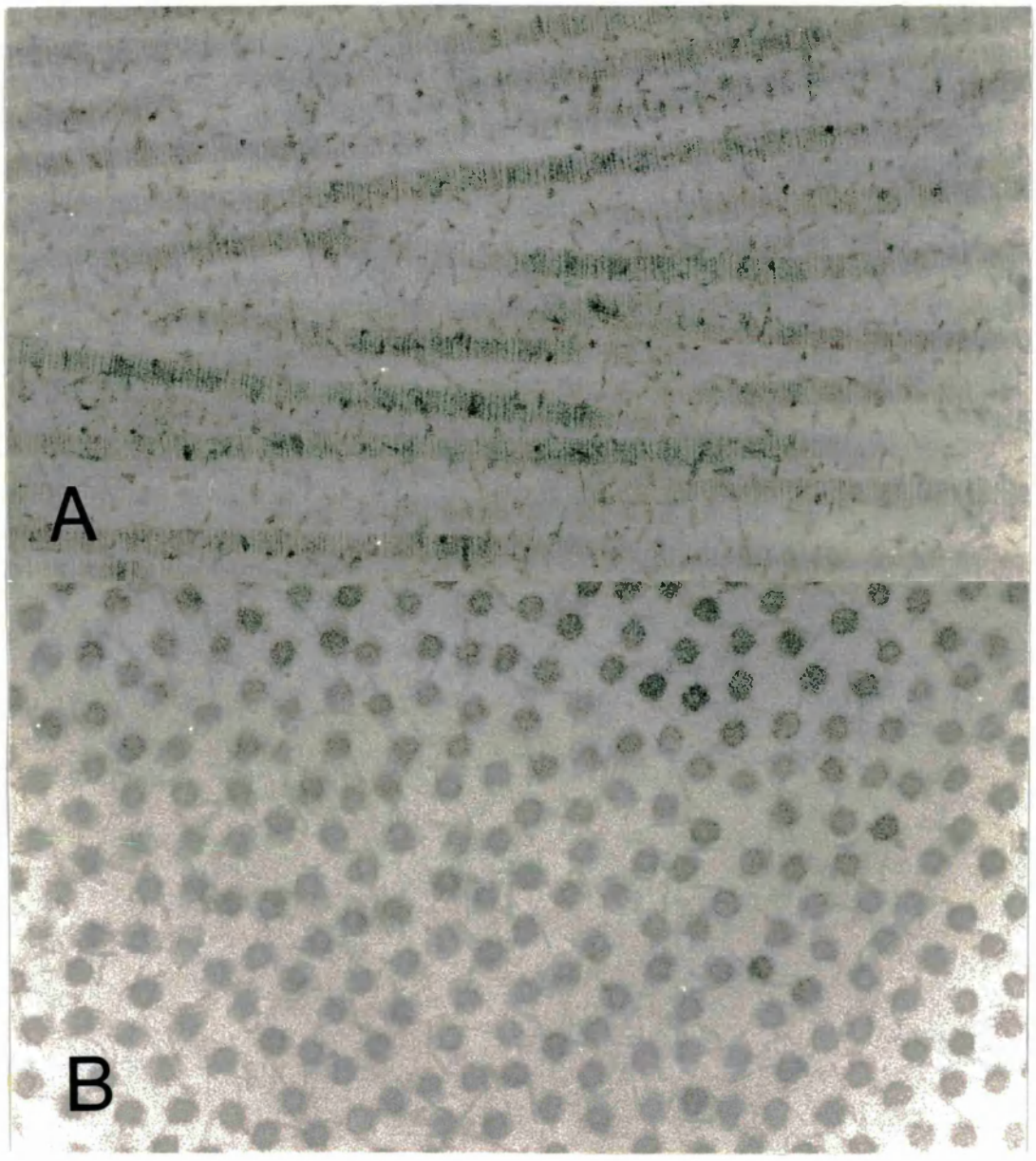

Figure 3.2 A TEM micrograph of (A) normal corneal stroma. The collagen fibrils are arranged parallel to one another with small proteoglycans filaments which are situated between the collagen fibrils. (B) Collagen fibrils in cross-section of normal rabbit cornea show the regular interfibrillar spacing. Stained with cuprolinic blue and counterstained with 2% uranyl acetate. Magnification A and B 115K

(figure 3.2). The rest of the filaments appear to be randomly organised. The proteoglycans are up to about 65 nm long with no observable larger filaments. These filaments represent proteoglycans whose glycosaminoglycan side chains have been precipitated by the cationic dye, probably onto the protein core. The filaments, although representing the distribution and size of the proteoglycans, give no information about proteoglycan morphology in vivo.

3.3 Superficial Lamellar Keratectomy

Following superficial lamellar keratectomy, re-epithelialisation of the wound surface was complete by the fourth day post wounding.

3.3.1 One week post wounding

TEM examination of 1-week-old tissue showed an epithelium 5 to 8 cells thick. Examination of the stroma beneath the resurfaced epithelium showed that there was a high density of stromal keratocytes in this region although only visual observations were made and no quantification was carried out (figure 3.3). These keratocytes were not normal in cross sectional contour and contained dense endoplasmic reticulum, indicating active protein synthesis. Surrounding the keratocytes were spaces in the extracellular matrix where no collagen occurred. These spaces are referred to as lacunae. The lacunae were largest and most numerous around the anterior keratocytes and appeared to be reduced both in size and number further from the epithelium. Near the epithelium, lacunae were up to 2400nm across (figure 3.3). Abnormal proteoglycan filaments were associated closely with the lacunae around the keratocytes (figure 3.4). These proteoglycan filaments were much larger than filaments present in the normal stroma, with sizes up to 180 X 20nm, and were heavily stained (figure 3.4). The abnormal filaments had no ordered pattern of distribution and they were not associated closely with collagen fibrils. At this stage of the healing response, little or no collagen synthesis could be detected.

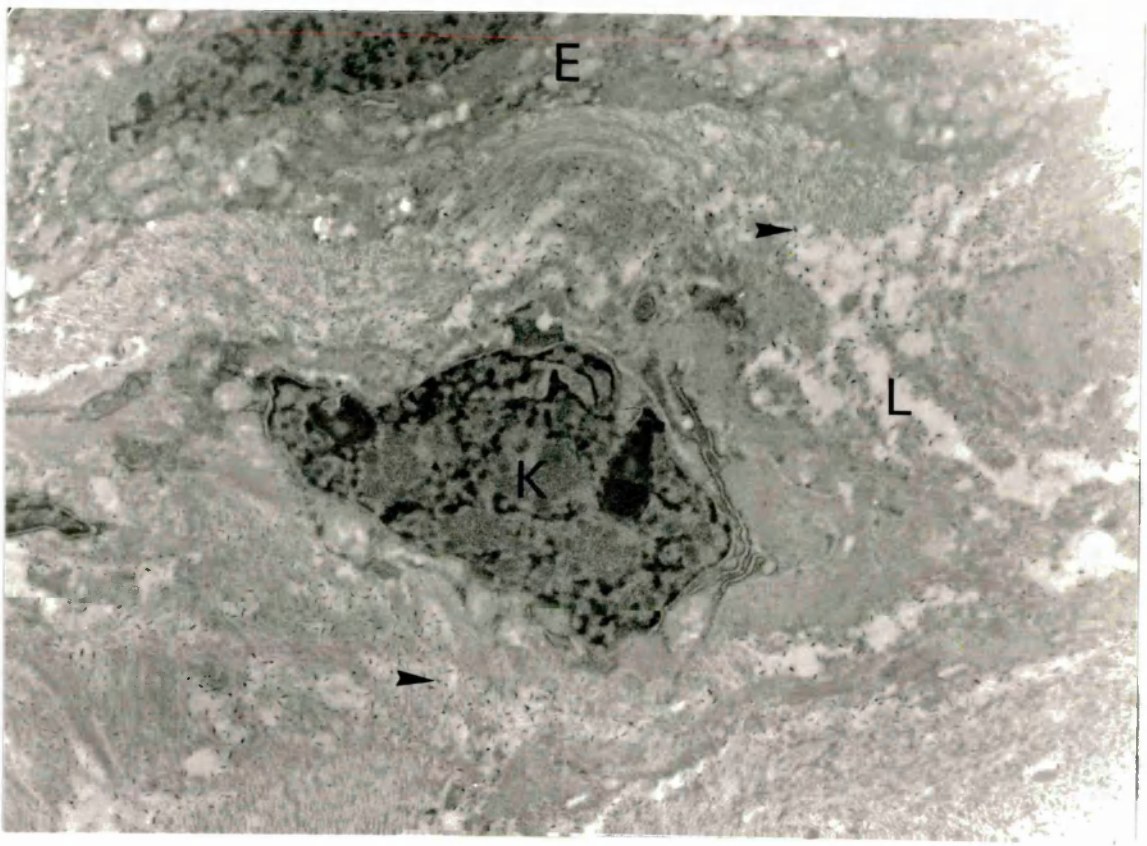

Figure 3.3 TEM micrograph of one-week S.L.K. scar tissue. Under the epithelium (E), can be seen keratocytes (K), lacunae (L), and abnormal proteoglycan filaments (➤). Stained with cuprolinic blue and counterstained with uranyl acetate. Magnification 8.3K

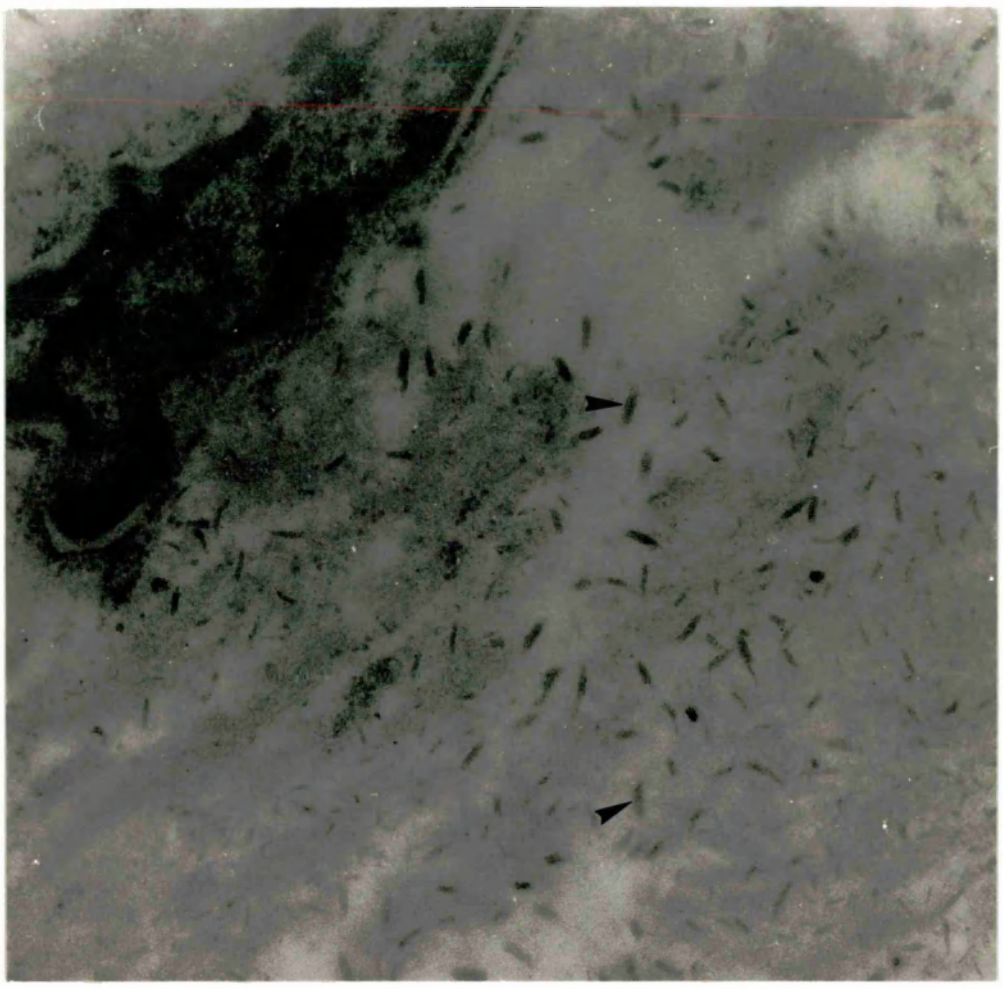

Figure 3.4 TEM of proteoglycans (➤) located within lacunae in one-week scar tissue. Stained with cuprolinic blue and counterstained with uranyl acetate. Magnification 47K

3.3.2 Two weeks post wounding

By two weeks of scar development, secretion of collagen fibrils had occurred. Much of this collagen was in bundles which had a wave-like pattern, and which ran essentially parallel with the surface epithelium (figure 3.5). The section through a keratocyte shown in figure 3.7 shows bundles of collagen fibrils in both longitudinal and cross-section in close association with the keratocyte. This image could therefore be interpreted as showing that collagen was being secreted in bundles, comprising different numbers of collagen fibrils. Normal-sized proteoglycan filaments were secreted into the extracellular matrix apparently already associated with the collagen fibrils. However, the most striking feature of the scar tissue at this age was the abundance of abnormal sized proteoglycan filaments, and the proliferation of lacunae within the tissue compared with controls. The proteoglycan filaments appeared to consist of two varieties (figure 3.6). The first were up to 140 X 15nm and occurred mostly within the collagen bundles, and were randomly orientated. The second type were larger and were mostly located around the perimeters of the lacunae. The sizes of this second type were diverse, being up to 600 X 35nm. The lacunae were very large, some being of the order of microns in length.

3.3.3 Four and Six weeks post wounding

At four to six weeks, the frequency and size of the abnormal proteoglycan filaments were observed to be reduced, as were the number of lacunae. At six weeks, the number of lacunae was strikingly reduced, though many were still present (figure 3.8). Abnormal proteoglycan filaments were still

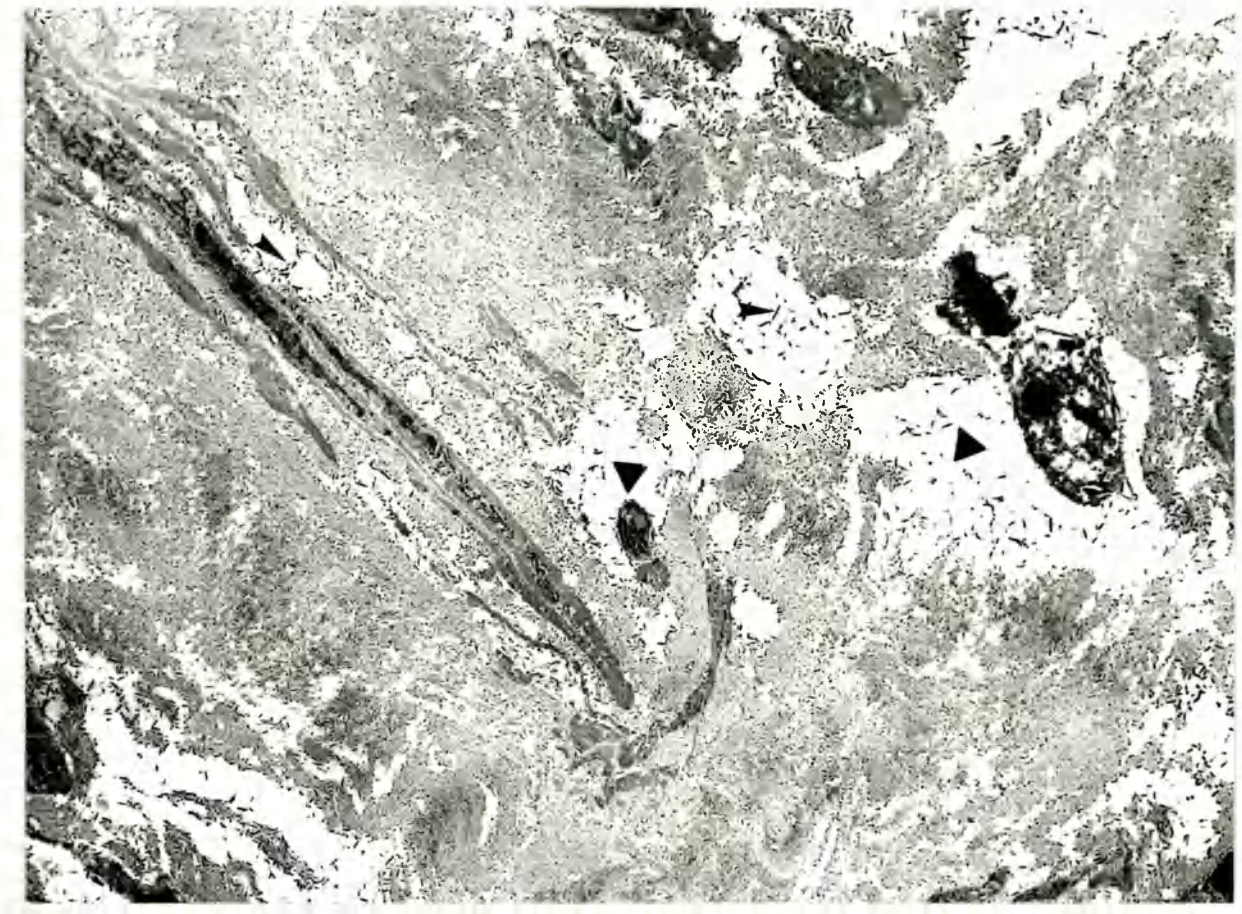

Figure 3.5 TEM of 2-week S.L.K. scar tissue. Areas free of collagen are evident (▶) and many large proteoglycan filaments (►) occur predominantly in and around the collagen-free areas. Stained with cuprolinic blue and counterstained with uranyl acetate. Magnification 6.3K

Figure 3.6 TEM of 2-week old S.L.K. scar tissue. At higher magnification some normal sized proteoglycans are seen (⟶) together with abnormal filaments. These appear to be of two types , one between the collagen fibrils (➤) and the second within the collagen-free spaces (⟶). Stained with cuprolinic blue and counterstained with uranyl acetate. Magnification 60K

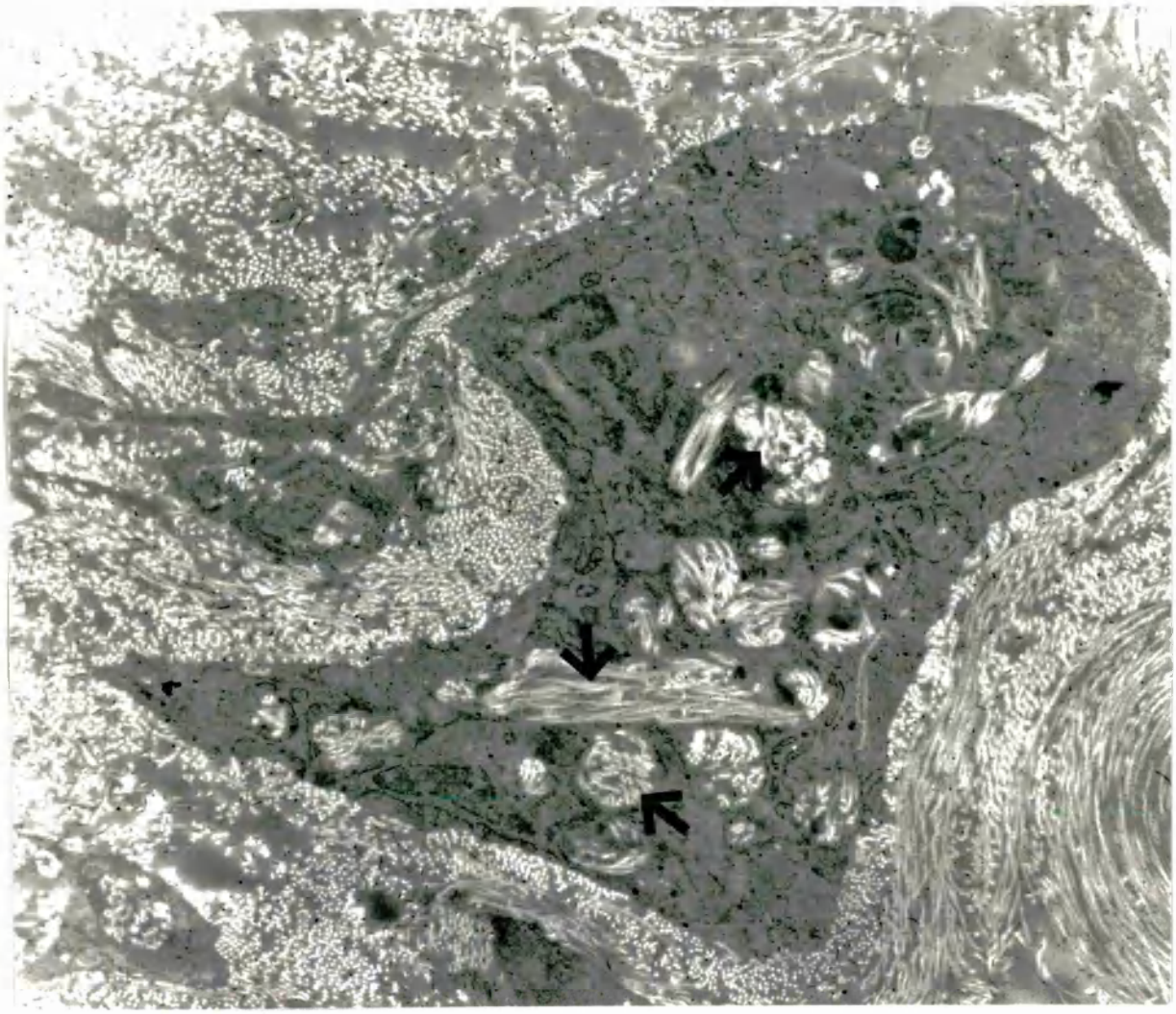

Figure 3.7 TEM micrograph of 2-week-old S.L.K tissue. A fibroblast secreting bundles of collagen fibrils (→) associated with proteoglycan filaments. Stained with cuprolinic blue and counterstained with uranyl acetate. Magnification 35K

associated with these lacunae; these filaments were up to 160nm X 15nm. Abnormal proteoglycans were also distributed throughout the extracellular matrix. The cell density appeared to decrease as the scar development progressed, possibly due partly to the increased volume of the scar tissue.

3.3.4 Two and Three months post wounding

At two months and three months, most of the extracellular spaces were occupied by collagen fibrils, there were very few lacunae, and many of the collagen bundles had come together to form a more uniform structure. Figure 3.9 shows scar tissue after three months of healing. Abnormal proteoglycan filaments were still present in the now more complete collagen matrix. The interfibrillar spacing was irregular and there were still a number of gaps in the matrix which were not seen in the control samples.

3.3.5 Six and Nine months post wounding

In the latter stages of healing, a normal proteoglycan staining pattern was seen, and this was accompanied by a higher level of ordering of the collagen fibrils. However, even after extended healing, the normal and scarred regions were still clearly distinguishable by the reduction in the fibrillar organisation in the scarred compared to the unscarred areas (figure 3.10). A few lacunae containing clusters of proteoglycans filaments persisted in the scarred tissue.

Figure 3.8 TEM of 6-week old S.L.K. scar tissue. The number of collagen-free spaces (▶) appears to have greatly reduced although abnormal proteoglycans (►) are still evident. The epithelium (**E**) is seen at the top of the micrograph. Stained with cuprolinic blue and counterstained with uranyl acetate. Magnification 10K.

Figure 3.9 TEM of three month old S.L.K tissue. The collagen bundles have come together but gaps remain in the tissue (➧). Stained with cuprolinic blue and counterstained with uranyl acetate. Magnification 10K

Figure 3.10 TEM of 6-month old S.L.K. scar tissue. A considerable amount of tissue restructuring has occurred. However, the distinction between normal stroma (**N**) and scar tissue (**S**) above it is still evident. Stained with cuprolinic blue and counterstained with uranyl acetate. Magnification 10K.

3.4 Electron Microscopy of Excimer Laser Ablated Corneal Stroma

3.4.1 Examination Prior to Sacrifice

Prior to sacrifice, broad beam slit-lamp photography was performed by Mr. R Zabel at the University of Minneapolis. This demonstrated that a corneal haze had developed in all the ablated corneas, but this haze was not graded. The haze was observed to have increased from week 1 (figure 3.11) to week 4 (figure 3.12) and was most intense between week 4 and week 8 and showed no improvement after week 16 (figure 3.13). In steroid treated corneas the corneal haze was less intense compared to that of the untreated corneas of the equivalent age (figure 3.14). [Figures 3.11-3.14 courtesy of Mr R. Zabel.]

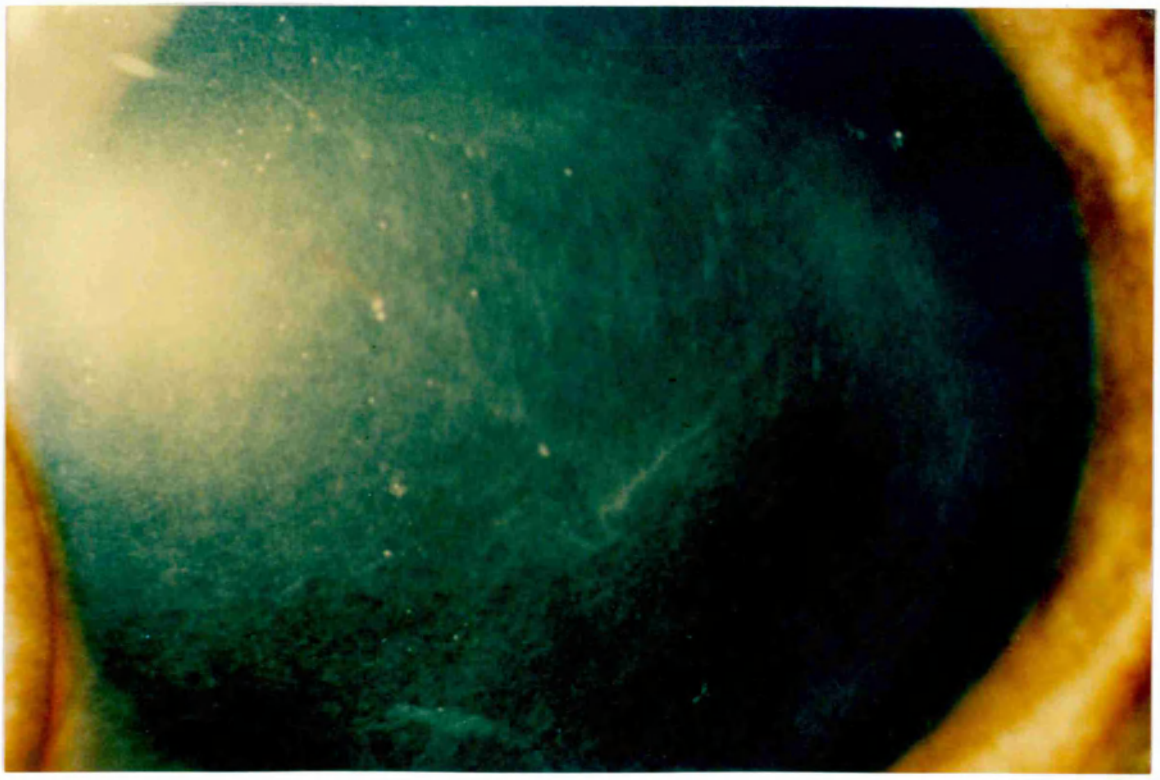

Figure 3.11 Photography of the corneal haze at 1 week.

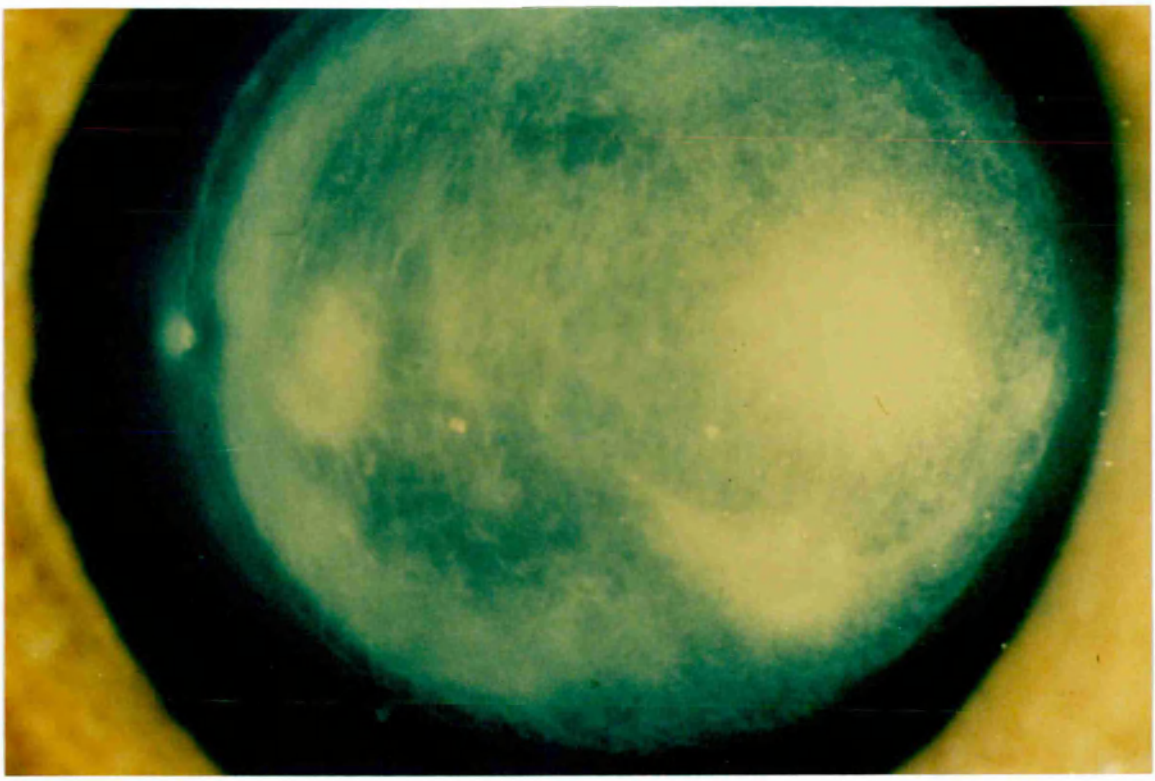

Figure 3.12 Photography of the corneal haze at 4 weeks.

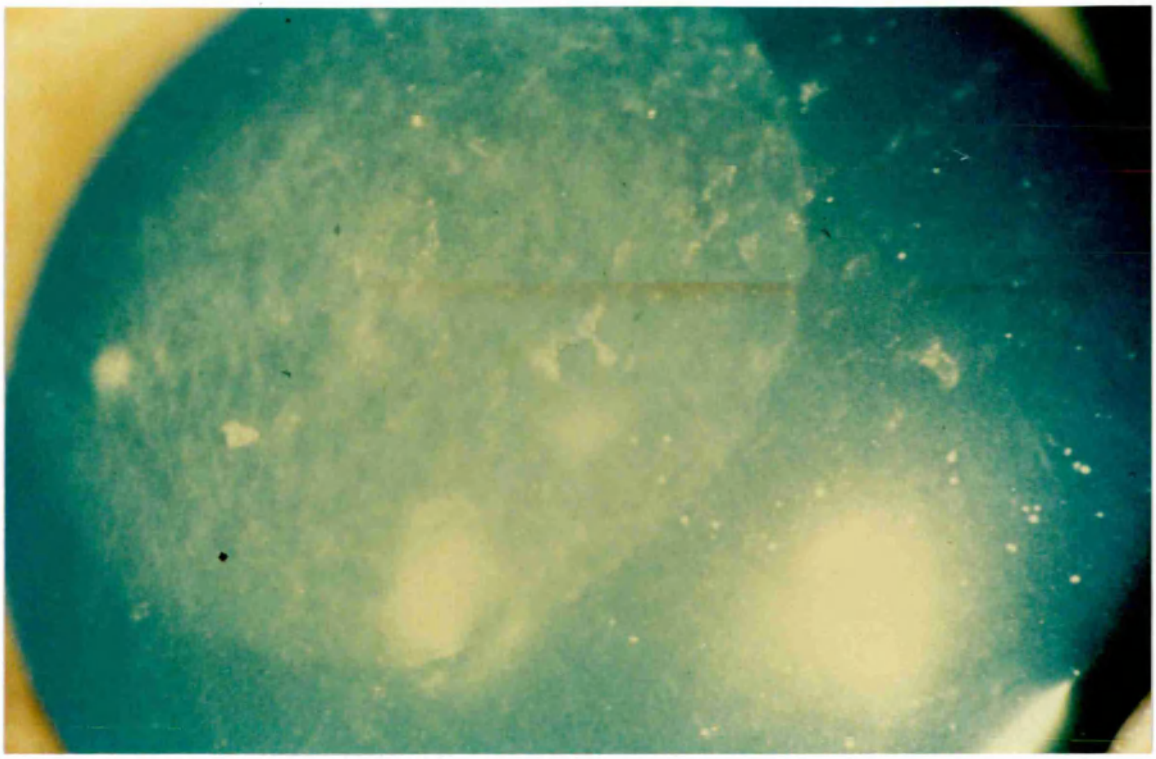

Figure 3.13 Photography of corneal haze at 16 weeks. (The white specks have resulted from the transfer of slide photograph to print).

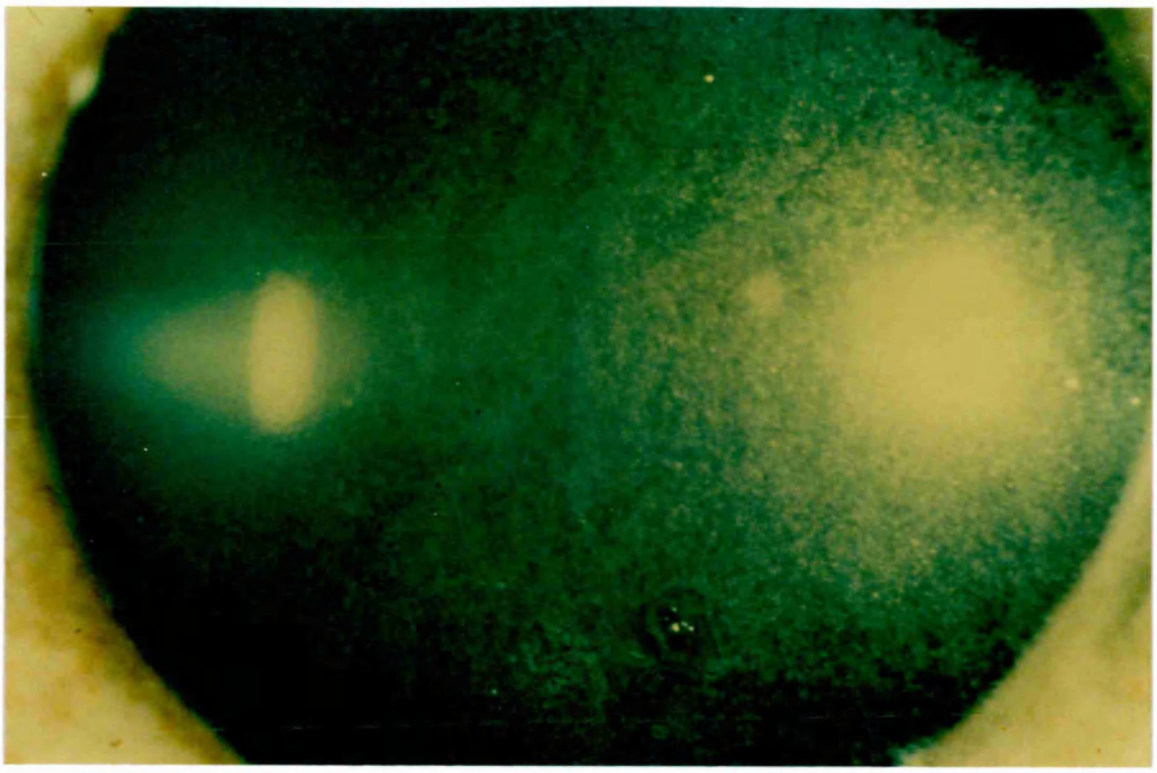

Figure 3.14 Photography of the corneal haze at 15 weeks with steroid treatment

3.4.2 One Week Post Laser Ablation

Comparison of the tissue one week after laser ablation with the control tissue showed an increased population of keratocytes situated immediately below the epithelium in the scar tissue. Primarily near and around these keratocytes were lacunae up to 2000nm x 500nm (figure 3.15). Much smaller lacunae were seen away from the edges of the keratocytes. Cuprolinic blue-staining filaments were of abnormal size and were located mainly around the edges of the lacunae but were also present in the ECM away from the keratocytes. Keratocytes further below the epithelium had smaller lacunae around them and fewer numbers of large proteoglycans. The general structure of the stromal tissue indicated that very little new collagen synthesis appeared to have taken place since the surrounding matrix appeared to look normal At a higher magnification the abnormally large proteoglycan filaments and the spaces in the ECM could be clearly seen (figure 3.16). Some of the proteoglycan filaments were up to 225nm in length.

3.4.3 Two Weeks Post Laser Ablation

At 2 weeks of healing larger lacunae were in abundance and this indicated, because of the presence of many hydrophilic proteoglycans, that the tissue was very hydrated (figure 3.17). Furthermore, many of these lacunae contained patchy background staining. The sizes of the lacunae had increased up to 5700nm in length and 2100nm in width. At this stage (week 2) a greater quantity of newly synthesized collagen fibrils occurred compared with 1 week of healing, where little newly synthesized collagen

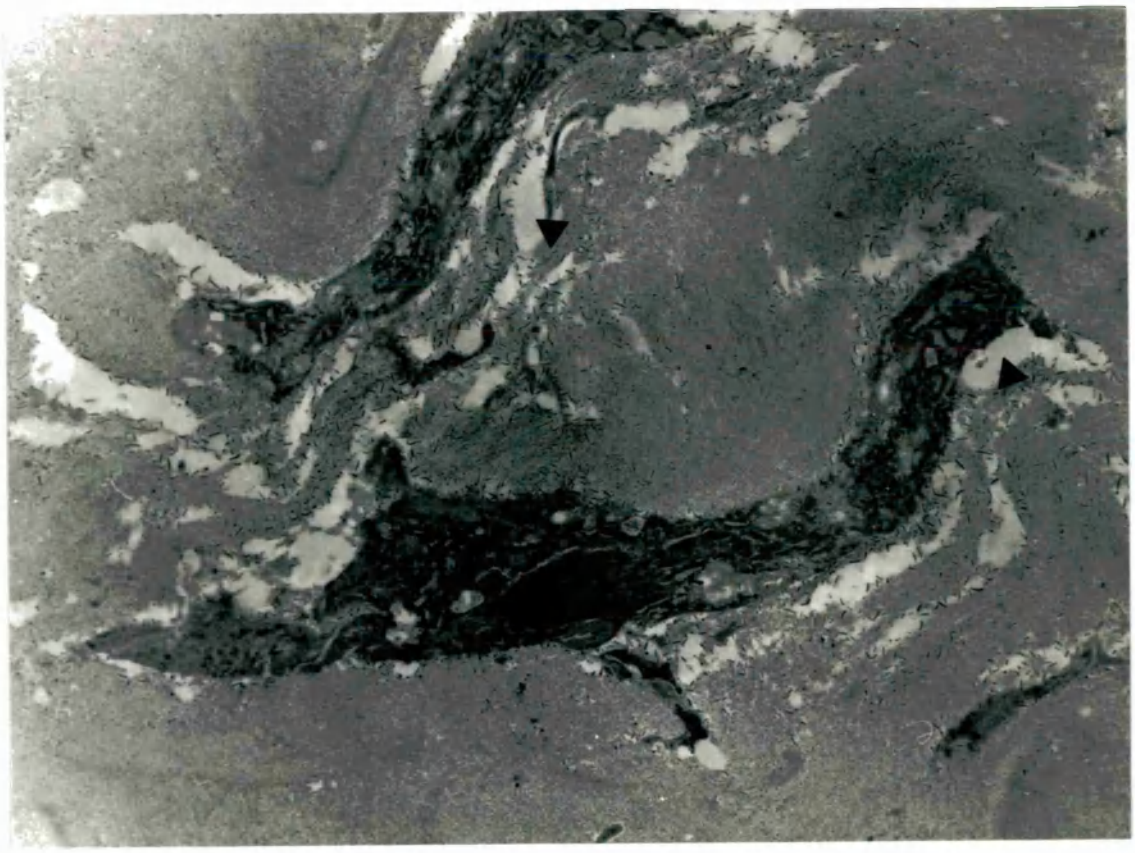

Figure 3.15 A TEM micrograph of one-week-old laser keratectomy tissue immediately below the epithelium. The stromal keratocytes (**K**) have areas free of extracellular matrix closely associated with them (▶). Stained with cuprolinic blue and counterstained with 2% uranyl acetate. Magnification 7.5K

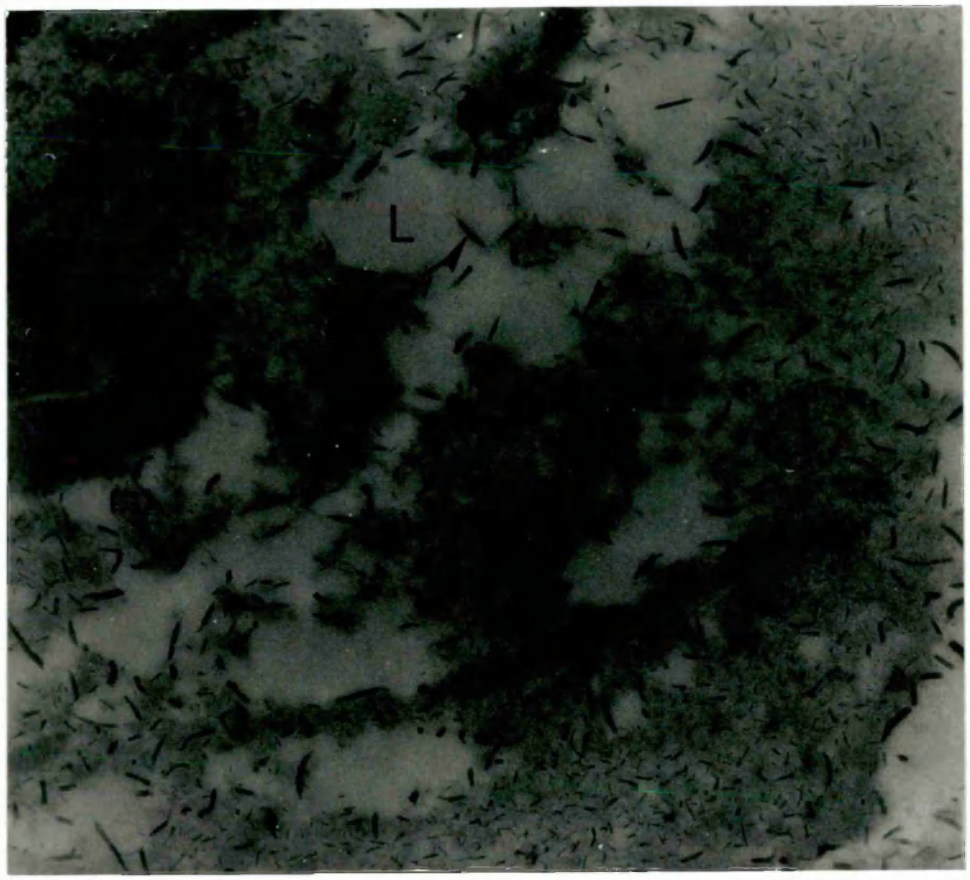

Figure 3.16 A TEM micrograph of one-week-old laser tissue. Associated with the areas free of extracellular matrix (**L**) are abnormally sized proteoglycan filaments (►). Stained with cuprolinic blue and counterstained with 2% uranyl acetate. Magnification 40K.

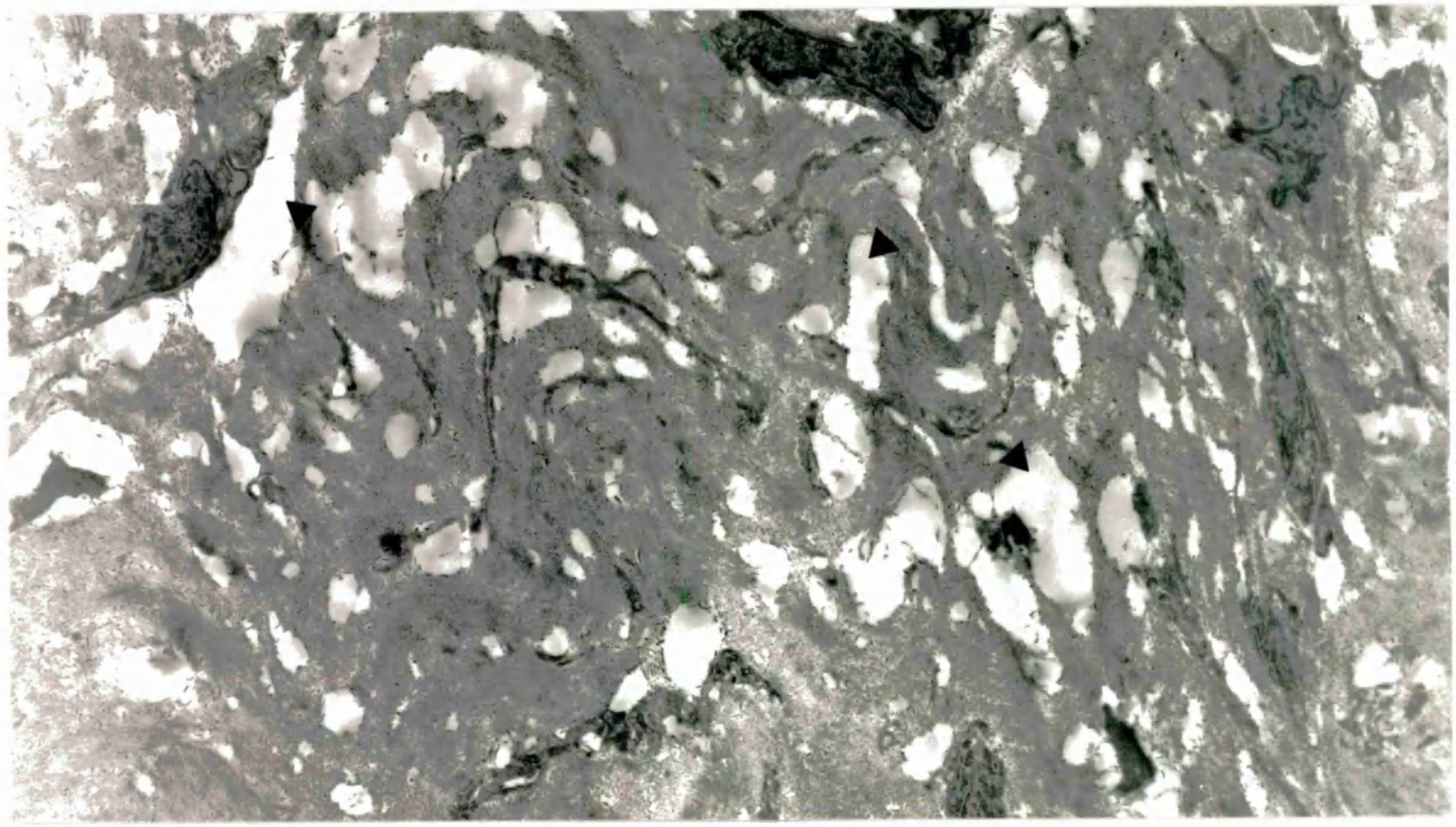

Figure 3.17 A TEM micrograph of two-week-old laser keratectomy tissue. The areas free of extracellular matrix are larger, more numerous and widespread (▶). Stained with cuprolinic blue and counterstained with 2% uranyl acetate. Magnification 6.3K.

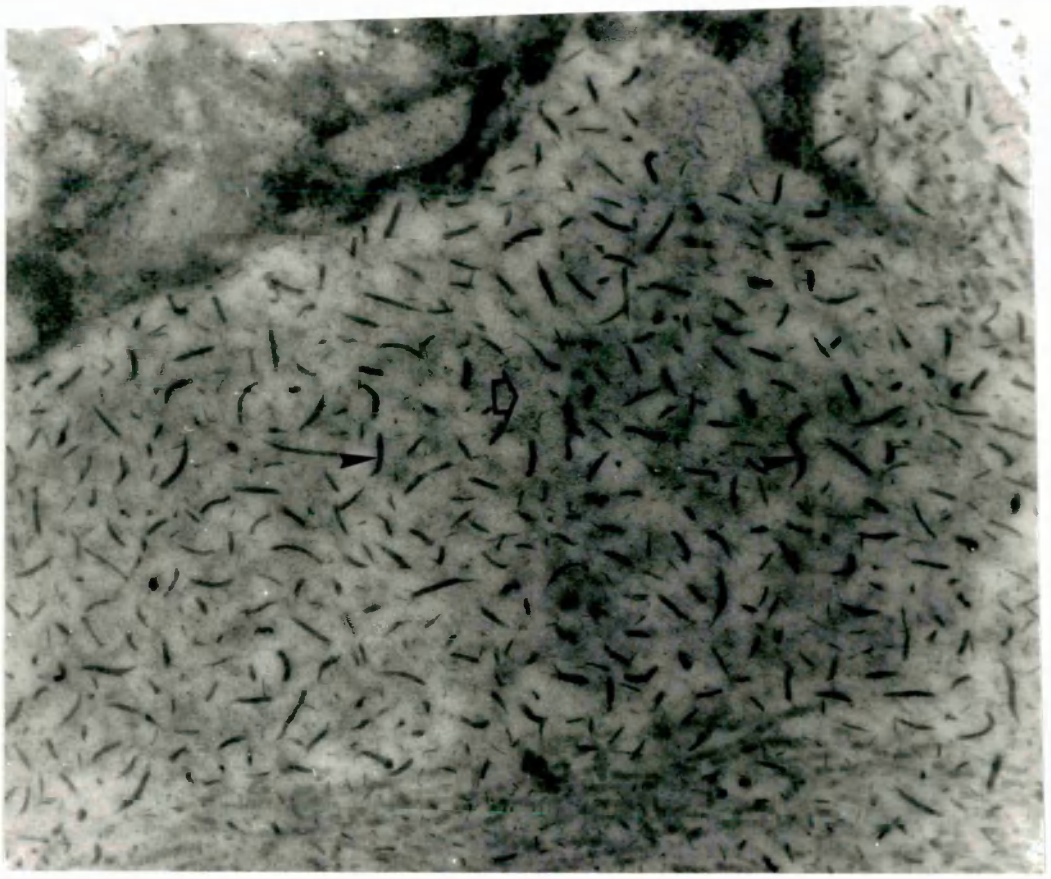

Figure 3.18 A TEM micrograph of two-week-old laser keratectomy tissue. The abnormal proteoglycans have increased in number (➤) and an amorphous material can be seen (⇨). Stained with cuprolinic blue and counterstained with 2% uranyl acetate. Magnification 40K.

was seen. These fibrils were in bundles but there were also many individual ones. Some collagen fibrils, in cross-section, were touching neighbouring fibrils and gave the appearance of merging into one larger fibril. There was an observed dramatic increase in the numbers of abnormal sized proteoglycans throughout the scarred region and many clumps of filaments were seen. These filaments had increased in size from those seen after one week, and some of them were now 530nm in length (not shown). Many of the proteoglycans were associated with the lacunae. Abnormal filaments were also located between the collagen fibrils resulting in a wide range of interfibrillar spacings. The small proteoglycans seen associated with collagen fibrils in normal corneal tissue (figure 3.19a), were reduced in number or absent from many collagen fibrils (figure 3.19b) in 2 week old scar tissue.

3.4.4 Four Weeks Post Laser Ablation

After 4 weeks of healing the vacuolated areas in the tissue were still present (figure 3.20), along with the large abnormal proteoglycans filaments (figure 3.21). However, these areas were reduced in size and number as were the abnormal proteoglycan filaments, which were up to 220nm in length. These abnormal filaments were located with lacunae which were in turn closely associated with the keratocytes in the tissue. The variation in the interfibrillar spacing and the presence of abnormal proteoglycan filaments between the fibrils created large spaces in the matrix (figure 3.22).

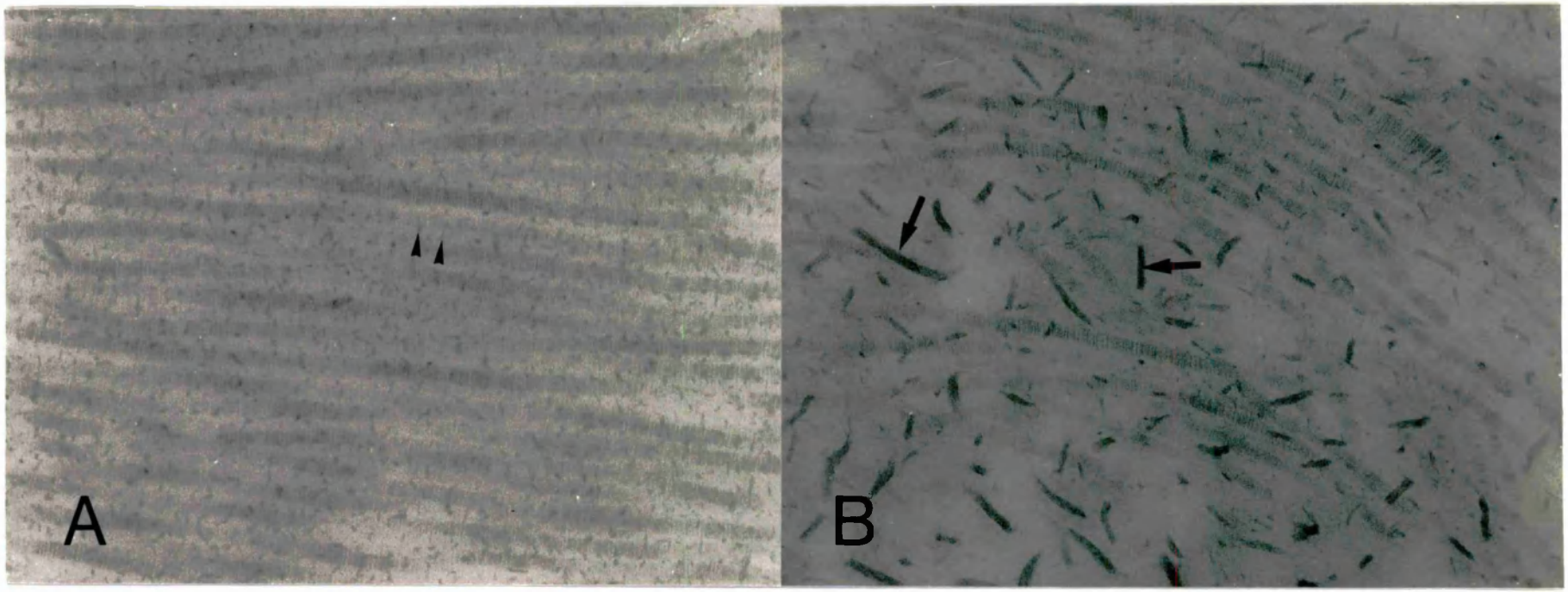

Figure 3.19 (A) In normal corneal stroma the collagen fibrils are arranged parallel to one another; small proteoglycan filaments are situated between the collagen fibrils (►). (B) In healing tissue 2 weeks after wounding many of the small proteoglycans filaments are absent, and the tissue contains proteoglycan filaments of abnormal size (⟷) between disordered collagen fibrils. Stained with cuprolinic blue and counterstained with uranyl acetate. Magnification (A) and (B) 60K.

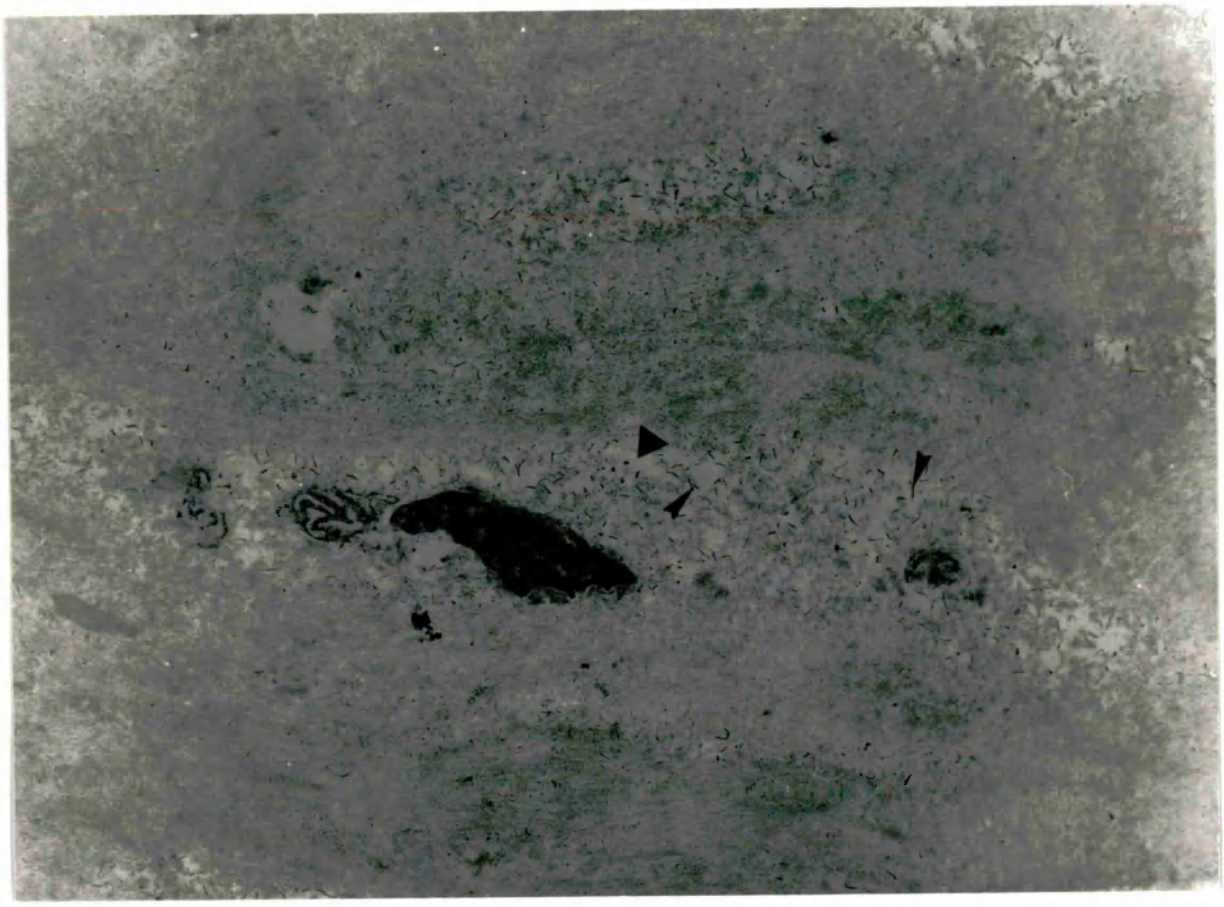

Figure 3.20 A TEM micrograph of four-week-old laser keratectomy tissue. Areas free of extracellular matrix (▶) are still present and associated with abnormal proteoglycan filaments (➤). Stained with cuprolinic blue and counterstained with 2% uranyl acetate. Magnification 7.5K.

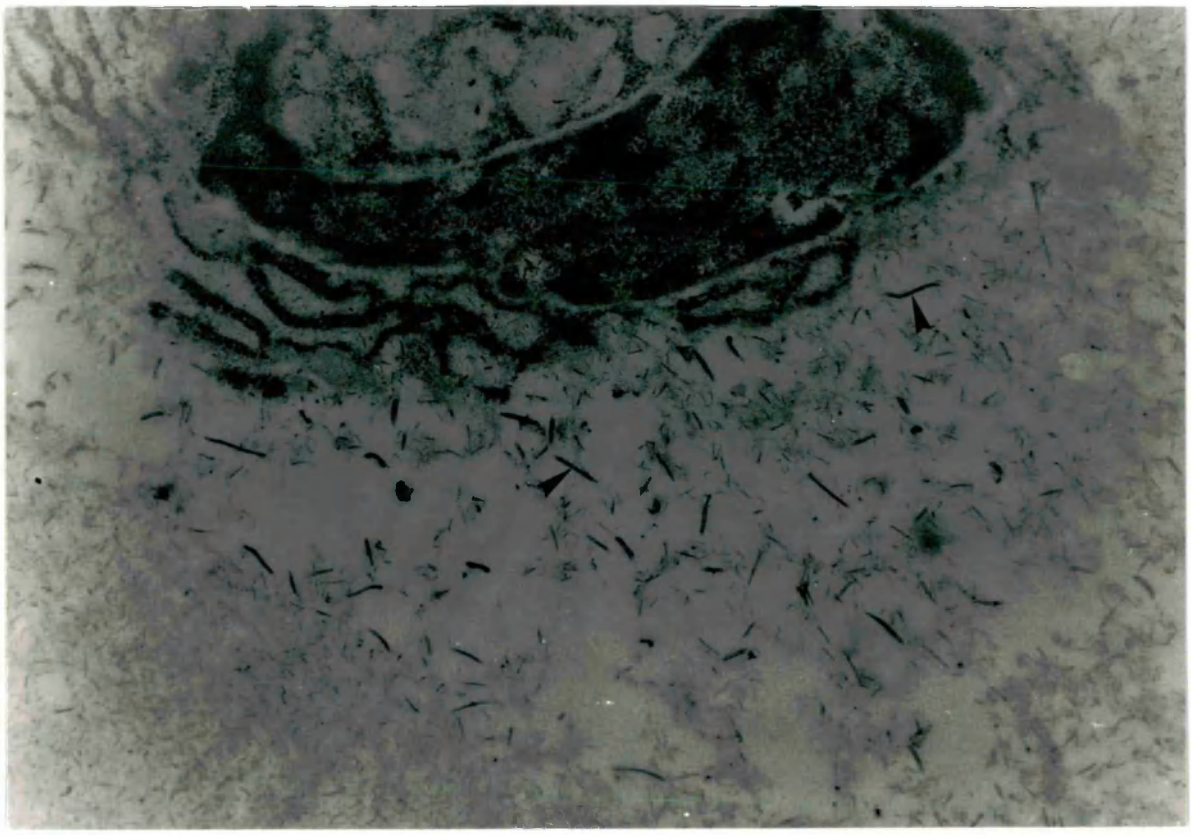

Figure 3.21 A TEM micrograph of four-week-old laser keratectomy tissue. Abnormal proteoglycans (►) are still present in the tissue but are reduced in number. Stained with cuprolinic blue and counterstained with 2% uranyl acetate. Magnification 40K.

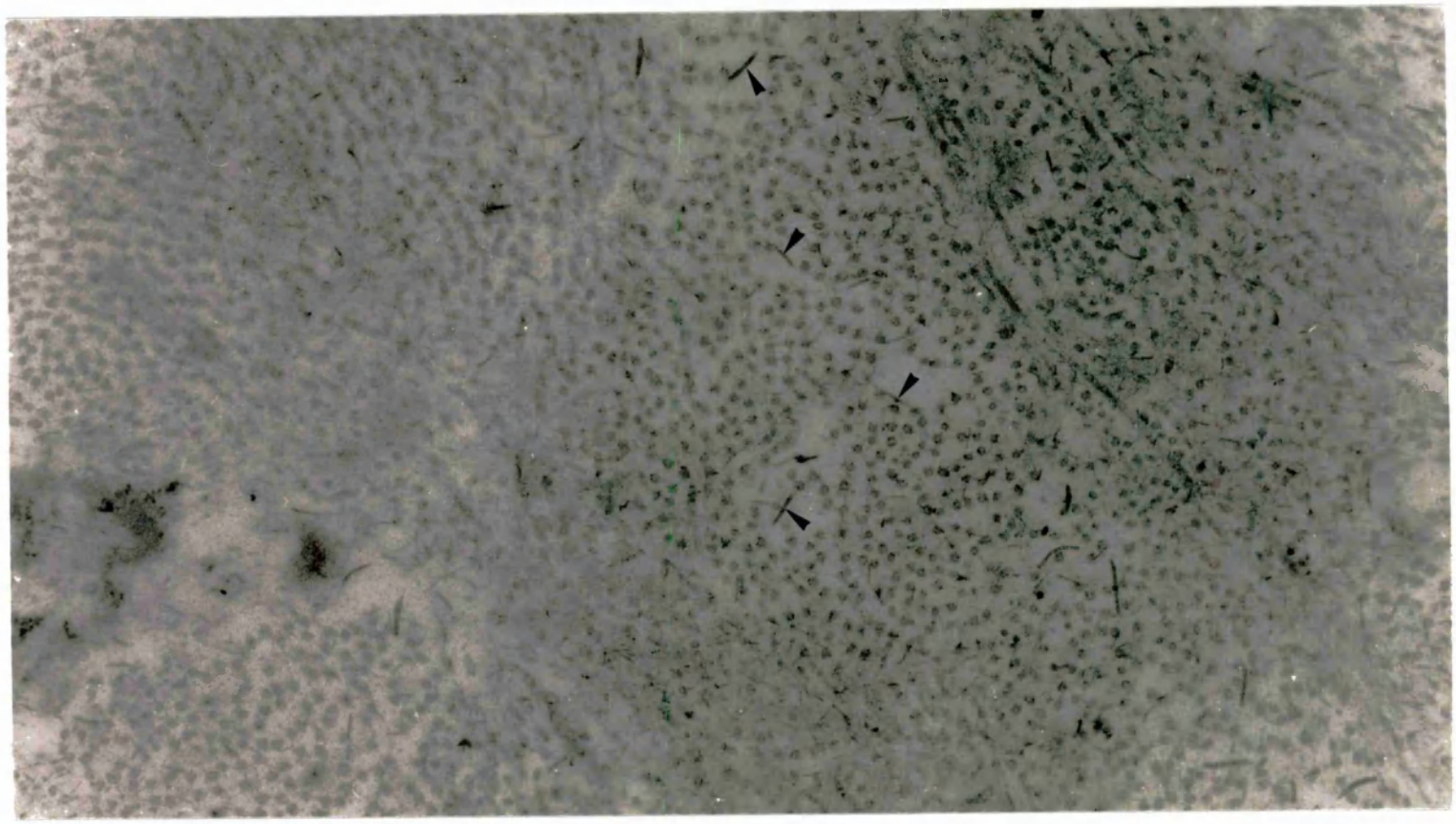

Figure 3.22 Four-week old laser keratectomy scar tissue. Collagen can be seen in cross section with large interfibrillar spaces between the collagen bundles occupied by abnormal sized proteoglycans filaments (►). Stained with cuprolinic blue and counterstained with 2% uranyl acetate. Magnification 40K.

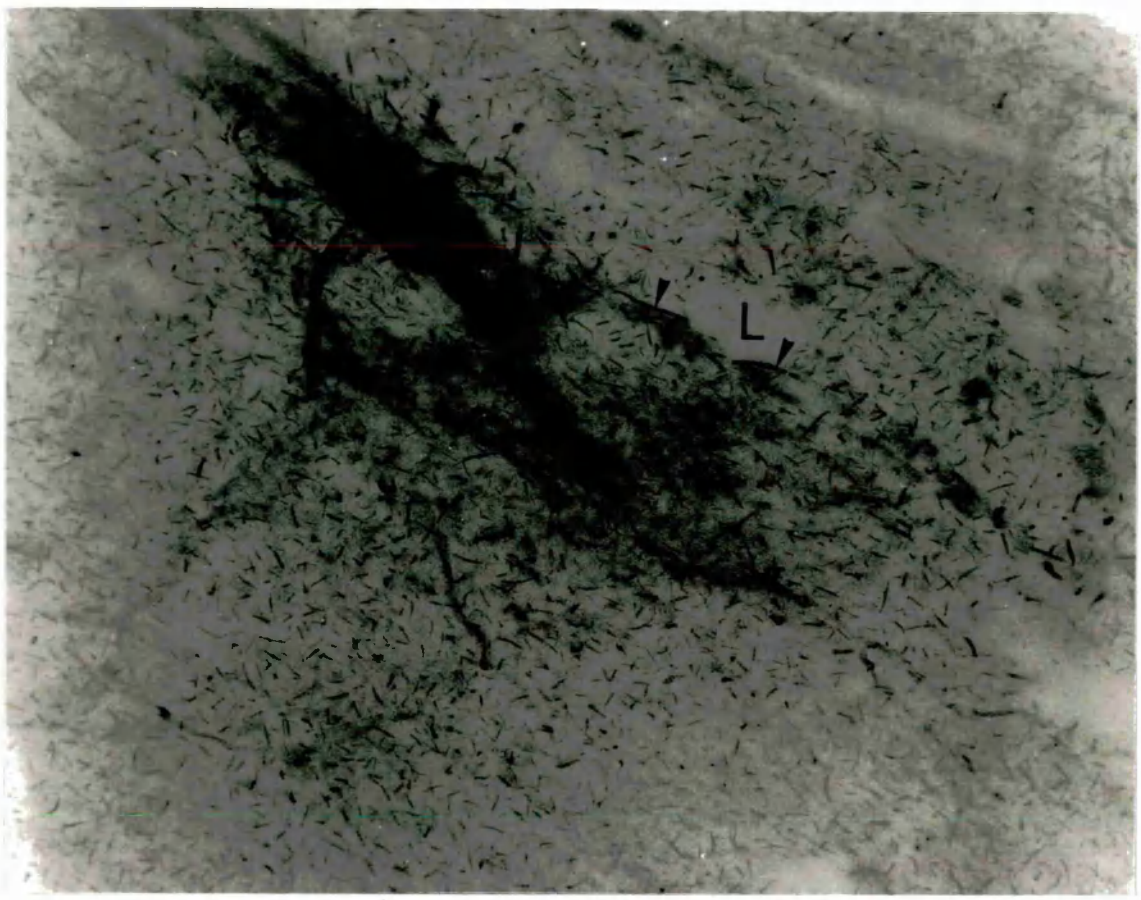

Figure 3.23 A TEM micrograph of eight-week-old laser keratectomy tissue. Abnormal proteoglycan filaments (➤) are still present along with lacunae (L) free spaces mainly located next to keratocytes. Stained with cuprolinic blue and counterstained with unranyl acetate. Magnification 40k.

3.4.5 Eight Weeks Post Laser Ablation

The abnormal proteoglycan filaments were still present in the tissue, though again they appeared fewer in number and were associated with ECM-free spaces. Both the spaces and the abnormal proteoglycan filaments were a almost entirely located adjacent to stromal keratocytes (figure 3.23). However larger than normal filaments were present individually in the regenerated stromal tissue.

3.4.6 Later Stages of Scar Formation

The pattern of decreasing numbers of abnormal proteoglycan filaments along with fewer lacunae continued through the next stages of wound healing, week 16, 38 and 45. At the later stages (35 and 45 weeks) scar tissue could still be identified from original stroma by the level of order observed in the tissue (figure 3.25B). The interfibrillar spacing appeared to have a wider range and there was no well defined lamellar structure in the scar tissue compared to normal stroma (figure 3.25A,B). There were no distinct differences between the proteoglycan staining pattern along the collagen in scar tissue and normal tissue at this time. The small proteoglycans had the same regular arrangement and location relative to the collagen fibrils. However, larger filaments (figure 3.24) could still occasionally be seen within the matrix. Areas that contained groups of proteoglycan filaments that were not associated with collagen were still seen in the scar tissue even after prolonged healing (figure 3.25C.), but these were not quantified.

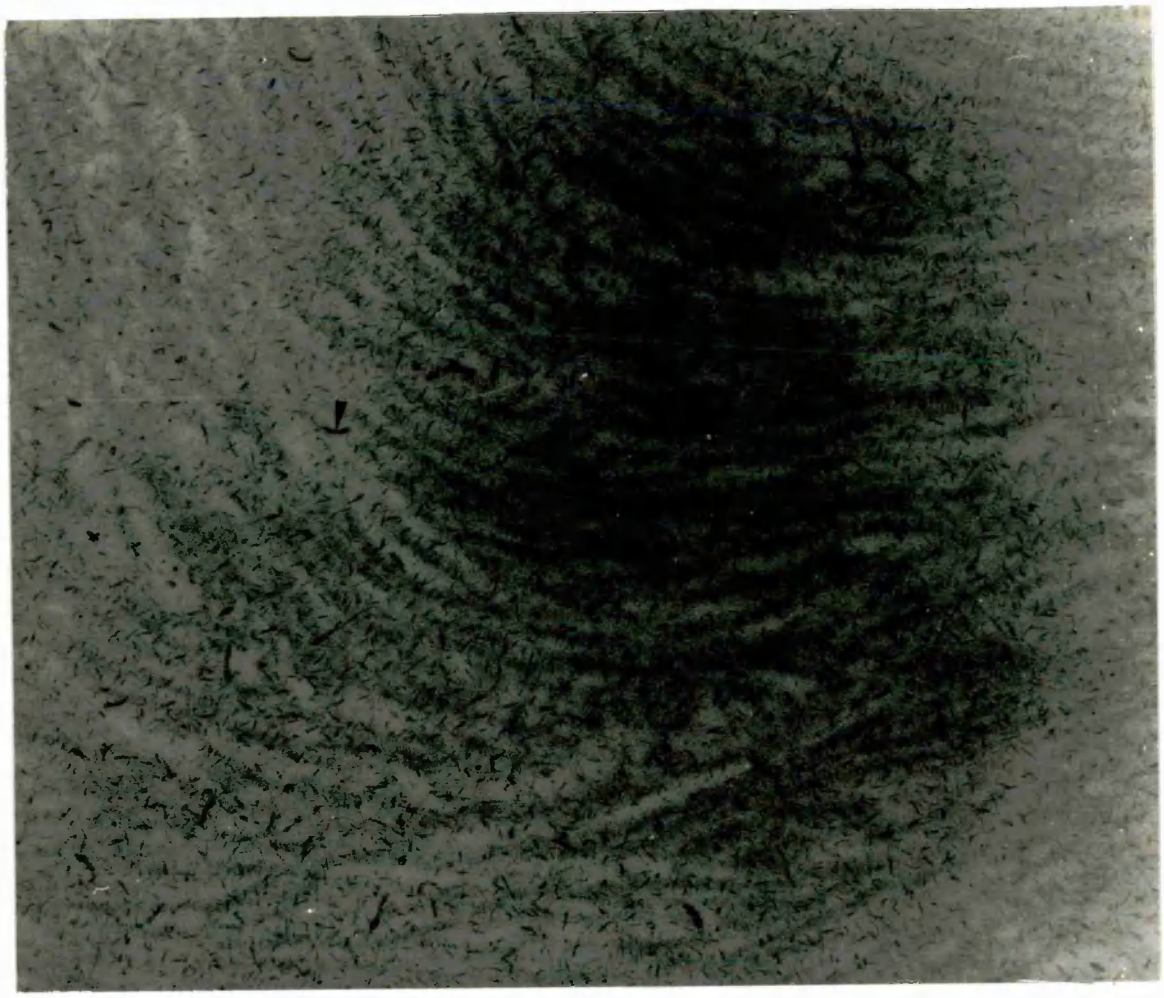

Figure 3.24 At 38 weeks of healing larger than normal proteoglycans (►) are seen in the extracellular matrix in steriod treated tissue. Stained with cuprolinic blue and counterstained with 2% uranyl acetate. Magnification 50K.

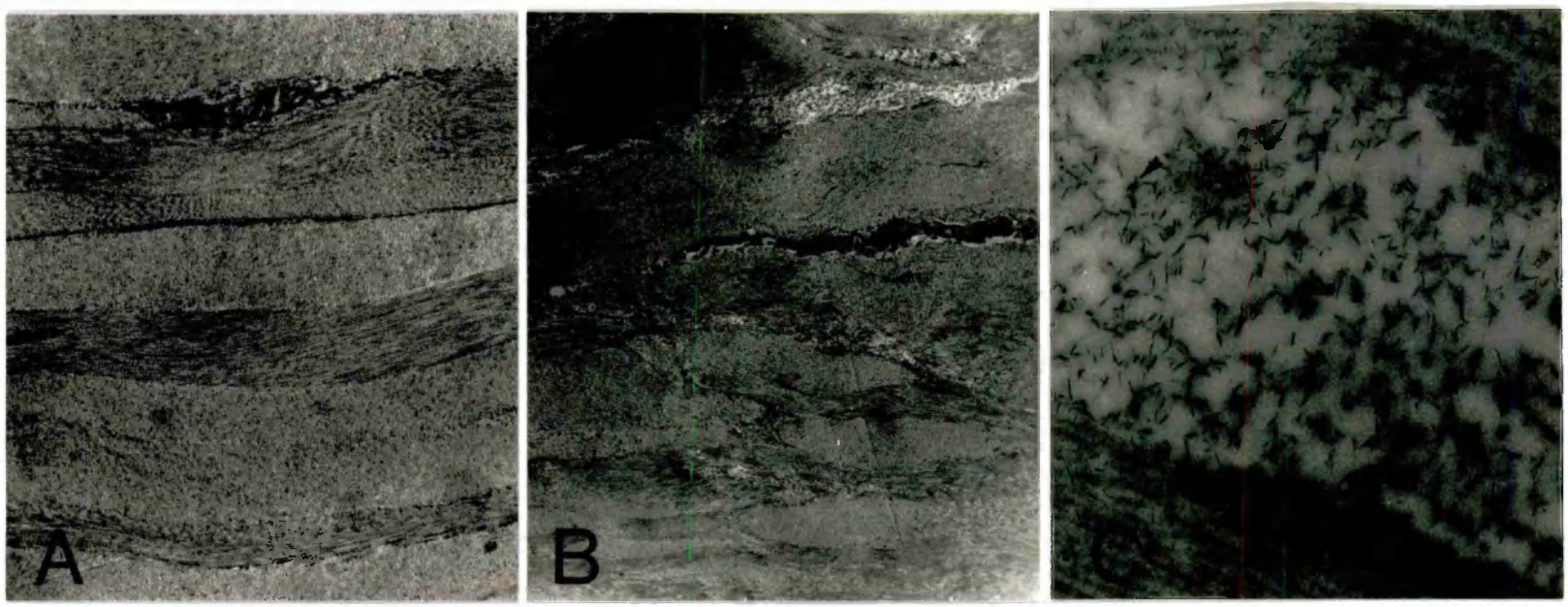

Figure 3.25 A TEM micrograph of (A) normal corneal stroma, (B) fourty-five-week-old laser keratectomy tissue the collagen fibrils are not formed into well-defined lamellae compared to normal. (C) Furthermore, in scar tissue, clumps of proteoglycans (➤) exist that are not associated with a collagen matrix. Stained with cuprolinic blue and counterstained with 2% uranyl acetate. Magnification (A,B) 5K, (C) 40K

3.4.7 Steroid-Treated Corneas

After 15 weeks of healing, steroid-treated corneas contained large proteoglycans and areas free of extracellular matrix similar to those observed after 16 weeks of healing in untreated corneas. At the later stages (35 and 45 weeks) steroid-treated corneas contained some abnormal proteoglycans both within the scar tissue matrix (figure 3.24) and also clustered in areas free of collagen.

3.5 Analysis of Electron Micrographs

3.5.1 Fibril Number per Unit Area

Electron microscopy, fibril number and statistics of the full-thickness corneal scars was carried out by Dr. Cintron and Dr Takahashi at the Schepens Eye Institute, Boston. The number of collagen fibrils were counted in 10 X 1μm^2 regions from sactions covering the whole of the scar tissue and the results were averaged (table 1). One sample of scar tissue was used except for 14 months were two different samples were used (a and b). The significance of the results was assessed by carrying out Student t-tests.

Table 1 The number of collagen fibrils per μm^2

Age of Scar	Fibril Number	+/-
3 week	161.3	46.4
6 week	168.0	31.6
7 month	211.9	40.3
14(a) month	217.2	38.0
14(b) month	316.0	77.5
21 month	230.3	49.9
Normal	326.2	69.7

The results of the t-tests showed that there was a significant difference between the number of collagen of 6 weeks and 7 months ($p < 0.05$). Also, there was a significant difference between 7 and 14(b) months $p <$

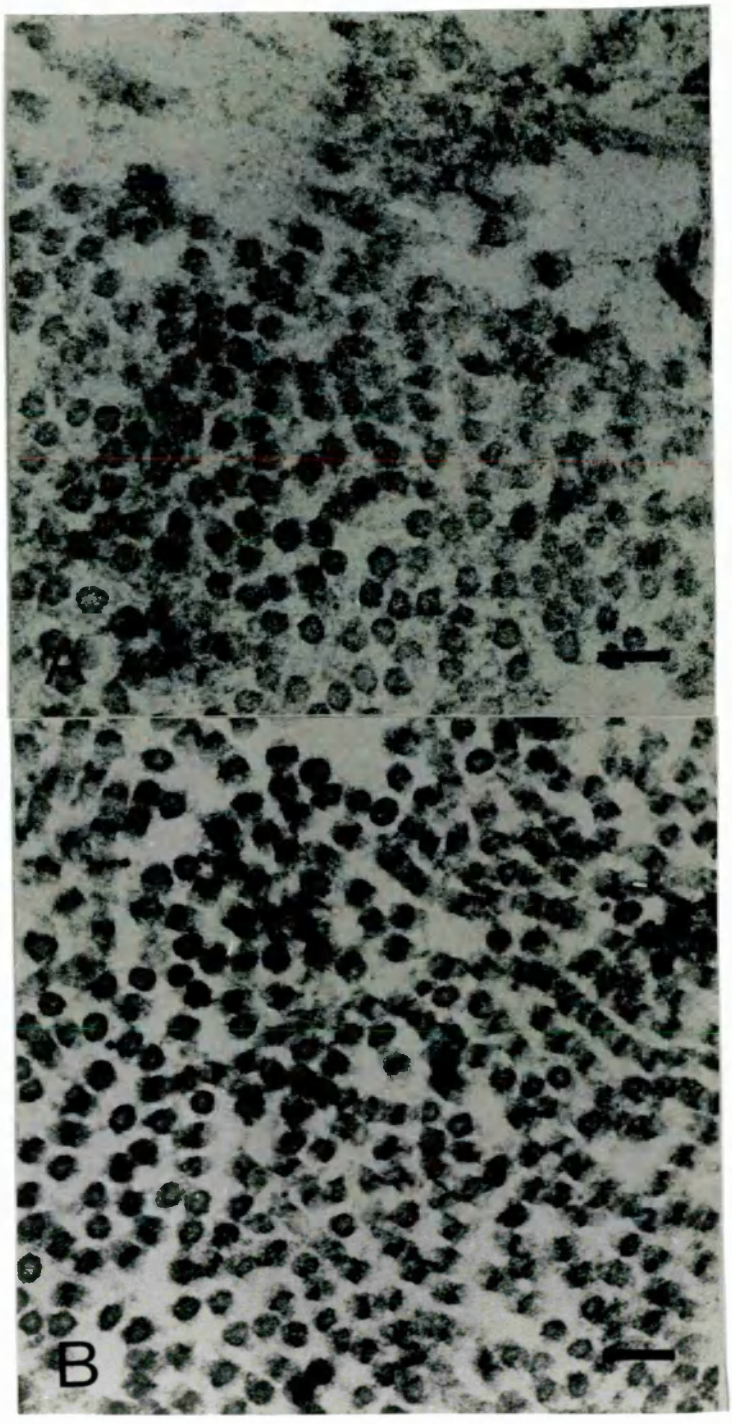

Figure 3.26 TEM of fibrils in cross-section of (A) 3 weeks and (B) 7 months full-thickness scar. Stained with tannic acid. Magnification 100,000

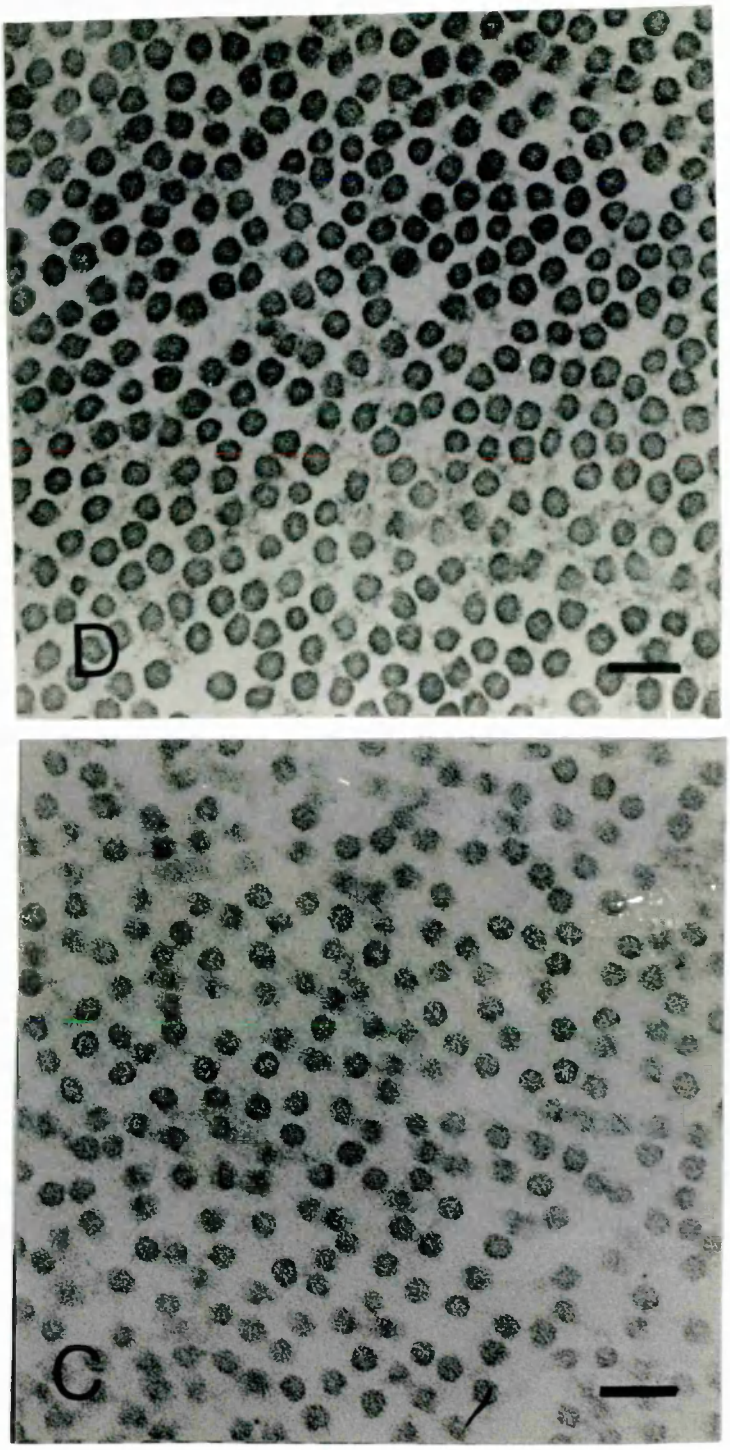

Figure 3.27 TEM of fibrils in cross-section of (C) 14 months full-thickness scar tissue and (D) normal tissue. Stained with tannic acid. Magnification 100,000

0.01 and 14(b) and 21 months $p < 0.01$. Comparison of scar tissue of 3,6 weeks and 7 and 14(a) months and the control show a significance of $p < 0.001$. The control and 14(b) month show no significant difference and the control and 21 months a significance of $p < 0.01$. Figures 3.26 and 3.27 show the change in the number of the fibrils with increasing age of the scar tissue compared to normal tissue.

3.5.2 Collagen Fibril Diameters

Several electron micrographs were produced of collagen fibrils in cross-section from 2,4,6,16 and 45 (two samples a and b) week SLK and PRK scar tissue and from collagen fibrils in normal rabbit cornea. Micrographs were taken from several regions of each tissue (scar and normal) to give a representative sample of each tissue, at least 250 fibrils were counted in each case. The fibril diameters were measured by capturing the image of the electron micrograph using a video camera. This image was then analysed using a computer program (2.2.1). No differences were observed between SLK and PRK wounds. The range of fibril diameters was calculated together with the mean diameter (table 2).

Table 2 The range and mean diameter of collagen fibrils in scar tissue.

Age of Scar	Diameter Range	Mean Diameter
2 week	22-38nm	28.5
4 week	20-32nm	26.1
6 week	8-52nm	32.7
16 week	22-36nm	28.3
45 week(a)	26-36nm	27.8
45 week(b)	14-36nm	25.6
Control	24-32nm	27.6

The results showed that in all of the scar tissues, the range in fibril diameters had increased. This increase was small in all but 6 week and 45(b) week scar tissue. The 6 week scar tissue had the largest range of fibril diameters, some of the fibrils being 52nm wide. In 45(b) the increased range of fibril diameters was due to the presence of smaller diameter fibrils (figure 3.29). All the mean diameters were close to the control mean value except that of the 6 week sample which was the only sample that had a higher mean fibril diameter. In 2 week scar tissue, fibrils up to 90nm wide were seen. However, these wider fibrils appear to comprise more than one smaller fibril, several small fibrils apparently having merged to form one larger one (figure 3.28).

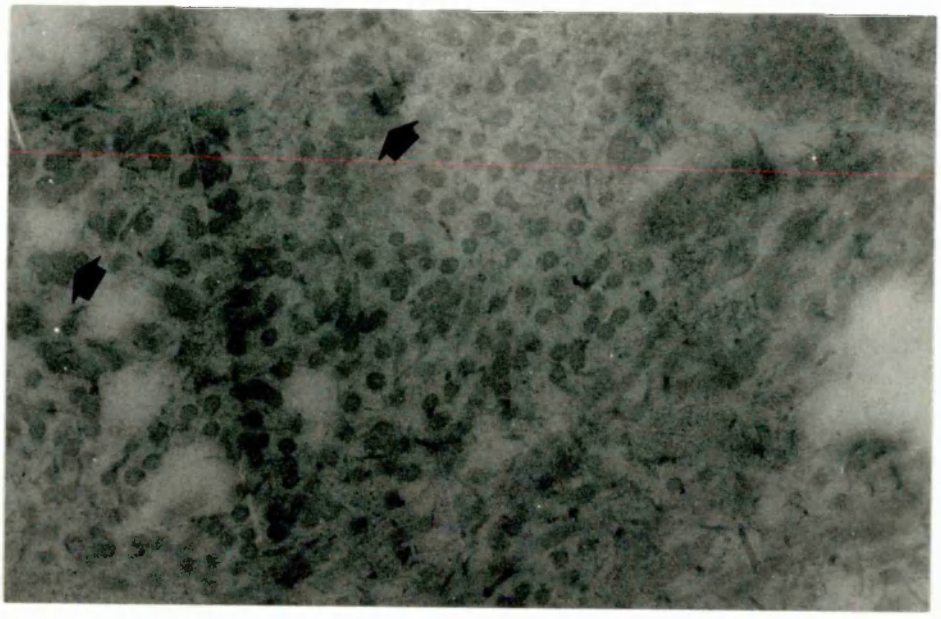

Figure 3.28 TEM of 2 week scar tissue showing the presence of merging collagen fibrils (➧). Stained with cuprolinic blue and counterstained with uranyl acetate. Magnification 77K

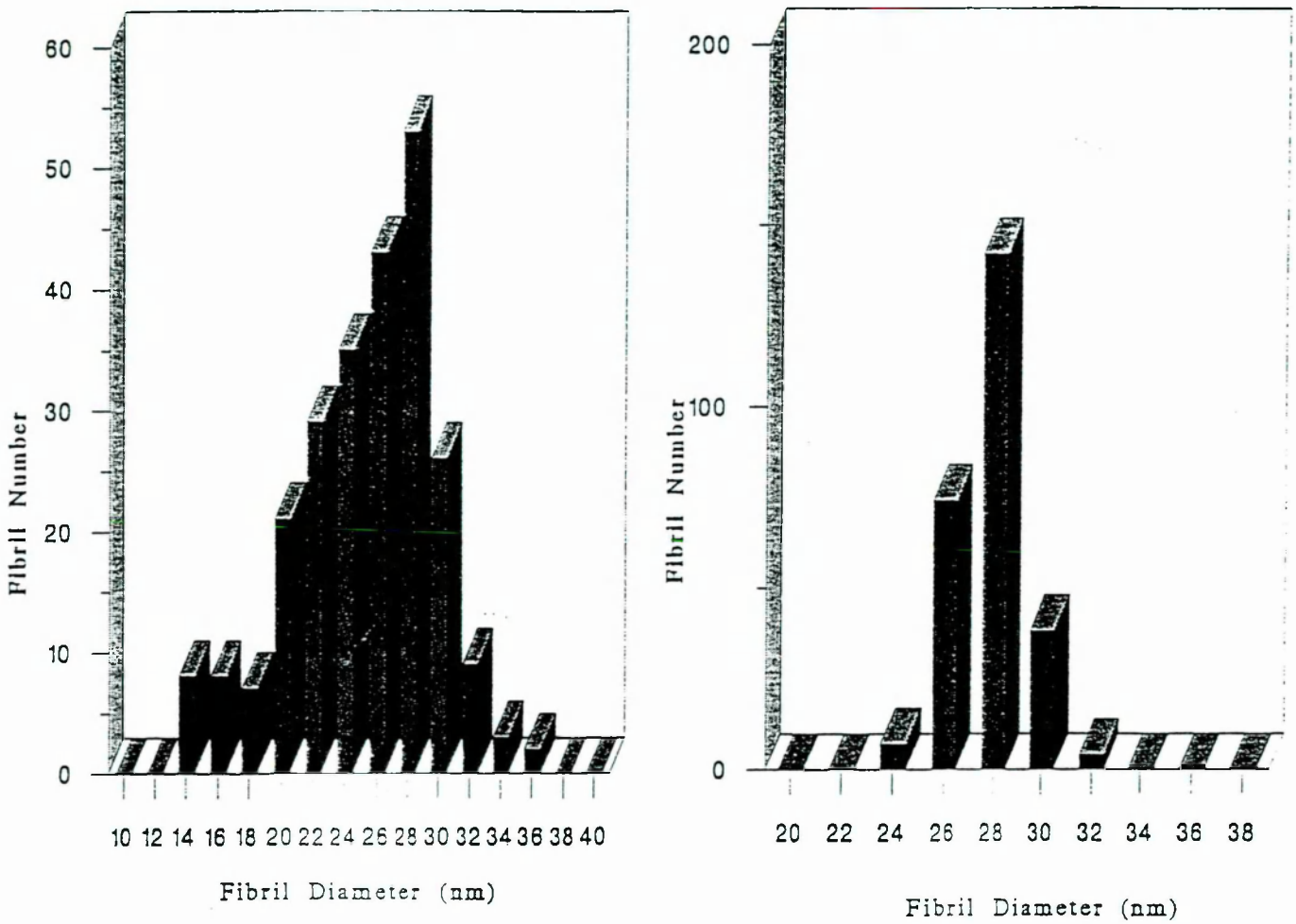

(A) Scar

(B) Control

Figure 3.29 Distribution of collagen fibril diameters in 45(b) weeks scar tissue and normal corneal tissue.

3.5.3 Radial Distribution Functions

The radial distribution function (RDF) is obtained from the measured fibril positions and displays the relative probability of finding another fibril as one proceeds out from any fibril that is chosen as a reference (McCally and Farrell, 1988). Data are averaged using all fibrils in the field of view in turn as the reference. The distance from the centre of the reference fibril is called the sample radius. RDFs of normal collagen fibrils in rabbit cornea and collagen fibrils of 45 week-old scar tissue were calculated to show the extent of order in the tissues. Figure 3.30 shows a typical RDF of collagen fibrils in normal rabbit cornea. The RDF has two or three peaks (1,2,3) at approximately 50nm, 100nm and 150nm. The RDF has spurious detail at large values of the sample radius because of the effect of reaching the edge of the micrographs during the counting. Figure 3.31 shows the RDF of 45 week-old scar tissue. In this RDF there is only one clear peak with a reduced intensity compared to normal. The RDF of normal rabbit cornea indicates that short range order exists in the tissue. The RDF of the 45 week scar tissue indicates that, in this tissue, the short range order is reduced.

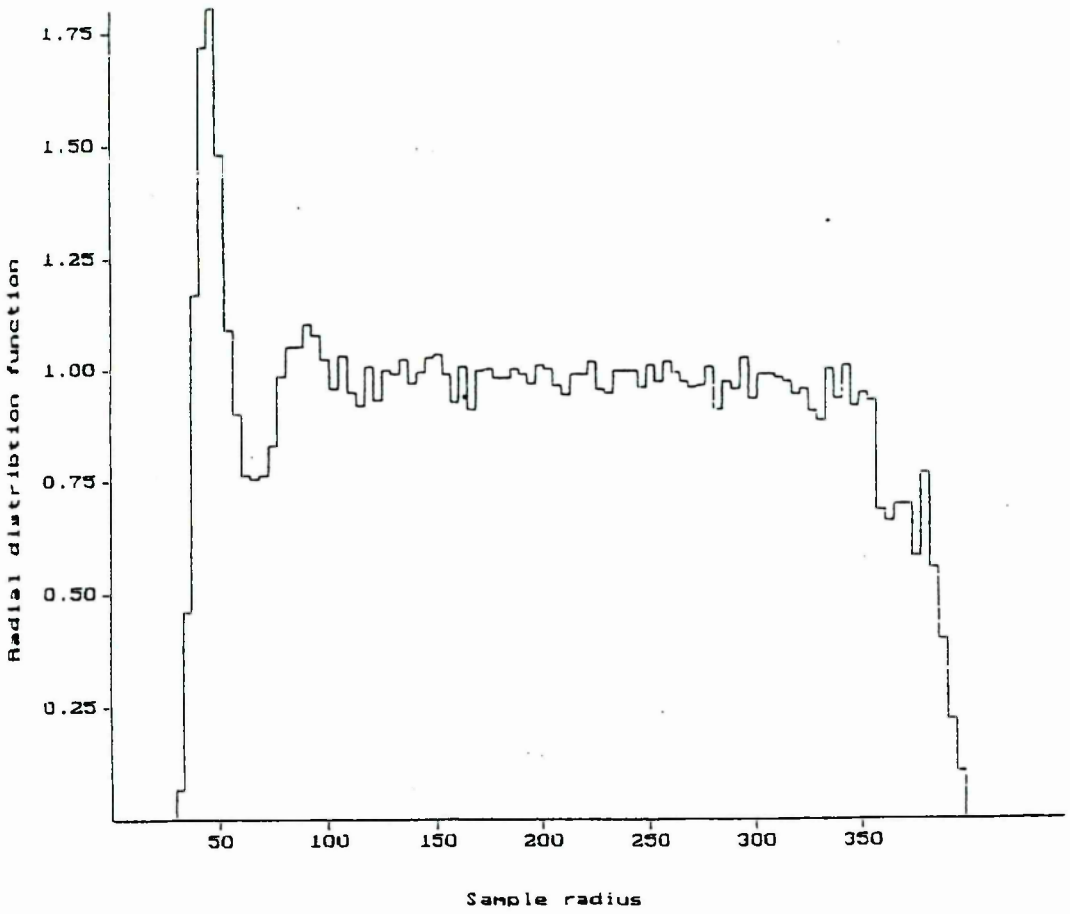

Figure 3.30 Radial distribution function of normal rabbit cornea

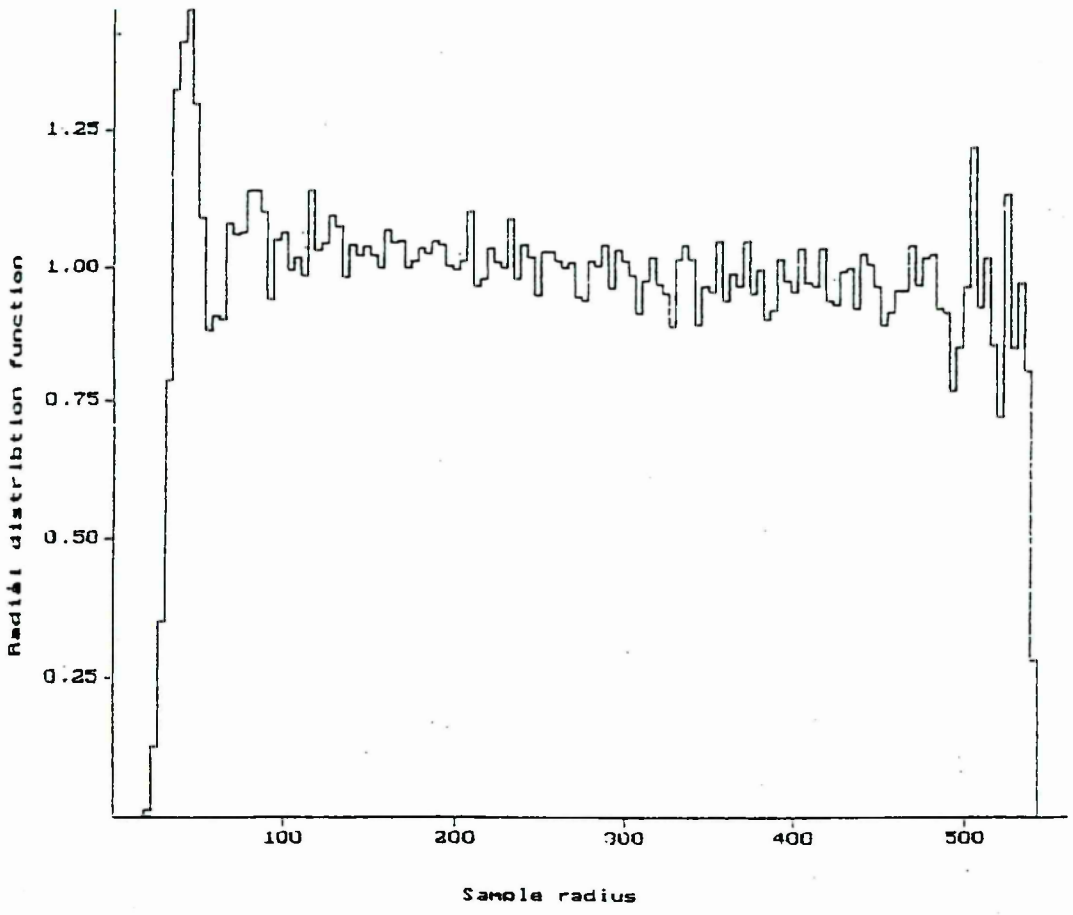

Figure 3.31 Radial distribution function of 45 week old scar tissue.

3.6 X-Ray Diffraction of Rabbit Corneal Scar Tissue

Synchrotron X-ray diffraction was carried out on the full-thickness rabbit corneal scars. To prevent excess drying, most of the scar tissue samples were not removed from the cornea. For the low angle diffraction, these corneas had not been frozen and were analysed within 36 hours of death. For the high angle X-ray diffraction, it was necessary to store the corneas frozen at -18^{o}C and to thaw them before use (2.4).

3.6.1 Interfibrillar Spacing

The interfibrillar spacing of full-thickness scar tissue and normal rabbit corneal tissue was calculated from the first order equatorial reflection. Figure 3.32(A) shows the first order reflection in normal cornea as a clear ring; in scar tissue this ring is more diffuse (figure 3.32(B)). This indicates a wider range of interfibrillar spacing and hence abnormal packing of the fibrils in the scar tissue compared to normal. However, the sharpness of this ring improves with the increasing age of the scar tissue. This is seen in figure 3.33,3.34 and 3.35, the densitometry traces of the interfibrillar ring from normal cornea and from 7 and 21 months scars.

The average interfibrillar spacing of 7,14 and 21 month scar tissue was significantly higher than that of normal tissue, though 3 and 6 weeks had an average spacing close to normal (table 3). The ratio of peak height to peak width (at half height), R1, gives a measure of the range of spacing within the tissue irrespective of the relative X-ray exposure time. Strictly

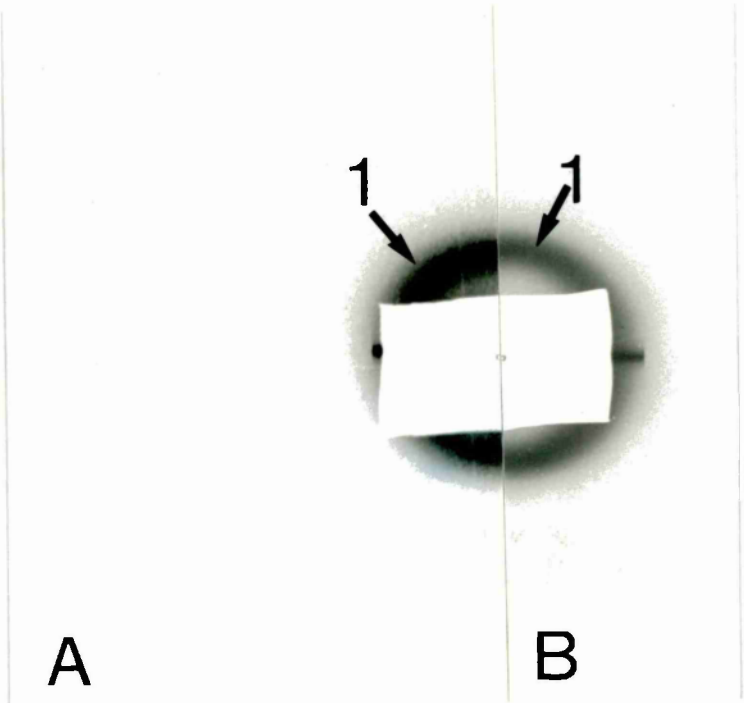

Figure 3.32. Low angle X-ray diffraction patterns of the first order reflection (1), A of normal rabbit cornea and B, the first order reflection of 7 month scar tissue.

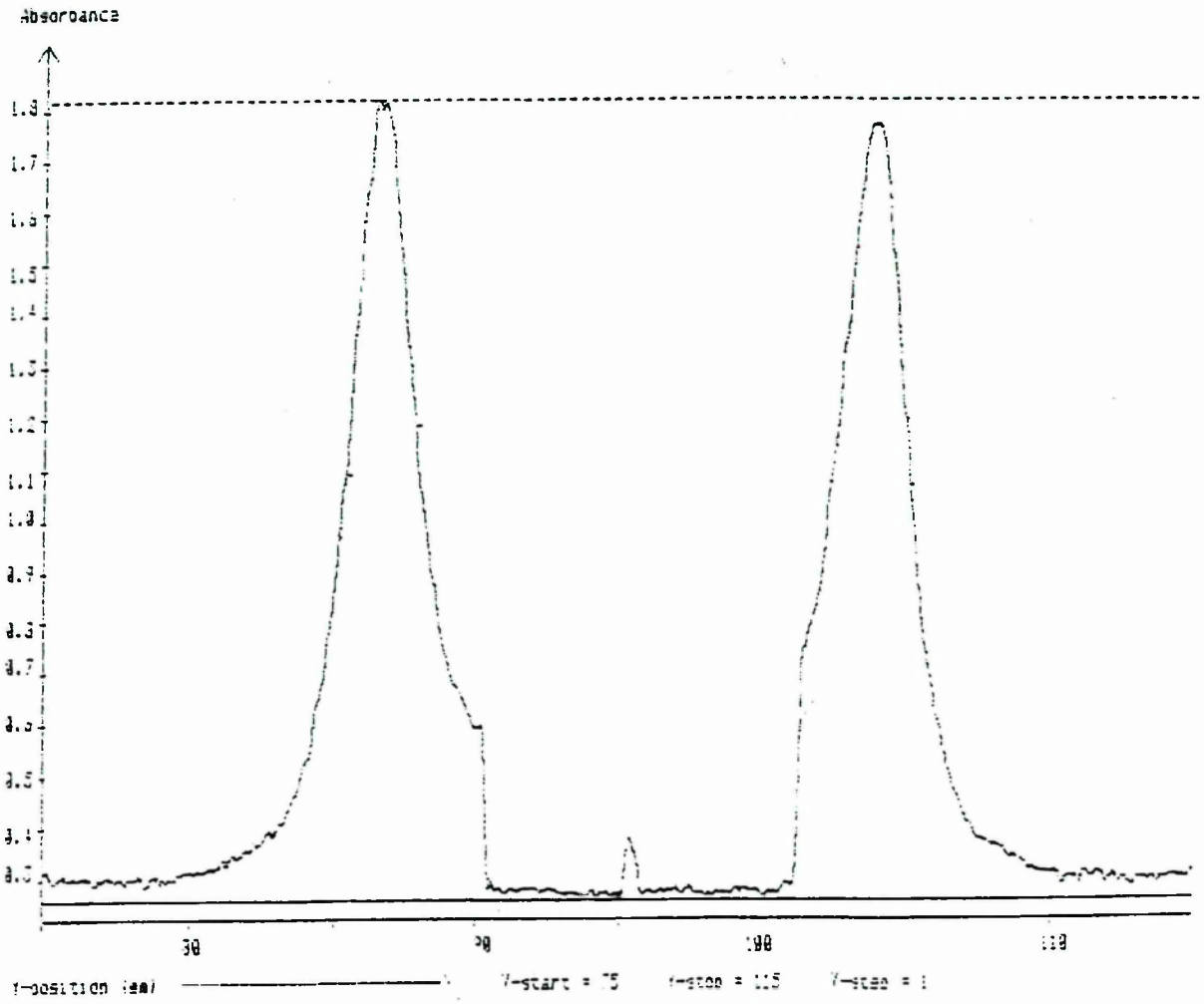

Figure 3.33 Densitometry trace of the first order reflection of normal rabbit cornea.

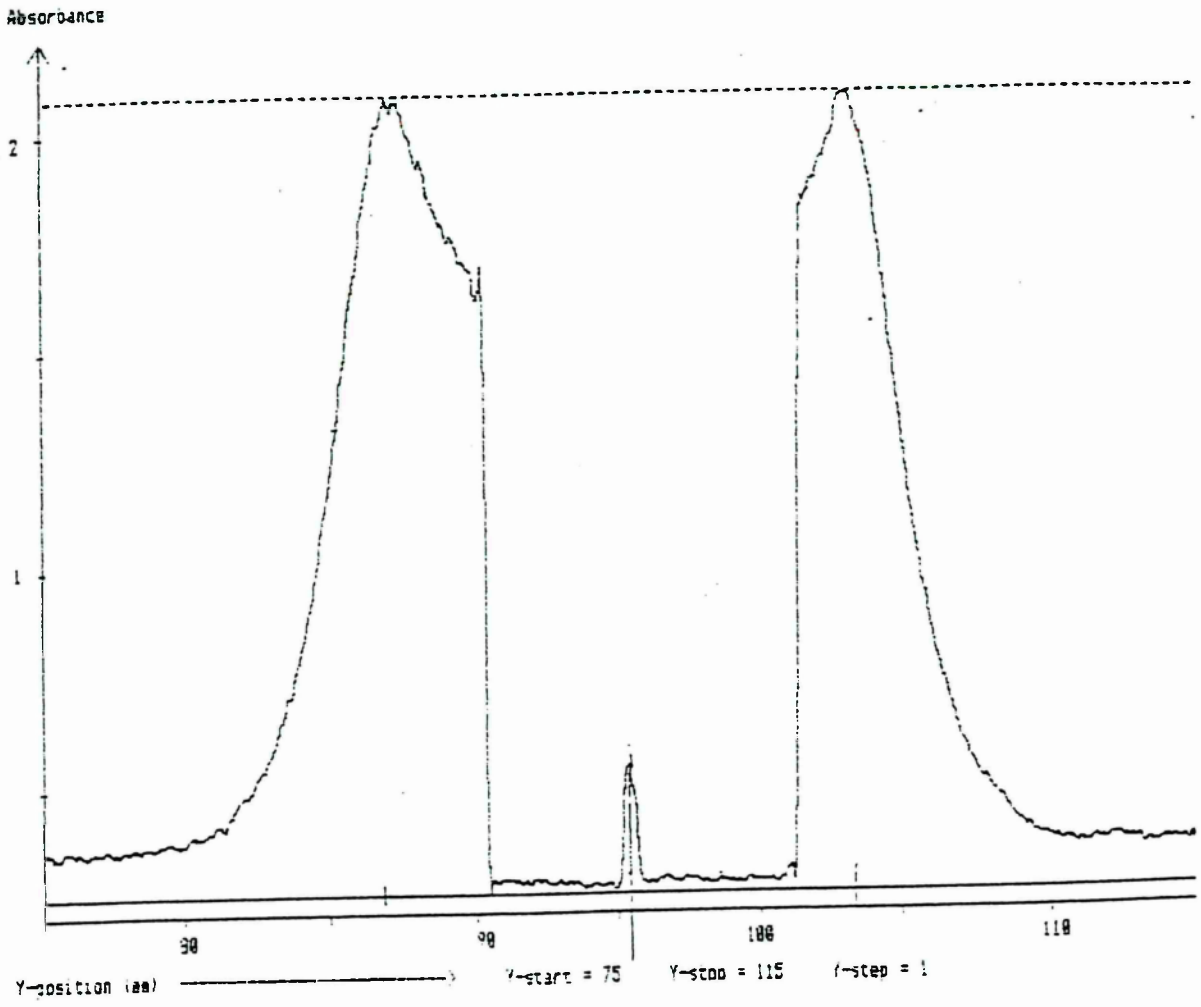

Figure 3.34 Densitometry trace of the first order reflection of 7 months scar tissue.

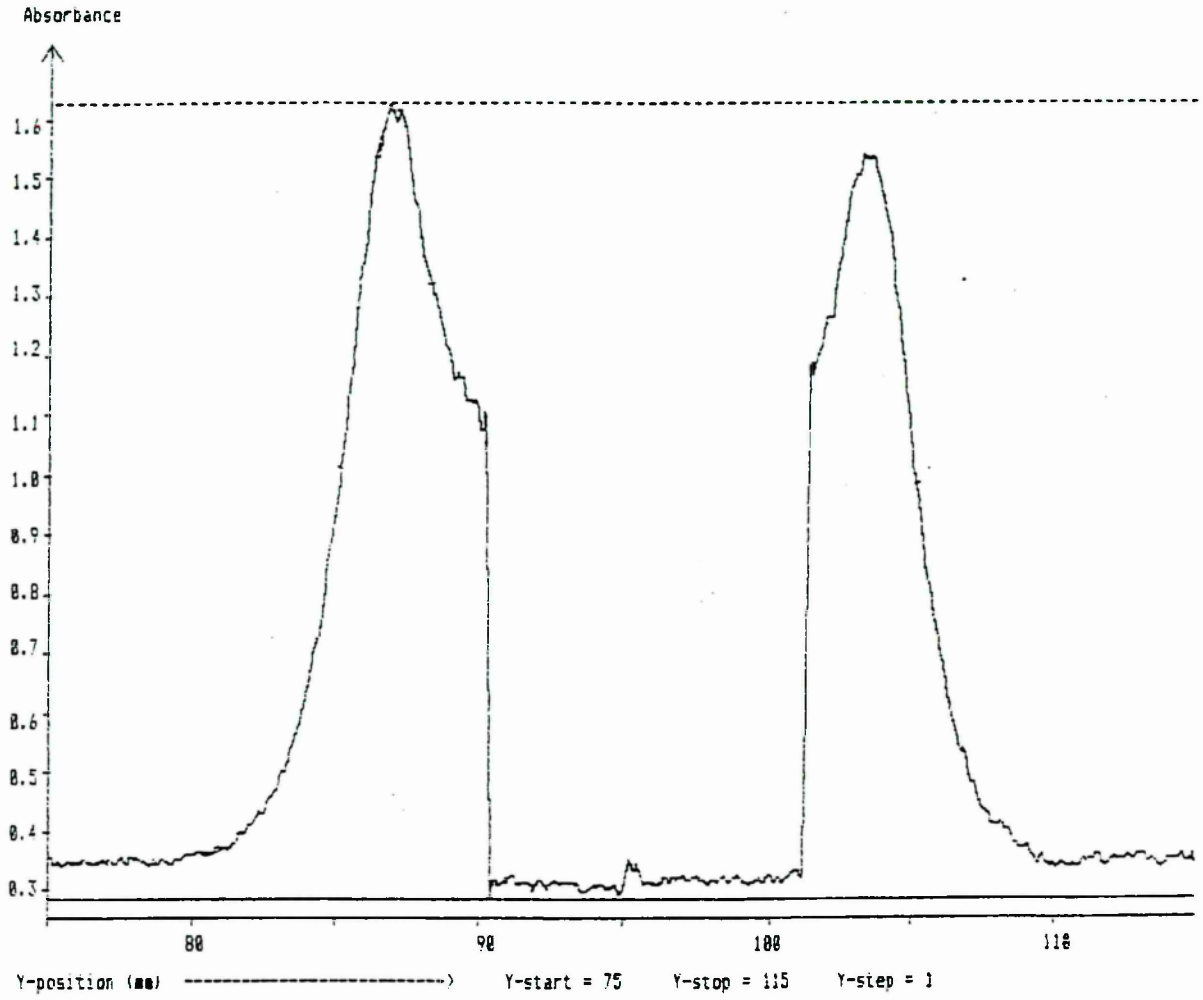

Figure 3.35 Densitometry trace of the first order reflection from 21 month scar tissue.

speaking, the X-ray data need to be converted to real space before the ratio R1 is calculated. However, since comparisons were being made over the same small region of reciprocal space, the height to width ratio could be measured directly from the densitometer scans. This ratio therefore gives information about the ordering of the collagen fibrils in the different tissues. R1 was very low in 3 weeks old scar, indicating a wide interfibrillar range. As the age of the scar increased, R1 increased, but after 21 months of wound healing, it had not returned to normal. The increase in R1 indicates a higher degree of interfibrillar order with increasing age of the scar, even though the average interfibrillar spacing remains elevated. Visual examination of the scar tissue *in vitro* showed that at 3 or 6 weeks the scar tissue was very opaque whereas after 21 months it was only lightly opaque. Densitomitry of the scar tissue supported this visual analysis (table 4).

Table 3. The average interfibrillar spacing and ratio of peak height to peak width at half height R_1, of rabbit corneal scar tissue at different ages.

Age of Scar	Interfibrillar Spacing	Ratio, R_1	No. of X-ray patterns
3 weeks	66.7 ±5nm	0.3	1
6 weeks	68.6 ±5nm	0.5	1
7 months	71.8 ±5nm	1.4	3
14 months	71.8 ±5nm	1.8	4
21 months	72.8 ±5nm	1.9	3
control	66.3 ±5nm	6.2	2

± refers to the estimated precision of measurement

Table 4. The maximum absorbance at 540nm of rabbit corneal scar tissue.

Age of Scar	Absorbance (a.u.)
3 week	0.48
6 week	0.50
7 month	0.35
14 month	0.26
21 month	0.24
control	0.02

± refers to the estimated precision of measurement

3.6.2 Fibril Diameter

The mean fibril diameter, was calculated for normal and scar tissue at physiological hydration from the first subsidary maximum (figure 3.35). For normal tissue, the mean diameter was 41.7nm, whereas in scar tissue, it was generally higher (table 5).

An estimate of the range of fibril diameters was obtained from the fibril transform peak, after digitization and background subtraction. The spread of diameters was quantified by calculating the ratio of peak height to peak width at half height, R2. The results indicated that, after 14 months of wound healing, the range of fibril diameters found in scar tissue had returned to normal.

Table 5 The mean fibril diameters of collagen in normal rabbit cornea and rabbit corneal scar tissue, with an estimation of the spread of fibril diameters R_2.

Age of Scar	Mean Diameter	Range,R_2	No. of X-ray patterns
6 weeks	>39.2nm	-	-
7 month	43.5 ±0.6nm	0.11	2
14 month	42.9 ±1.0nm	0.16	2
21 month	43.4 ±0.7nm	0.17	4
control	41.7 ±0.8nm	0.16	2

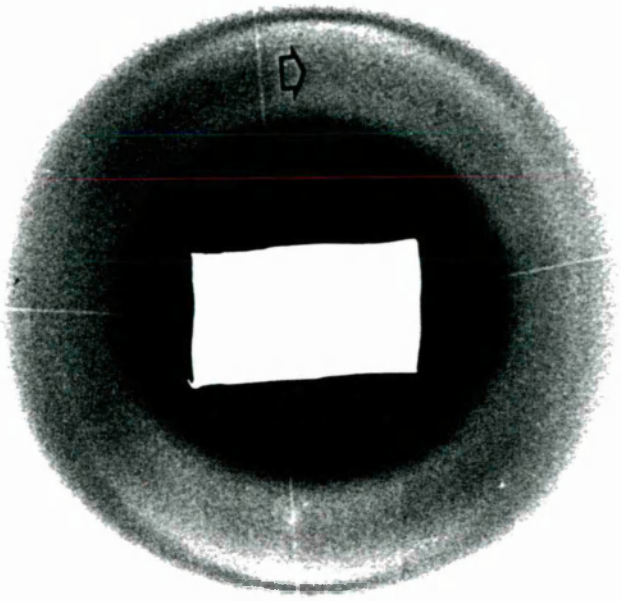

Figure 3.36 Low angle X-ray diffraction pattern of normal rabbit cornea showing the first maximum (⌷) derived from the scattering by the collagen fibrils (fibril transform)

3.6.3 Volume Fraction

The volume fraction q is the percentage of the tissue volume occupied by the hydrated collagen. The amount of water associated with each collagen molecule affects the intermolecular spacing and therefore the volume fraction. Tissue hydration was kept as close to physiological hydration as possible (2.3). By considering a transverse section through the fibrillar array, the mean volume fraction is defined by

$$q = \frac{V_f}{V_i}$$

where V_f is the average cross-sectional area of a single fibril and V_i is the area of the section associated with each fibril (equivalent to a unit cell). This is shown schematically in figure 3.37.

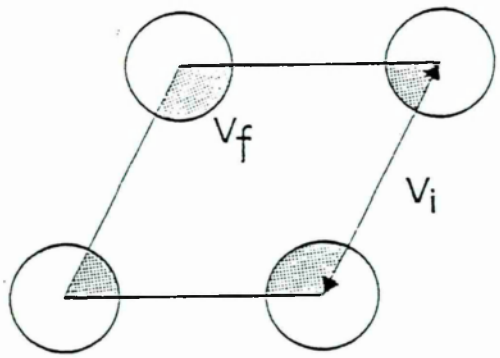

Figure 3.37

If the fibrils are packed with liquid-like order, V_i is given by:

$$V_i = 1.12d^2$$

where d is the interfibrillar Bragg spacing. Also, assuming that the fibrils have a circular cross-section of radius,r, we can write $V_f = \pi r^2$, and hence

$$q = \frac{\pi r^2}{1.12d^2}$$

In scar tissue of 7, 14 and 21 months, the mean volume fraction is lower than that of normal corneal tissue (table 6). However, the reduction in the volume fraction is only 3-4%.

Table 6. The volume fraction, Vf/Vi of corneal scar and normal corneal tissue.

Age of Scar	Vf/Vi
7 month	32%
14 month	31%
21 month	31%
Normal	35%

3.6.4 High angle X-ray diffraction

High angle X-ray diffraction was used to calculate the intermolecular spacing of the collagen in the full thickness scar tissue.

3.6.5. Intermolecular spacing

The intermolecular spacing of scar tissue and normal rabbit corneal tissue was calculated at physiological hydration. The intermolecular spacing of the scar tissue at each age examined was lower than that of normal corneal tissue (table 7).

Table 7. The intermolecular spacing of scar and normal corneal tissue.

Age of Scar	Average Intermolecular Spacing	No. of diffraction patterns
3 week	1.67 ±0.06nm	2
6 week	1.67 ±0.06nm	2
7 month	1.72 ±0.06nm	2
14 month	1.75 ±0.4nm	4
21 month	1.75 ±0.06nm	2
control	1.78 ±0.0.6nm	2

The intermolecular spacing of collagen molecules in a fibril depends on the hydration of the collagen fibrils. When the cornea dries the intermolecular spacing reduces (Fullwood et al., 1992). A normal rabbit cornea, a 3 week and a 2 month corneal scar were dried in a hot air drying cabinet, and the intermolecular spacing was calculated (table 8). On drying, the intermolecular spacing of the normal cornea reduced by 20%, whereas, the intermolecular spacing of the scar tissues reduced by only 4% (3wk) and 13% (2mn).

Table 8. The intermolecular spacing of dry rabbit scar and dry normal rabbit corneal tissue.

Age of Scar	Intermolecular Spacing (dry)	Intermolecular spacing (wet)	no. of diffraction patterns
3 week	1.60 ±0.03nm	1.67 ±0.07nm	1
2 month	1.47 ± 0.03nm	1.69 ±0.06nm	1
control	1.42 ±0.02nm	1.78 ±0.06nm	1

3.7 Morquio's Syndrome

3.7.1 X-ray Diffraction

The first-order equatorial diffraction ring was obtained from a short exposure. The ring showed maxima in the intensity distribution in two orthogonal directions, which is normal for human cornea (Meek et al. 1987). The interfibrillar spacing was calculated and compared to previously published values for human cornea (Fullwood et al., 1992) (table 9). The Morquio's syndrome (MS) cornea specimen showed a reduction in the interfibrillar spacing of approximately 10%. A longer exposure on the low-angle camera produced the fibril transform (figure 3.38a), which was very broad compared to normal human (figure 3.38b), indicating a wide range in the diameter of the fibrils. The average fibril diameter of (MS) was 30.2nm compared to normal 30.8nm, however, the maximum diameter in Morquio's syndrome was >42nm. A high angle X-ray pattern was produced from which the intermolecular spacing was calculated (table 9). The intermolecular spacing was reduced with respect to normal by 6%.

Table 9. The interfibrillar and intermolecular spacing of Morquio's syndrome and normal human cornea.

Specimen	Interfibrillar Spacing	Intermolecular Spacing
Morquio	56.4nm +/-3.1	1.74nm +/-0.06
Normal	61.9nm +/-4.5	1.85nm +/-0.07

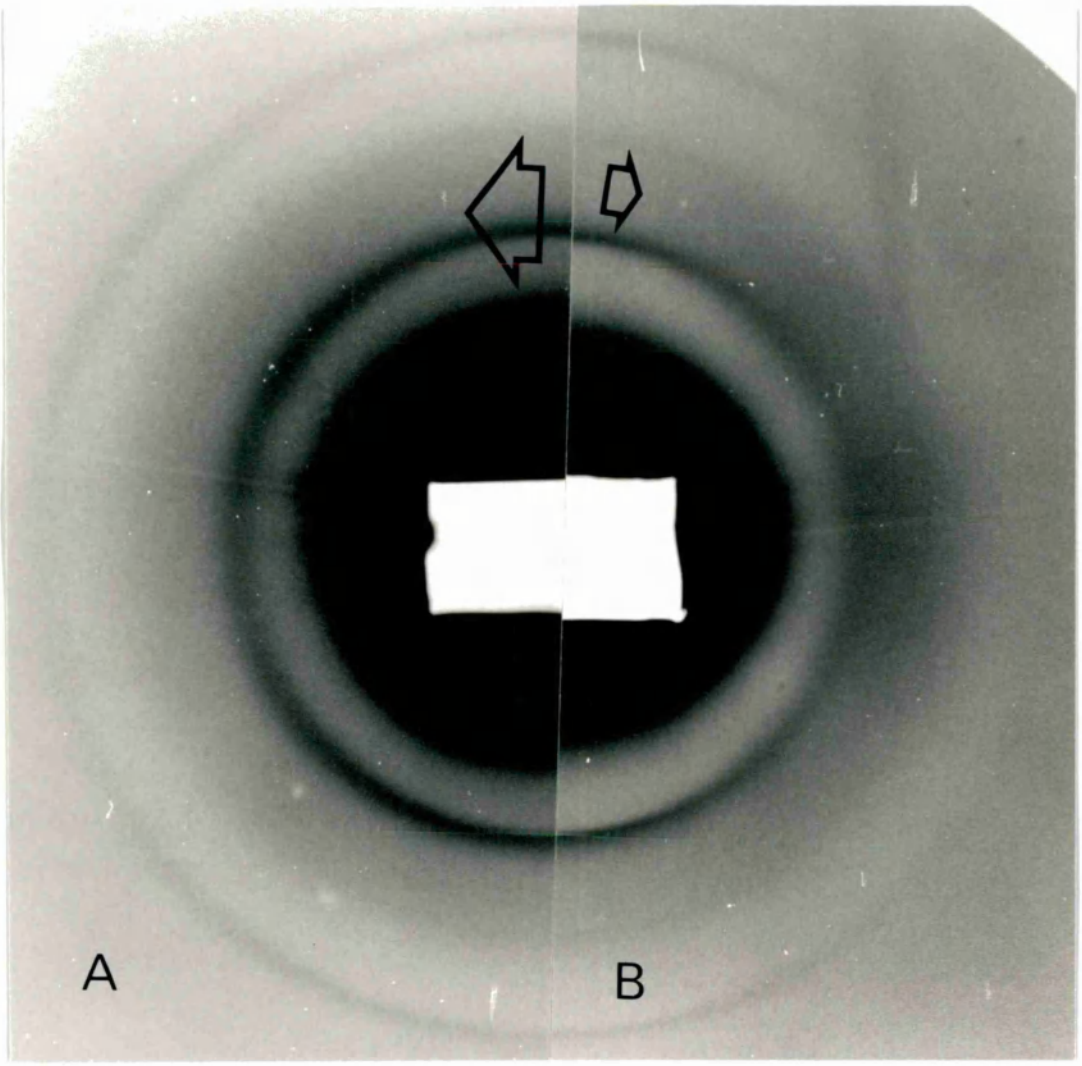

Figure 3.38 A low angle pattern of the fibril transform from A, morquio syndrome and B, normal human cornea.

3.7.2 Collagen Fibril Diameters

Collagen fibril diameters of Morquio's syndrome and normal human were measured from electron micrographs of fibrils in cross-section. The fibrils in human cornea had a diameter spread of 22-30nm (figure 3.39); in MS, the diameter range was much larger, 20-42nm (figure 3.40). The diameters in MS appeared to be composed of two populations. The first population had a distribution comparable to that in normal tissue (20-30nm) but the second contained of larger fibrils with a range of 32-42nm. The fibril diameters in the MS cornea thus displayed a bimodal distribution, a population of normal sized fibrils and a population of abnormally large fibrils.

The arrangement of the fibrils in the MS cornea also differed to normal in that some fibrils were very close to or touching their neighbours (figure 3.41). The larger abnormal sized fibrils were obviously not circular in shape and had a lobed appearance when compared to the normal sized fibrils (figure 3.41).

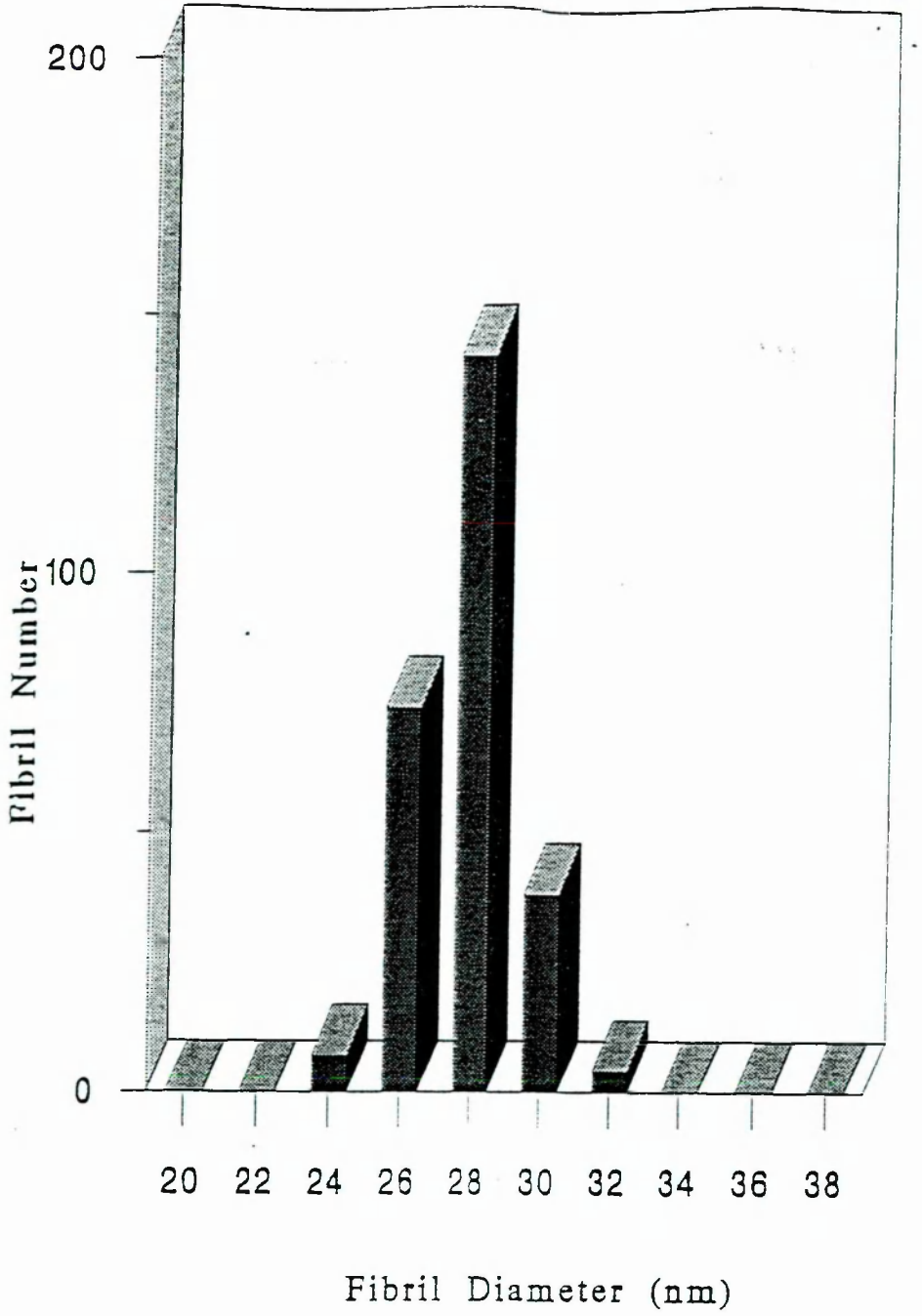

Figure 3.39 Diameter distribution of collagen fibrils from normal human cornea.

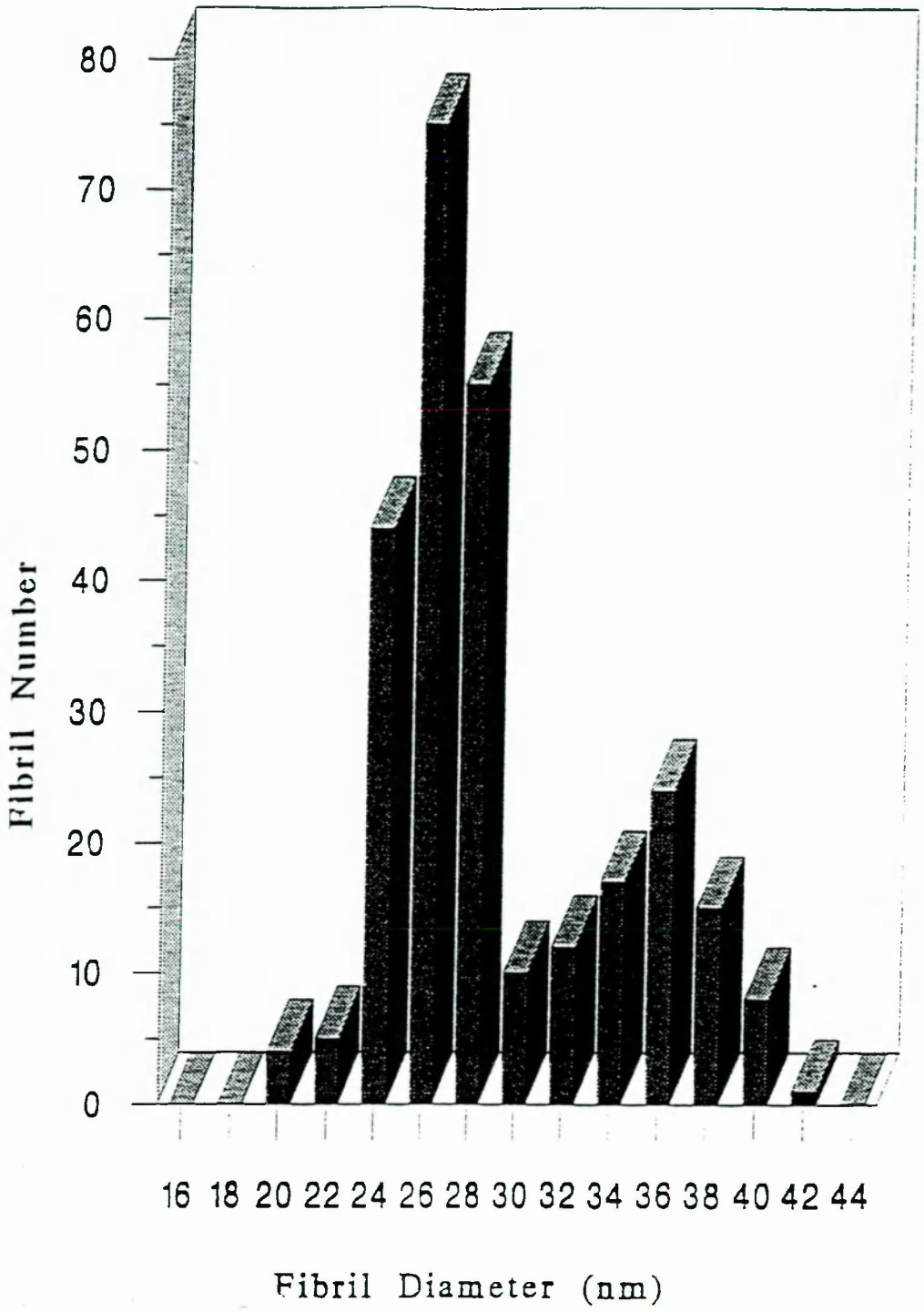

Figure 3.40 Diameter distribution of collagen fibrils from Morquio syndrome cornea.

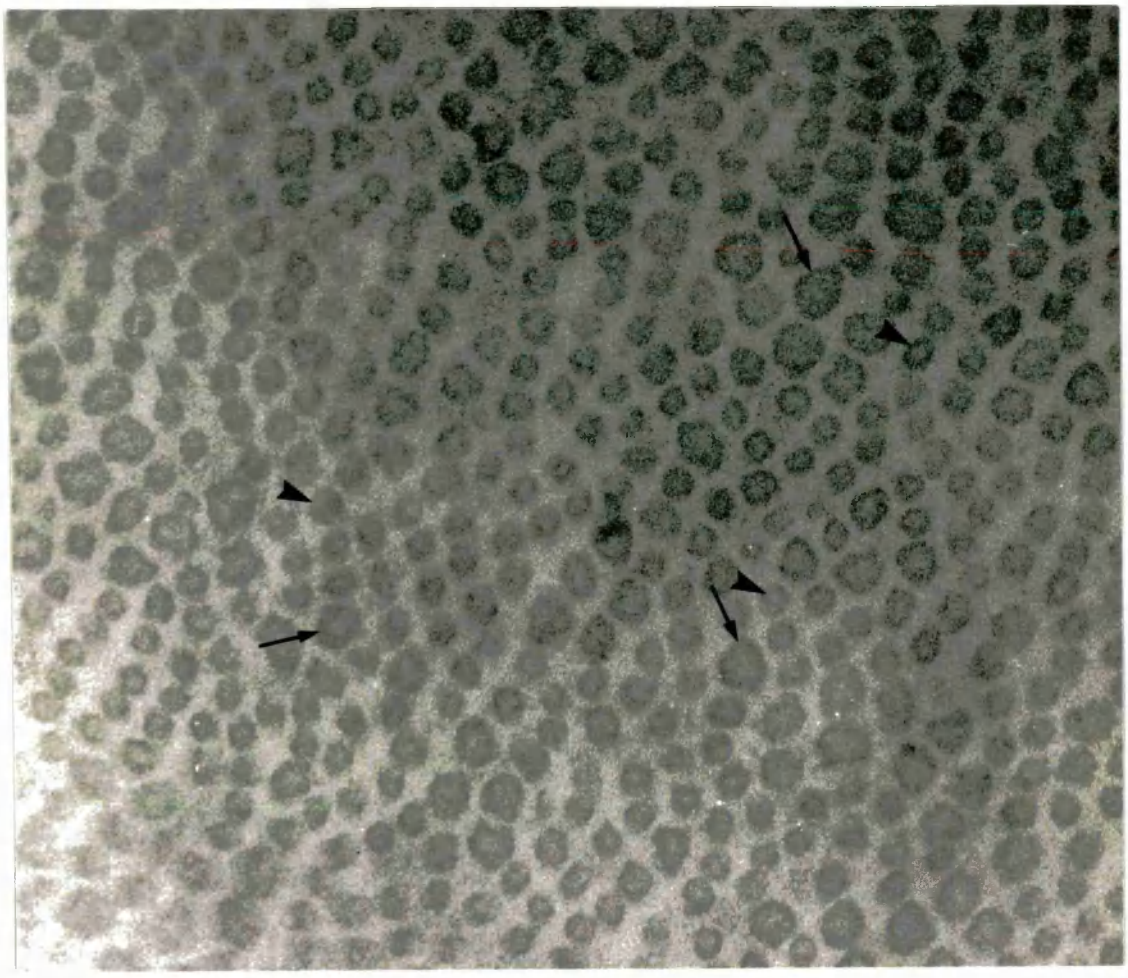

Figure 3.41 TEM of collagen fibrils in cross-section from Morquio's syndrome. Abnormally large fibrils (⟶) and normal size fibrils (➤) are present. Stained with cuprolinic blue and counterstained with uranyl acetate and phosphotungstic acid. Magnification 150k

3.7.3 Proteoglycan Staining

Proteoglycan staining in normal human cornea, revealed a regular arrangement of proteoglycan filaments along each individual collagen fibril (figure 3.42). Many of these filaments were orientated crosswise from one fibril to its neighbour. The proteoglycan staining throughout the bulk of the MS cornea showed the same arrangement of interfibrillar proteoglycans although by visual inspection the number of these proteoglycans seemed to be elevated (figure 3.43). However, this difference may be due to the relative ages of the two donors.

In the anterior stroma, abnormal filaments (up to 400nm long) were seen, randomly orientated in the collagen matrix. Other large proteoglycan filaments were found throughout the stroma and also in close proximity to the keratocytes (figure 3.44), these were not seen in the normal human control cornea. The structure of the keratocytes was not normal, many of the cells appearing to be disrupted. This disruption took the form of circular structures in the cell body which gave the impression that the cells were disintegrating.

Long-spacing structures (possibly long spacing collagen) with a periodicity of 110nm were also frequently observed (figure 3.45). Similar structures have been reported to occur in the corneas from old individuals (Marshall et al., 1992) but not in younger, normal human corneas and in Scheie's Sydrome (Quantock et al., 1993).

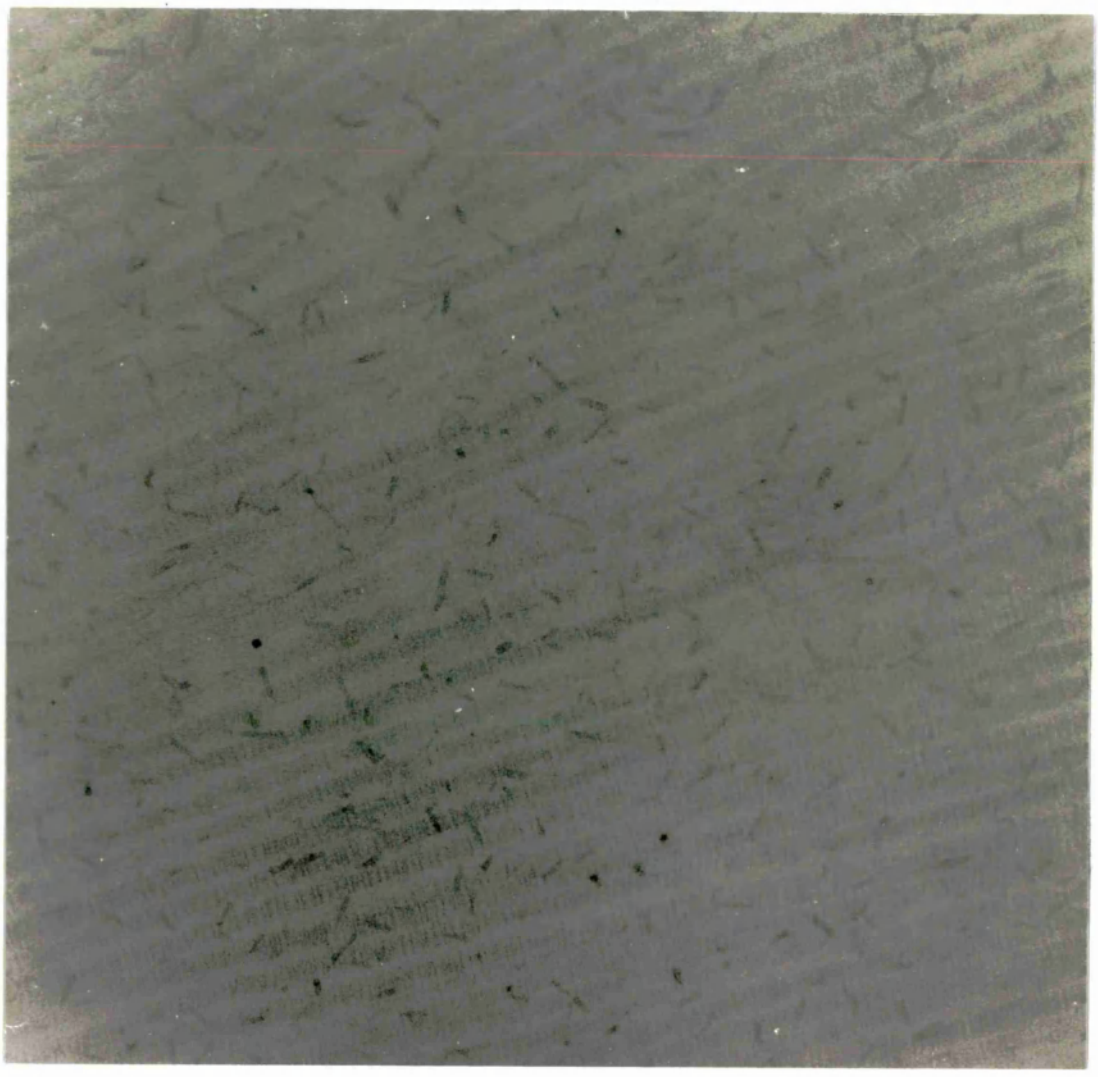

Figure 3.42. Electron micrograph of proteoglycan staining in normal human corneal stroma (age 74 years). Stained with cuprolinic blue and counterstained with uranyl acetate.

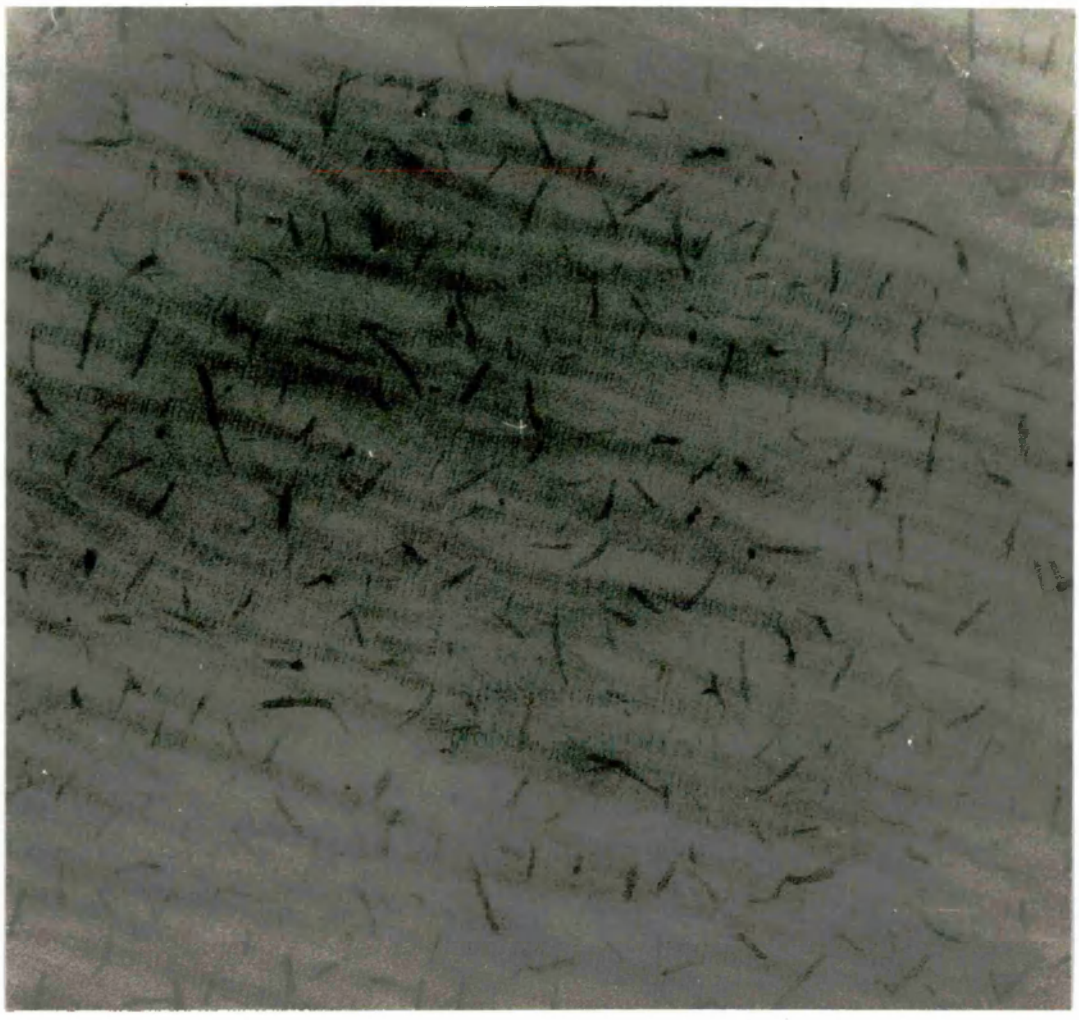

Figure 3.43 Electron micrograph of proteoglycan staining in Morquio's syndrome cornea (age 34 years). Stained with cuprolinic blue and counterstained with uranyl acetate.

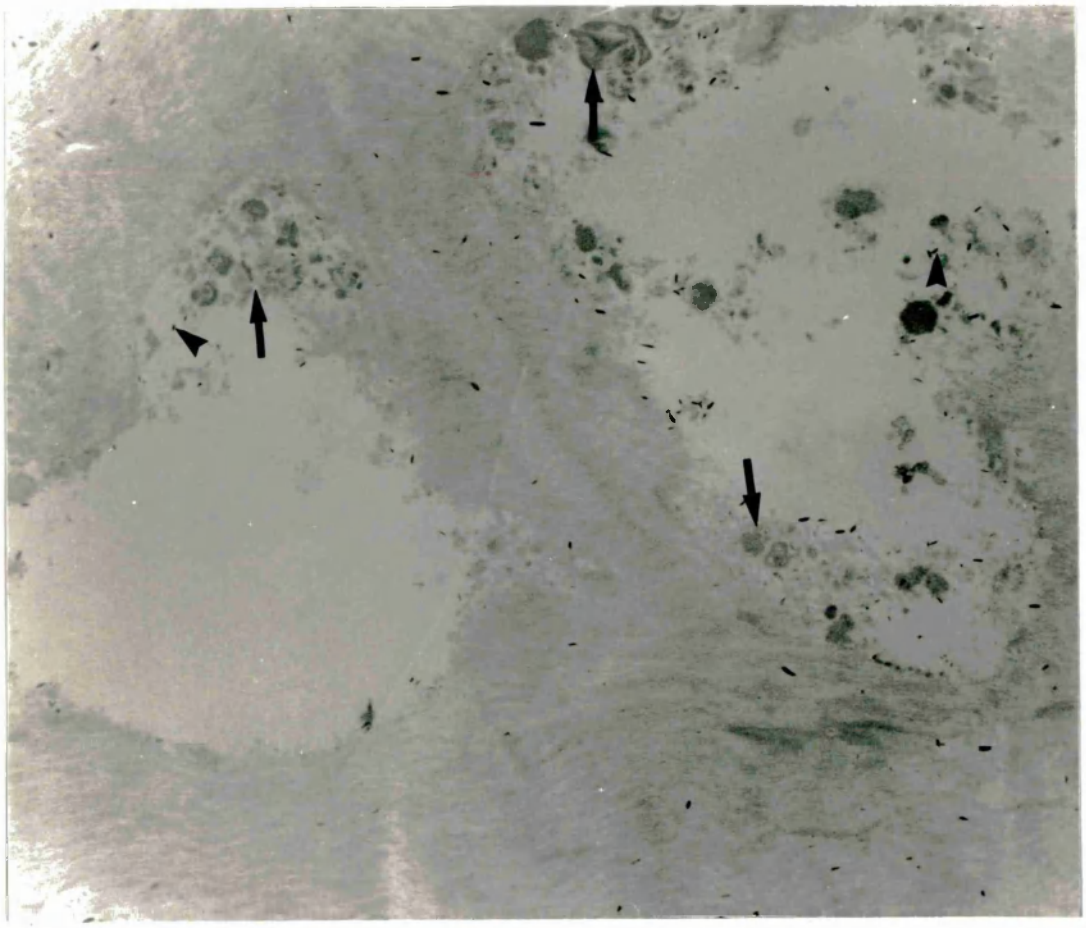

Figure 3.44 Electron micrograph of large proteoglycan filaments (↔) located with disrupted keratocytes (►) of Morquio's syndrome cornea. Stained with cuprolinic blue and counterstained with uranyl acetate. Magnification 6K

Figure 3.45 Electron micrograph of banding structure (⟷) in Morquio's syndrome and large proteoglycan filaments (►) located in the anterior stroma. Stained with cuprolinic blue and counterstained with uranyl acetate. Magnification 30K

Chapter 4

4.0 Discussion

4.1 Superficial Lamellar Keratectomy

In this study of S.L.K. wounds, the major differences in the number, size and distribution of proteoglycans occurred 2 weeks after wounding. The stroma at this stage appeared very hydrated and contained much larger than normal proteoglycans distributed throughout the scarred tissue. Previous researchers have shown that, in full thickness wounds, the highest tissue hydration also occurs after two weeks, as too do the largest size and number of abnormal proteoglycans (Cintron et al., 1990). At this age the predominant proteoglycan has been shown to be a highly sulphated dermatan sulphate, with hyaluronic acid and possibly some undersulphated keratan sulphate (Cintron et al., 1990). The present results from S.L.K. wounds also show abnormal proteoglycan filaments (as observed by cuprolinic blue staining) which occur after one week, proliferate after two weeks and then gradually reduce in size and in number, having virtually disappeared by six months. In comparison with other studies (Funderburgh & Chandler 1989) both types of wound, are likely to consist predominantly of dermatan or chondroitin sulphate, with relatively little keratan sulphate. However, whereas in full thickness wounds the maximum proteoglycan filament length is about 170nm (anterior scar, 2 weeks)(Cintron et al., 1990), the corresponding filaments in S.L.K. scars are longer (up to 500nm). However, in general, the same sequence of events appears to take place in both full-thickness wounds

and in S.L.K. wounds. This suggests that, in contrast to previous reports (Cintron et al., 1990), there is no difference with respect to the types of proteoglycans synthesized between the anteriorly located and posteriorly located stromal fibroblasts. Furthermore, the proliferation of an oversulphated dermatan sulphate at the same time during healing in both types of wound suggests that these molecules, which are not found in normal tissue, play a key function in the wound-healing process. It is not surprising, therefore, that a similar sequence of events occurs during corneal development (Cintron & Covington, 1990).

Since the proteoglycans of normal tissue are known to play an important role in regulating the hydration of the stroma, it can be concluded that the abnormal size, level of sulphation and numbers of proteoglycans observed in 2-week wounds increase the swelling pressure and result in the wound having a high level of hydration. A major function of these large proteoglycans may be to hydrate the tissue and perhaps compensate, by swelling, for the volume of the tissue removed by the wounding. This may allow easier tissue restructuring; a fluid environment would probably make large amounts of synthesized collagen, which is laid down by fibroblasts as bundles of parallel fibrils, easier to deposit in an ordered structure. Furthermore, it has been shown that collagen accumulation is very rapid up to 2 weeks of healing but becomes gradual after the second week (Cintron et al., 1977; Menasche et al., 1988). The highly swollen environment in the first few weeks of wound repair would also, therefore, allow easier passage of cells through the collagen framework, both for the synthesis of collagen and for the removal of breakdown products.

In contrast, however, there seems to be a correlation between the presence of large dermatan sulphate proteoglycans and the extent of disruption to the collagen interfibrillar spacing, however this has not been quantified. The collagen fibrils synthesised in the early stages of healing were deposited in parallel bundles (figure 3.5) and the constituent fibrils were associated with small proteoglycans. The constituent collagen fibrils in the matrix had a range of interfibrillar spaces. The very large proteoglycans (up to 500nm x 25nm) appeared mostly in collagen-free spaces, but the medium-sized ones (up to 140nm x 15nm) occurred between the disordered collagen fibrils. Ordering within the scar tissue did, however, gradually increase. But it is evident from figure 3.10 that the scar tissue of 6 months is clearly distinguishable from the normal tissue with respect to the ordering within the tissue.

The gradual restoration of interfibrillar order in S.L.K. wounds was accompanied by a reduction in the size and number of the collagen free spaces, in the abnormal proteoglycans which fill them, and in the abnormal proteoglycans located between the collagen fibrils. This sequence of events strongly suggests that there is a direct correlation between normal proteoglycans and normal fibril arrangement and, conversly, between abnormal proteoglycans and fibril disruption.

4.2 Excimer Laser Photorefractive Keratectomy

The rabbit has a vigorous corneal wound healing response and, like other techniques, excimer laser PRK excites this response. A similar response occurs in monkey and human corneas but to a lesser degree (SundarRaj et al., 1990).

By this regenerative reaction, the area of the stroma lost to the ablation is being repaired. In the stroma, the sequence of events of stromal regeneration is keratocyte death and then proliferation of the keratocytes in higher than normal numbers under the epithelium. These keratocytes then appear to produce, by their location, larger than normal proteoglycan filaments which are associated with amorphous, densely stained material. The nature of this material is unknown, although scar tissues are known to contain large amounts of specialised proteins such as fibronectin and tenascin (Van Setten, et al., 1991). Proteoglycans are thought to play a role in controlling corneal hydration and these abnormally large filaments may increase the hydration around the keratocytes and result in the observed areas free of extracellular matrix seen next to and near these cells. As little or no new collagen synthesis was seen at this stage, the production of large proteoglycan filaments may be one of the first steps in stromal regeneration, as appeared to be the case during S.L.K. wound healing.

A dramatic change in the morphology of the healing tissue occurs by the second week; the distribution, number and size of the abnormal

proteoglycan filaments all increase. Newly synthesized collagen can be seen and the tissue contains more areas free of extracellular matrix.

It has been postulated that proteoglycans play a role in collagen fibril development by controlling fibril diameters (Scott, et al., 1981; Scott, 1984) (4.4.2). We observed that the small proteoglycan filaments closely associated with collagen fibrils in normal cornea are absent between the fibrils within early healing tissue. However, the collagen fibrils in the healing tissue appear to be of approximately normal diameter (figure 3.19). This suggests that proteoglycans do not play a role in governing the diameter of collagen fibrils (4.4.2). As the age of the healing tissue advances, the numbers of the large abnormal filaments deceases and there is also a corresponding reduction in the number and size of the spaces within the matrix.

Steroids are thought to act by inhibiting the fibroblastic response by blocking DNA and protein synthesis. In this study, nothing can be concluded from the small sample, however the corneas that were treated with steroid during healing were observed to have a decreased amount of corneal haze compared with corneas of the equivalent age that were untreated. However corneal haze did develop indicating that the action was limited. The scar tissue produced in the corneas that were treated had a very similar structural morphology to untreated corneal scar tissue. Larger than normal proteoglycans were observed in the scar tissue up to 45 weeks post wounding and clumps of filaments were also observed. However, because of the small number of specimens used, no firm conclusions could be drawn from this experiment.

4.3 Laser and Manual Keratectomy and Transparency

The excimer laser photoablation and superficial lamellar keratectomy of rabbit corneas provoked the same characteristic wound healing response, which resulted in the formation of an opaque scar. In both cases the wound healing response was characterised by the appearance of large numbers of abnormal chondroitin/dermatan sulphate proteoglycan filaments seen mainly in the first weeks of healing. After long term healing (up to 9 months), lacunae containing clumps of proteoglycans and abnormal proteoglycans were located within the matrix of both scar tissues.

The haze that is associated clinically with corneal scar formation is thought to derive from the structural features of the scar tissue. There are three factors to consider. According to Benedek (1971), when a cornea swells, some of the water imbibed goes into 'lakes', that is, areas devoid of collagen fibrils. These 'lakes' may occur within or between the stromal lamellae. When the size of such a region reaches approximately half the wavelength of light (approx 250nm) it will scatter light and the tissue will start to appear cloudy. The presence of collagen free regions in regenerated tissue, even after 45 weeks of healing (figure 3.25) suggests that they might be responsible for at least some of the corneal haze. The second factor to consider is the corneal lamellae themselves. Certainly, in scar tissue, there appears to be no layering of the collagen fibrils into lamellae. However, the presence of lamellae is thought not to be required

for transparency (Hart & Farrell, 1969) and the optical purpose of these structures is not yet understood. The third, and perhaps the most important, structural difference between corneal scar tissue and normal stroma, is the reduction in the degree of ordering of the collagen fibrils. Proteoglycans are thought to play a major role in the transparency of the cornea by maintaining interfibrillar spacing. Corneal scar tissue produced by both procedures contains proteoglycan filaments that are not seen in a normal stroma. There are larger then normal filaments distributed in the matrix in addition to the groups or clumps of proteoglycans, even at 45 weeks post wounding. The larger than normal individual filaments in the scar tissue matrix may stimulate the corneal keratocytes to continue remodelling the tissue, since turnover of scar tissue occurs at an elevated rate compared to normal stromal collagen turnover (Cintron, 1990). The presence of clumps of proteoglycan filaments may be an indication that remodelling of the scar tissue is still occurring.

4.4 Analysis of Electron Micrographs

4.4 1 Fibril Number Density

The study of the fibril number per unit area in different ages of scar tissue revealed that the number of fibrils in early scar tissue is significantly reduced when compared to normal tissue. As the age of the scar tissue increased the number of fibrils significantly increased. At 21 months the number of fibrils was still significantly lower (< 0.01) than normal tissue. However one 14 month(b) sample showed no significant difference when compared to the control.. The increase in the fibril number with age can be seen from figures 3.26 and 3.27, as can the return to a more ordered structure in the tissue. This is reflected in the X-ray results (section 3.5) where an increase in fibril order was seen with time.

4.4.2 Fibril Diameter

It can be seen that the average fibril diameter does not change significantly during the healing process. The distribution of fibril diameters is however less regular for the wounded corneas than for the control. This is seen by the increased range of fibril diameters in the scar tissue which shows that in scar tissue the regulation of the collagen fibril diameters is disrupted. In one sample (6 week) the mean fibril diameter was much larger than normal and the range of diameters (8-52nm)was much greater than normal (26-32nm). It is not clear why this sample contained such a wide range of diameters.

Over the years there has been controversy over the size of collagen fibril diameters in corneal scar tissue from various species, with reports indicating collagen fibril diameters of up to 120nm in man (Kenyon, 1987). The electron microscopy study of fibril diameters in S.L.K. and laser ablated corneas did not show the presence of very large fibril diameters (except in one sample). Although an increased spread of diameters was measured, the results indicate that, in most cases, the fibril diameter is close to the mean value. It has been suggested that collagen fibril diameters are controlled by some other tissue component, such as hydroxylysine-linked glucosides (Harding et al, 1980), type V collagen (Birk et al, 1990) or 'small' proteoglycans (Scott, 1984,1988)

The answer to the reports that indicated very large (Kenyon et al. 1987) fibril diameters may lie with the observation of collagen fibrils coming together and merging to form one large fibril. This clearly would produce fibrils of much larger diameter, and may have been responsible for the large fibril diameters measured in the 6 week sample.. This process of fibril fusion was seen in early scar tissue (2 weeks, figure 3.28) where fibrils were 90nm in diameter. In the early stages of wound healing, the collagen showed less staining of the 'small' proteoglycans normally associated axially with the individual fibrils. This would suggest that small proteoglycans prevent fibrils from fusing together to form a larger fibril, probably by hydrating the tissue and preventing fibrils coming into contact.

4.4.3 Radial Distribution Functions

RDF's of fibril centres show the extent of order in the tissue. For a regular lattice structure the RDF would show long-range ordering. In the RDF of normal rabbit, the short range order in the arrangement of the collagen fibrils is demonstrated by the appearance of only 2 or 3 peaks. The RDF of the 45 week scar tissue contained only one clear peak which indicates that the order in this tissue was reduced with respect to normal. The RDF of the scar tissue was produced from regions that were, in comparison to the rest of the tissue, highly ordered, some regions were too disordered to produce a meaningful RDF. From this it is clear that the short-range ordering in scar tissue is reduced with respect to normal after 45 weeks healing with different regions in the tissue having different degrees of order. This clear reduction in the ordering of the collagen fibrils may play a significant part in the reduction of the transparency of the scar tissue.

Interpretation of X-ray diffraction patterns (Sayers et al. 1982) indicated that the packing of the fibrils in the bovine cornea has short range order extending over approximately three times the fibril diameter (100nm). The RDFs produced from the normal rabbit also cornea indicate a short range order of approximately 100nm.

4.5 X-ray Diffraction

Transparency of the cornea is thought to be due to the narrow uniform diameter of the collagen fibrils and the ordered packing of the fibrils. Hart and Farrell (1969), and Bendeck (1971) have shown theoretically that short range order in the corneal stroma should be sufficient to ensure transparency. The results from the work on the packing arragement of the cornea by Sayers et al., (1982) confirm the presence of short range order. The loss of corneal transparency in corneal scar tissue may be due to a number of factors: (1) The loss of short range order of the collagen fibrils. The results presented in Chapter 3 showed that even after prolonged healing, the order is much reduced in scar tissue compared with normal cornea. (2) The increase in diameter of some of the collagen fibrils. Scattering goes as the fourth power of the fibril diameter (Benedek, 1992). This means that a two-fold increase in diameter would increase light scattering by 16 times. (3) The presence of 'lakes' (Benedek, 1971). These are areas devoid of collagen fibrils. Such areas would be expected to scatter light if they are greater than half the wavelength of light. In Chapter 3, many such areas were seen to occur during the early stages of wound healing, but their numbers reduce as healing progresses. (4) A change in the refractive index of the ground substance or of the collagen fibrils. At present , it is not clear whether the copious abnormal proteoglycan filaments synthesised during wound healing lead to a change in the refractive index of the ground substance compared to that of the collagen.

Synchrotron X-ray diffraction of cornea produces an average value from the whole thickness of the cornea, though, in the scar tissue, the X-ray beam will pass through areas which contain no collagen fibrils. The average values for the interfibrillar centre-to-centre separation showed that scar tissue of 3 and 6 weeks had a normal fibril spacing (61.9nm), whereas, the average interfibrillar spacing of 7, 14 and 21 months scar tissue was 8-9% higher than that of normal tissue. However, as suggested, it is the spread of the spacing rather than the average spacing (representing the degree of disorder) that is more likely to affect transparency.

The ratio of peak height to peak width at half height gives a value R1, that provides a quantitative estimate of the spread. At the ages of 3 and 6 weeks, the first order diffraction ring was very broad and hence R1 was low, indicating a low degree of fibril order in the tissue. The interfibrillar X-ray pattern of the 7 month scar tissue was still broad when compared to normal (figure 3.32) and this is reflected in the densitometry trace and again in the low value of R1. The value of R1 in the 14 (1.7) and 21 (1.9) month scar tissue increased, but it remained lower than normal (6.2). However, the increase in R1 does indicate that the fibril order of the collagen fibrils in scar improves with the increasing age of the scar tissue.

The X-ray diffraction showed that the average fibril diameters were higher in the scar tissue, but by only 4% at 7, 14 and 21 months. The range of the fibril diameters R2, is lower than normal in 7 month scar tissue but has returned to normal after 14 months. These results suggest, that in early scar tissue, the range of fibril diameters is greater than that present in normal tissue. However, after extended healing (> 7 months), the range of

fibril diameters returns to normal but with a slightly increased average value.

The X-ray results suggest that collagen molecules have a normal axial arrangement within the fibrils of scar tissue (D = 65nm) but have a slightly altered lateral spacing that gradually returns to normal. The slighty reduced intermolecular spacing indicates that the hydration of the collagen fibrils is normal. Therefore the increased collagen fibril diameters are probably due to a higher number of collagen molecules per fibril and this would also indicate that the collagen fibrils have a normal refractive index. When a 3 week scar tissue was dried, the reduction of the intermolecular spacing was less compared to dry normal tissue. This reduction in the intermolecular spacing was closer to normal in dry 2 months scar tissue. This may reflect that, in early scar tissue, factors controlling the collagen molecular arrangement are altered. In scar tissue the composition of the fibrils is known to change, it has been shown that there is an increase/appearance of type III collagen and this may alter the response of the lateral spacing of the collagen molecules to drying. Other factors may also be important, such as the number and nature of the intermolecular bonds and the level of glycosylation.

Meek & Leonard (1993) have demonstrated that, in all species examined, including aquatic and land animals, the volume fraction of the hydrated collagen fibrils was constant. The volume fraction calculated from the average fibril diameter and interfibrillar spacing was reduced in scar tissue but this reduction was only minimal 3-4%. The 8-9% increase in the average interfibrillar spacing appears to be compensated by the increase in

average fibril diameter therefore maintaining a volume fraction close to normal.

The visual observations and densitometry clearly showed that the scar tissue under study was opaque, but with increasing age, the transparency of the tissue improved. However, even at 21 months, the transparency of the tissue was still reduced compared to normal. Electron microscopy has shown that in early stages of scar tissue development, (up to a few months), there are considerable areas free of collagens fibrils which would scatter light and cause the tissue to be opaque. In the 7- 21 month scar tissue the light scattering may result from the presence of 'lakes' in the tissue, an increase in the fibril diameter or the loss of short range order. The results suggest that the fibril diameter, though increased, would not increase light scattering sufficiently to effect transparency. Electron microscopy has shown that lakes persist in scar tissue up to 9 months but these do not appear to be of sufficient in size and number to greatly effect transparency. The parameter that changes with increasing age was the estimation of the range of interfibrillar spacing. Therefore it seems that, as the scar tissue increases in age, it is the level of fibril order that increases, and with it the transparency of the tissue.

4.6 Morquio's Syndrome

The X-ray diffraction results demonstrated that the mean centre-to-centre collagen fibril spacing the Morquio's syndrome is approximately 51.7nm. This is lower than the value of 61.9nm found for normal human corneas (Fullwood et al., 1992). Dehydration of the specimen, which would reduce interfibrillar spacing, was kept to a minimum by storage of the specimen tightly wraped in clingfilm and use of air tight X-ray cells. TEM also showed a reduction in interfibrillar spacing (figures 3.41, 4.1) confirming the X-ray result, the tissue sample used for TEM was processed immediately after keratoplasty, therefore the sample was at physiological hydration prior to processing. The degree of order in the tissue can be estimated from the first order diffraction ring. When compared to the first order reflection of normal cornea, the intensity and width of the first order diffraction ring are both similar, implying that the Morquio's syndrome cornea has the same degree of ordering of the collagen fibrils. This suggests that the reduced spacing occurs throughout the stroma. The calculation of the fibril diameters showed that the range of diameters was much greater in Morquio's syndrome than in normal human which agrees with the results from the electron microscope measurements discussed below. The intermolecular spacing, which is slightly lower than normal, indicates that the packing arrangement of the collagen molecules in the fibrils in Morquio's syndrome is the same as in normal tissue.

Transmission electron microscopy showed the range of collagen fibril diameters in Morquio's syndrome to be 22-42nm and in normal cornea 24-

30nm. Other reports have indicated this range to be 24-28nm (Craig & Parry, 1981) for normal human cornea.. Variations occur in diameter studies in the electron microscope because of the different extent of tissue dehydration in processing protocols used. The histogram of the diameters (figure 3.40) shows the distribution to be bimodal. The first population ranges from 24-28nm, a distribution that is seen in normal human corneas (figure 3.39) and the second population ranges from 30-42nm. This bimodal distribution of fibril diameters has also been demonstrated in Scheie's syndrome (Quantock et al., 1993)). From the electron micrographs, the larger than normal fibrils occur amongst normal diameter fibrils (figures 3.41, 4.1) and it can be seen that some collagen fibrils are touching their neighbours and are possibly merging. This would explain the presence of the larger diameter fibrils, their lobed appearance their and irregular shape (figure 4.1).

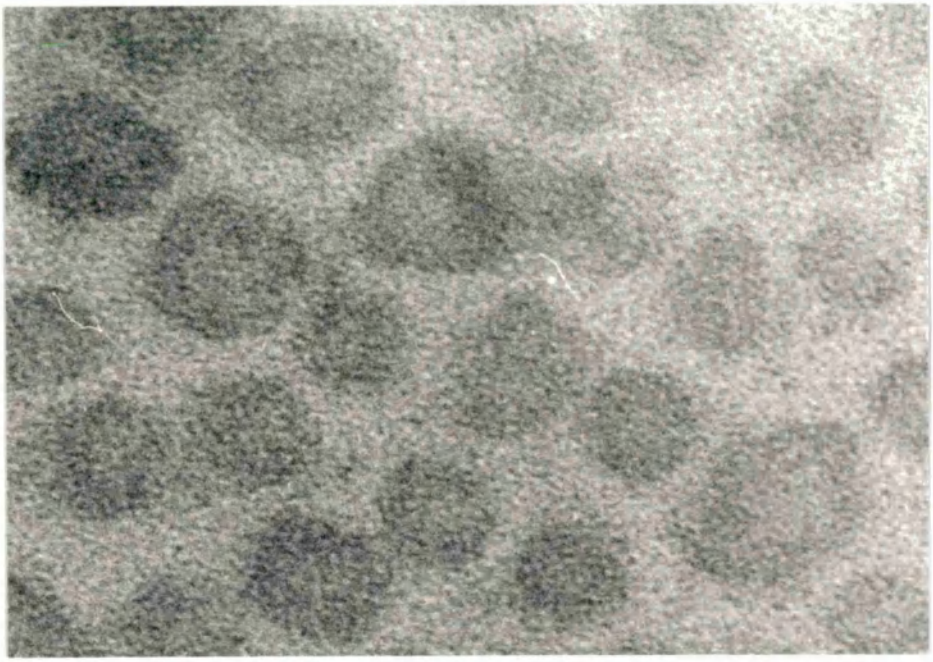

Figure 4.1 TEM of collagen fibrils in Morquio's syndrome showing the irregular shape of the fibrils. Stained with uranyl acetate and phosphotungstic acid. Magnification 530K

Further evidence for the possibility of the fibrils merging comes from the calculation of the addition of fibril areas. For example, the addition of two fibril areas calculated from the commonest fibril diameters (26nm) gives:

fibril area = πr^2

$= 3.141 \times 169nm^2 = 530.9nm^2$

Thus two merged fibrils would have an area of,

$2 \times 530.9nm^2 = 1061nm^2$

A fibril with area $1061nm^2$, when reshaped into a cylindrical form, will have a radius given by,

$$r = \frac{\text{area}}{\pi}$$

$$r = \frac{1061}{3.141} \text{ nm}$$

$r = 18.3nm$

The merging of two fibrils with a diameter of 26nm would therefore result in a fibril with a diameter of approximatly 36nm, this diameter falling within the population of larger fibril diameters measured in the Morquio's syndrome.

Proteoglycan staining with Cuprolinic blue revealed an apparent increase in the amount of stained material, as well as abnormal sized filaments.

With an increased population of interfibrillar proteoglycans one would expect the interfibrillar separation to increase. However, in the Morquio's syndrome cornea, increased number of interfibrillar proteoglycans should logically increase the stromal hydration and result in an increased interfibrillar separation. The results however show a decrease in the interfibrillar spacing of the collagen fibrils. This suggests that the above hypothesis may be an over simplification, to which I will return below.

It has also been postulated that proteoglycans play a role in controlling fibril diameters by preventing fibril fusion. The results from the Morquio's cornea oppose this because the fibrils appear to merge while in the presence of increased numbers of interfibrillar proteoglycans.

In Morquio's syndrome, the interfibrillar spacing is decreased and fibrils appear to merge, even in the presence of interfibrillar proteoglycans. The reduction of the interfibrillar spaces may be due to a decrease in hydration of the interfibrillar matrix. Most of the abnormal proteoglycans occur in spaces within the stroma. These proteoglycans may be responsible for creating lakes in the extracellular matrix by drawing water from the surrounding tissue and thereby reducing the interfibrillar water. This loss of interfibrillar water leads to a reduction in the interfibrillar separation and, in some cases, to fibril merging. It would therefore seem that the interfibrillar proteoglycans in Morquio's syndrome do not prevent the merging of the collagen fibrils simply by their physical presence. This

may have consequences for the mechanism of fibril spacing in the normal cornea and, perhaps, in connective tissue generally.

5.0 Conclusions

The aims of this thesis were to examine the ultrastructural changes that occur in the corneal stroma during wound healing and to compare the sequence of events in manual anterior keratectomy, photorefractive keratectomy and full-thickness wounds. The results showed that, all three types of wound follow a similar sequence of ultrastructural changes over a similar time period during healing. This process involves (i), the presence of abnormal proteoglycan filaments in the earliest stages which considerably hydrate the tissue and facilitate the movement of cells and (ii), the presence of lacunae, many of which are filled with abnormal proteoglycans. These lacunae, which would be expected to contribute to light scattering, persist in the scar tissue, even after long healing periods (9 months). Quantitative analysis of scar tissue using electron microscopy and X-ray diffraction showed that there is an increased range of diameters that returns to normal after 14 months. There is also a reduction in the ordering of the collagen fibrils compared to normal stroma. the increased spread of the interfibrillar spacing is still present after 21 months healing though it improved throughout the healing period studied, as did the transparency of the scar tissue.

In the study of Morquio's syndrome, the collagen fibrils had a reduced interfibrillar spacing in the stroma, and the fibrils appear to merge in the presence of normally arranged interfibrillar proteoglycans, forming collagen fibrils of larger fibril diameters. Morquio's syndrome, therefore, is a potentially useful model in which to study the factors that control fibril diameters and spacing in the corneal stroma.

6.0 Future Work

The electron microscopy of scarred corneal tissue using specfic staining of matrix components will be a useful technique for observing the effects of drug intervention to prevent scarring. The animal model will be the testing ground of new drugs to prevent the formation of scar tissue, with particular attention being paid to the effects of drugs on the nature and distribution of proteoglycans synthesised in the healing tissues.

The X-ray diffraction of the full-thickness scars could be taken further. In theory it should be possible to obtain the RDF from the X-ray pattern. This could then be used to calculate the tissue transparency and the results of the calculations could be compared with measured values if a suitably refined transparency measurement system could be devised. The RDF's generated from the electron micrographs could also be used in transparency calculations.

Disorders such as Morquio's Syndrome and other mucoploysaccharidoses are good systems for examining the structural role of individual components and their role in the organisation of the ultrastructure of the corneal matrix.

7.0 List of Publications

Papers:

Rawe, IM., Tuft, SJ. and Meek, KM. (1992) Proteoglycan and collagen morphology in superficially scarred rabbit cornea. Histochem. J. 24,311-318.

Rawe, IM., Zabel, RW., Tuft, SJ., Chen, V. and Meek, KM. (1992) A morphological study of rabbit corneas after laser keratectomy. Eye 6,637-642.

Abstracts

Rawe, IM., Tuft, SJ., Meek, KM., Elliott, GF., Cintron, C. and Kublin, CL., (1991) X-ray diffraction and electron microscopical studies of rabbit corneal scar tissue. Invest. Ophthalmol. Vis. Sci. 32,1164

Rawe, IM., Tuft, SJ., Zabel, RW. and Meek, KM (1992) Proteoglycans and collagen in rabbit excimer laser, manual keratectomy and ulcerated corneal scar tissue. Pro. Int. Soc. Eye Res. 7,101

Meek, KM., Rawe, IM., Cintron, C. and Takahashi, T. (1993) X-ray diffraction from corneal scar tissue. Proc. Vis. Sci. 2,7

Rawe, IM., Zabel, RW. and Meek, KM. (1993) Morquio's syndrome: a structural investigation using synchrotron X-ray diffraction and TEM. Ass. Eye Res. Documenta Ophthalmologica 9.

8.0 References

Adachi, E. & Hayashi, T. (1987) Comparison of axial banding patterns of type V collagen and type I collagen. Coll. Rel. Res., 7,27.

Azar, D.T., Spurr-Michaud, S., Tisdale, A.S., Gipson, I.K. (1989) Decreased penetration of anchoring fibrils into the diabetic stroma. Arch. Ophthalmol. 107:1520.

Benedek, G.B. (1971) Theory of transparency of the eye. Applied Optics 10:459.

BenEzra, D., Tanishima, T. (1978) Possible regulatory mechanisms of the cornea. I. Epithelial-stromal interaction in vitro. Arch. Ophthalmol. 96:1891.

Berman, M. (1989) The pathogenesis of corneal epithelial defects. in Advances in Applied Biotechnology Series. Vol 1. Healing processes in the cornea. ed. Beuerman, R.W., Crosson, C.E. & Kaufman, H.E. Gulf Publishing Co, Houston.

Birk, D.E., Trelstad, R.L. (1984) Extracellular compartments in matrix morphogenesis: collagen fibril, bundle and lamellar formation by corneal fibroblasts. J Cell Biol. 99, 2024.

Birk, D.E., Fitch, J.M., Babiarz, J.P., Doane, K.J. & Linsenmayer, T.F. (1990) Collagen fibrillogenesis in vitro: interaction of types I and V collagen regulates fibril diameter. J. Cell Science. 95, 649.

Borcherding, M.S., Blacik, L.S., Sittig, R.A., Bizzel, J.U., Breen, M. & Weinstein, H.G. (1975) Proteoglycans and collagen fibre organisation in human corneascleral tissue. Exp. Eye. Res. 21,59.

Brown, S.I., Weller, C.A.. (1970) Cell origin of collagenase in normal and wounded corneas. Arch Ophalmol 83,74.

Buckley, R.J. (1987) The cornea: Clinical Ophthalmology (ed Miller, S.)129, I.O.P. Publishing Ltd., Bristol.

Cho, H., Covington, H.I. & Cintron, C. (1990) Immunolocalization of type VI collagen in developing and healing rabbit cornea. Invest. Ophthalmol. Vis. Sci. 31,1096.

Chapman, J.A., Tzaphlidou, M., Meek, K.M. & Kadler, K.E. (1990) The collagen fibril - A model system for studying the staining and fixation of a protein. Electron Microsc. Rev. 3, 143.

Cintron, C., Schneider, H. & Kublin, C.L. (1973) Corneal scar formation. Exp. Eye Res. 17, 251.

Cintron, C. & Kublin, C.L. (1977) Regeneration of corneal tissue. Developmental Biol. 61, 346.

Cintron, C., Hassinger, L.C., Kublin, C.L., Cannon, D.J. (1978) Biochemical and ultrastructural changes in collagen during wound healing. J. Ultrastruct. Res. 65,13.

Cintron, C. & Covington, H.I. (1990) Proteoglycan in developing rat cornea. J. Histochem. Cytochem. 38, 675.

Cintron, C., Covington, H.I. & Kublin, C.L. (1990) Morphologic analyses of proteoglycans in rabbit corneal scars. Invest. Ophthalmol. Vis Sci. 31,1789.

Craig, A.S., Parry, D.A.D. (1981) Collagen fibrils of the vertebrate corneal stroma. Mol. Struct. Res. 74,232.

Crosson, C.E. (1989) The pathogenesis of corneal epithelial defects. in Advances in Applied Biotechnology Series. Vol 1. Healing processes in the cornea. ed. Beuerman, R.W., Crosson, C.E. & Kaufman, H.E. Gulf Publishing Co, Houston.

Crosson, C.E., Klyce, S.D. & Beuerman, R.W. (1986) Epitheilial wound closure in the rabbit cornea. Invest. Ophthalmol. Vis Sci. 27:464.

Dunnington, J.H., Weimar V. (1958) Influence of the epithelium on the healing of corneal incisions. Am. J. Ophthalmol 45,89

Engel, J., Furthmayr, H., Odermatt, E., von der Mark, H., Aumailley, M.,Fleischmajer, R. and Timpl, R. (1985) Structure and macromolecular structure of type VI collagen. Ann. NY Acad. Sci. 460:25.

Engvall, E., Hessle, H. and Kl;eir G. (1986) Molecular assembly, scretion, and matrix depostion of type VI collagen. J Cell Biol. 102:703.

Fantes, F.E., Hanna, K.D., Waring III, G.O., Pouliquen, Y., Thompson, K.P. & Savoldelli, M. (1990) Wound healing after excimer keratomileusis (photorefractive keratectomy) in monkeys. Arch. Ophthalmol. 108,665.

Fini, M.to fluid influx to the cornea, and a pump mechanism that E., Matsubra, M., Zieske, J.D., Cintron, C., Girard, M.T. & Kublin, C.L. (1991) Type IV collagenase expression in normal cornea and healing corneal wounds. Invest. ophthalmol. Vis. Sci. 32,1070.

Fitzsimmons, T., Fagerholm, P., Schenholm, M. & Harfstrand, A. (1991) Hyaluronic acid in the rabbit cornea after superficial keratectomy with the excimer laser. Invest. Ophthalmol. Vis. Sci. 32,1247.

Friedlaender, M.H. (1987) Metabolic diseases. in The Cornea ed Smolin, G. and Thoft, R.A. Little, Brown and Co. Boston/Toronto.

Fullwood, N.J., Tuft, S, J., Malik, N, S., Meek, K, M., Ridgway, A, E, A, R and Harrison, R, J. (1992) Synchrotron X-ray diffraction studies of keratoconus corneal stroma. Invest. Ophthalmol. Vis. Sci. 33,1734

Fullwood, N.J. & Meek, K.M. (1994) An ultrastructural time-resolved study of freezing in the corneal stroma. J. Mol. Biol. 236,749.

Funderburgh, J.L., Cintron, C., Covington, H.I. & Conrad, G.W. (1988) Immunoanalysis of keratan sulphate proteoglycan from corneal scars. Invest. Ophthalmol. Vis. Sci. 29, 1116.

Funderburgh, J.L. & Chandler, J.W. (1989) Proteoglycans of rabbit corneas with nonperforating wounds. Invest. Ophthalmol. Vis. Sci. 30,435.

Furthmayr, H., Wiedemann, H., Timpl, R., Odermatt, E. and Engel, J. (1983) Electron-microscopical approach to a structural model of intima collagen. Biochem J. 211:303.

Fujikawa, L.S., Foster, C.S., Harrist, T.J., Lanigan, J.M. (1981) Fibronectin in healing rabbit corneal wounds. Lab Invest 45,120.

Fujikawa, L.S., Foster, C.S., Gipson, I.K., Colvin, R.B. (1984) Basement membrane components in healing rabbit corneal epithelial wounds: Immunofluoresscence and ultrastructural studies. J. Cell Biol. 98,128.

Gartry, D.S., Kerr Muir, M.G., Marshall, J. (1991) Photorefractive keratectomy with an argon fluoride excimer laser: a clinical study. Refract. Corneal Surg. 7,420.

Gipson, I.K. & Anderson, R.R. (1977) Actin filaments in normal and migrating epithelial cells. Invest. Ophthalmol. Vis. Sci. 16:161.

Gipson, I.K., Spurr-Michaud, S.J. & Tisdale, A.S. (1987) Anchoring fibrils form a complex network in human and rabbit cornea. Invest. Ophthalmol. Vis. Sci. 28:212.

Gipson, I.K., Spurr-Michaud, S.J. & Tisdale, A.S. (1988) Hemidesmosomes and anchoring fibril collagen appear synchronously during development and wound healinng. Dev. Biol. 126:253.

Gipson, I.K., Spurr-Michaud, S.J., Tisdale, A.S. & Keough, M. (1989) Reassembly of the anchoring structures of the corneal epithelium during wound repair in the rabbit. Invest. Ophthalmol. Vis. Sci. 30:425.

Goldman, J.N., Benedek, C.H., Dohlman, C.H. & Krauitt, B. (1968) Structural alterations affecting transparency in swollen human corneas. Invest. Ophthalmol. Vis. Sci. 7, 501.

Goodfellow, J.M., Elliott, G.F., Woolgar, A.E. (1978) X-ray diffraction studies of the corneal stroma. J. Mol. Biol. 119,237.

Goodman, W.M., SundarRaj, N., Garone, M., Arffa, R.C. & Thoft, R.A. (1989) Unique parameters in the healing of linear partial thickness penetrating corneal incisions in rabbit: immunohistochemical evaluation. Current Eye Res. 8, 305.

Gordon, J.M., Bauer, E.A. Eisen, A.Z. (1980) Collagenase in human cornea: immunological localisation. Arch. Ophthalmol. 98,341.

Graf, B., Pouliquen, Y., Frouin, M-A., de Montaut, F. (1972) The phenomena of reabsorption in the course of cicatrization of experimental wounds of the cornea (ultrastructure study). Exp. Eye Res. 13,24.

Gyi, T.J., Meek, K.M., Elliott, G.F. (1988) The interfibrillar spacings of collagen fibrils in the corneal stroma; a species study. Int. J. Biol. Macromol. 10,256.

Hanna, K.D., Pouliquen, Y.M., Savoldelli, M., Fantes, F., Thompson, K.P., Waring III, G.O. & Samson, J. (1990) Corneal wound healing in monkeys 18 months after excimer laser photorefractive keratectomy. Refractive & Corneal Surgery. 6,340.

Harding, J. J., Crabbe, M. J. C. & Panjwani, N.A. (1980) Corneal Collagen: A Review. Colloques Int. Cent. Natl. Rech. Sci. 287, 51.

Hardingham, T.E. & Fosang, A.J. (1992) Proteoglycans: many forms and many functions. FASEB J. 6,861.

Hart, R.W., Farrell, R.A. (1969) Light scattering in the cornea. J. Opt. Soc. Am. 59,766.

Hassell, J.R., Cintron, C., Kublin, C. & Newsome, D.A. (1983) Proteoglycan changes during the restoration of transparency in corneal scars. Arch. Biochem. Acta 882, 136.

Hedbys, B.O. (1961) The role of polysacharides in corneal swelling. Exp. Eye Res. 1:81.

Hersh, P.S., Rice, B.A., Baer, J.C., Wells. P.A., Lynch, S.E., McGuigan, L.J.B. & Foster, C.S. (1990) Topical nonsteriodal agents and corneal wound healing. Arch. Ophthalmol. 108, 577.

Hodge, A.J., Schmitt, F.O. (1960) The charge profile of the tropocollagen macromolecule and the packing arrangement in native-type coolagen fibrils. Proc. Natl. Acad. Sci. USA, 46,186.

Johnson-Wint, B. (1980) Regulation of stromal cell collagenase production in adult rabbit cornea. In vitro stimulation and inhibition by epithelial cell products. Proc. Nat. Acad. Sci. USA 77:5331.

Kanski, JJ. (1984) Disorders of the cornea and sclera. In: Clinical Ophthalmology, 2nd edition (ed Kanski) 87, Butterworth & Co. Ltd,. London.

Katz, E.P., Wachtel, E.J., & Maroudas, A. (1986) Exrafibrillar proteoglycans osmotically regulate the molecular packing of collagen in cartilage. Biochem. Biophys. Acta 882, 136.

Keen, D.R., Engvall, E. and Glanville, R.W. (1988) Ultrastructure of type VI collagen in human skin and cartilage suggests an anchoring function for this filamentous network. J Cell Biol 107:1995.

Kenyon, K.R. (1987) Morphology and Pathologic response of the cornea to disease. In The Cornea (Smolin, G & Thoft, R.A. eds.) 2nd edn. pp 63-98. Boston/Toronto: Little, Brown and Company.

Khodadoust, A.A., Silverstein, A.M., Kenyon, K.R. & Dowling, J.E. (1968) Adhesion of regenerating corneal epitheilium. The role of basement membrane. Am. J. Ophthalmol. 65:339.

Kuwabara, T., Perkins D.S., Coggan, D.G. (1976) Sliding of the epithelium in experimental corneal wounds. Invest. Ophthalmol. 15,4.

Labermeier, U., Kenney, M.C. (1983) The presence of EC collagen and type IV collagen in bovine Descemet's membranes. Biochem. Biophys. Res. Commun. 116,619.

Lapiere, Ch. M., Nusgens, B., Pierard, G.E. (1977) Interaction between collagen types I and types III in conditioning bundles organisation. Connect. Tissue Res. 5,21.

Leblond, CP. (1989) Synthesis and secretion of collagen by cells of connective tissue, bone, and dentin. The Anatomical Record 224,123.

Lee, R.E., Davison, P.F. & Cintron, C. (1982) The healing of linear nonperforating wounds in rabbit corneas of different ages. Invest. Ophthalmol. Vis. Sci. 23,660.

Maroudas, A., Wachtel, E., Grushko, G., Katz, E.P. and Weinberg, P. (1991) The effect of osmotic and mechanical pressures on water partitioning in articular cartilage. Biochim. Biophys. Acta. 1073,285.

Marshall, GE., Konstas, AG. and Lee, WR. (1991) Immunogold fine structural localization of extracelluar matrix components in aged human cornea. II. Collagen types V and VI. Graefe's Arch. Clin. Exp. Ophthalmol. 229,164.

Marshall, J., Trokel, S., Rothery, S., Kreuger, R.R. (1986) Photoablative reprofiling using the excimer laser: photorefractive keratectomy. Lasers Ophthalmol. 1,21.

Matsuda, H. & Smelser, G.K. (1973) Electron microscopy of corneal wound healing. Exp. Eye Res. 16, 427.

Maurice, D.M. (1957) The structure and transparency of the corneal stroma. J. Physiol. 136, 263.

Maurice, D.M. (1987) The biology of wound healing in the corneal stroma. Cornea 6, 162.

McCally, R. L. and Farrell, R. A. (1988) Interaction of light and the cornea: light scattering versus transparency. The Cornea: Transactions of the World Congress on the Cornea III, (edited by H. Dwight Cavanagh) Raven Press, Ltd., New York.

McDonald, M.B., Frantz, J.M., Klyce, S.D., Beuerman, R.W., Varnell, R., Munnerlyn, C.R., Clapham, T.N., Salmeron, B. & Kaufman, H.E. (1990) Central photorefractive keratectomy for myopia. The blind eye study. Arch. ophthalmol. 108,799.

McDonald, M.B., Frantz, J.M., Klyce, S.D., Salmeron, B., Beuerman, R.W., Munnerlyn, C.R., Clapham, T.N., Koons, S.J. & Kaufman. (1990) One-year refractive results of central photorefractive keratectomy for myopia in the nonhuman primate cornea. Arch. Ophthalmol. 108,40.

Meek, K.M., Elliott, G.F., Sayers, Z., Whitburn, S.B., Koch, M.H. (1981) Interpretation of the meridional X-ray diffraction pattern from collagen fibrils in corneal stroma. J. Mol. Biol. 149,477.

Meek, K.M., Elliott, G.F. & Nave, C. (1986) A synchrotron X-ray diffraction study of bovine cornea stained with cupromeronic blue. Collagen Res. Rel. 6, 203.

Meek, K.M. and Leonard, D. (1993) Ultrastructure of the corneal stroma: a comparative study. Biophys. J. 64,273.

Menasche, M., Robert, L., Payrau, P., Hamada, R. & Pouliquen, Y. (1988) Comparative biochemical and morphometric studies on corneal wound healing. Pathologie Biologie 36, 781.

Mishima, S., Hedbys, B.O. (1967) The permeability of the corneal epithelium and endothelium. Exp. Eye Res.6,10.

Montes, G.S. & Junqueira, L.C.U. (1988) Histochemical localization of collagen and of proteoglycans in tissues. In Collagen Vol II: Biochemistry and Biomechanics (Nimni, M.E. ed.) p 42 Boca Raton, Florida: CRC Press, Inc.

Newsome, D.A., Gross, J. and Hassel, J.R. (1982) Human corneal stroma contains three distinct collagens. Invest. Ophthalmol. Vis. Sci. 22/3,376.

Nimni, M.E., Harkness, R.D. (1988) Molecular structure and functions of collagen. *In*: Collagen , Volume 1: Biochemistry (Ed. Nimni, M.E.), C.R.C. Press Inc., Boca Raton, Florida.

Parry, D.A.D. (1988) The molecular and fibrillar structure of collagen and its relationship to the mechanical properties of connective tissue. Biophys. Chem. 29,195.

Quantock, A., Zabel, R. and Meek, K.M. (1993) "Scheie's Syndrome: An ultrastructural analysis of the cornea. II. Architecture of stromal collagen and distribution of stromal proteoglycans." In press.

Ramachandran, G.N. (1967) Structure of collagen at the molecular level. *In:* Treatise on collagen. (Ed. Ramachandran, G.N.) Academic Press, New York.

Sayers, Z., Koch, M.H., Whitburn, S.B., Meek, K.M., Elliott, G.F., Harmsen, A. (1982) Synchrotron X-ray diffraction study of the corneal stroma. J. Mol. Biol. 160:593.

Scott, J E (1984) The periphery of the developing collagen fibril. Biochem. J. 218, 229.

Scott, J.E. (1985) Proteoglycan histochemistry - a valuable tool for connective tissue biochemists. Collagen Res. Rel. 5, 541.

Scott, J.E. (1988) Proteoglycan - fibrillar collagen interactions. Biochem. J. 252, 313.

Scott, J.E. (1985) & Haigh, M. (1985) Proteoglycan-type 1 collagen interactions in bone and non-calcifying connective tissues. Bioscience Rep. 5, 71.

Smith, J.E. (1969) The transparency of the corneal stroma. Vision Res. 9,393.

Suda, T., Nishida, T., Ohashi, Y., Nakagawa, S., Manabe, R. (1982) Fibronectin appears at the site of corneal stromal wound in rabbits. Exp. Eye Res. 9:553.

SundarRaj, N., Geiss, M.J., Fantes, F., Hanna, K., Anderson, S.C., Thompson, K.P., Thoft, R.A. & Waring, G.O. (1990) Healing of excimer

ablated monkey corneas: An immunohistochemical evalution. Arch. Ophthalmol. 108, 1604.

Talamo, J.H., Gollamudi, S., Green, W.R., De La Cruz, Z., Filatov, V. & Stark, W.J. (1991) Modulation of corneal wound healing after excimer laser keratomileusis using topical mitomycin C and steriods. Arch. Ophthalmol. 109,1141.

Ten Cate, A.R., Deporter, D.A. (1975) The degenerative role of the fibroblast in the remodelling and turnover of collagen in soft connective tissue. Anat. Rec. 182:1.

Toft, R.A., Friend, J. (1983) The X, Y, Z hypothesis of corneal epithelial maintenance. Invest. Ophthalmol. Vis. Sci. 24,1442.

Tuft, S.J., Zabel, R.W. & Marshall, J. (1989) Corneal repair following keratectomy: a comparison between conventional surgery and laser photoablation. Invest. Ophthalmol. Vis. Sci. 30, 1769.

Woost, P.G., Brightwell, J., Eiferman, R.A., Schultz, G.S. (1985) Effect of growth factors with dexamethasone on healing of rabbit corneal stromal incisions. Exp. Eye. Res. 40:47.

Worthington, C.R., Inouye, H. (1985) X-ray diffraction study of the cornea. Int. J. Biol. Macromol. 7,2.

Young, R.D. (1985) The ultrastructural organisation of proteoglycans and collagen in human and rabbit scleral matrix. J. Cell Sci. 74, 95.

Yue, B.Y.J.T., Hsieh, P., Baum, J.L. (1986) Effects of corneal extracts on rabbit corneal stromal cells in culture. Invest. Ophthalmol. Vis. Sci. 27:14.

Zabel, R.W., Sher, N.A., Ostrov, C.S., Parker, P. & Lindstrom, R.L. (1990) Myopic excimer laser keratectomy: a preliminary report. Refractive & Corneal Surgery. 6, 329.

Zimmerman, D.R., Trueb, B., Winterhalter, K.H., Witmer, R. & Fischer, R.W. (1986) Type VI collagen as a major component of the human cornea. Fed. Eur. Biochem. Soc. 197,55.